VOL. 11 NO. 4 APRIL 1966
PUBLISHED MONTHLY

Journal of

ELECTROANALYTICAL CHEMISTRY

International Journal Dealing with all Aspects of Electroanalytical Chemistry, Including Fundamental Electrochemistry

ELSEVIER

GENERAL INFORMATION

See also Suggestions and Instructions to Authors which will be sent free, on request to the Publishers.

Types of contributions

(a) Original research work not previously published in other periodicals.
(b) Reviews on recent developments in various fields.
(c) Short communications.
(d) Bibliographical notes and book reviews.

Languages

Papers will be published in English, French or German.

Submission of papers

Papers should be sent to one of the following Editors:

Professor J. O'M. BOCKRIS, John Harrison Laboratory of Chemistry, University of Pennsylvania, Philadelphia 4, Pa., U.S.A.
Dr. R. PARSONS, Department of Chemistry, The University, Bristol 8, England.
Professor C. N. REILLEY, Department of Chemistry, University of North Carolina, Chapel Hill, N.C., U.S.A.

Authors should preferably submit two copies in double-spaced typing on pages of uniform size. Legends for figures should be typed on a separate page. The figures should be in a form suitable for reproduction, drawn in Indian ink on drawing paper or tracing paper, with lettering etc. in thin pencil. The sheets of drawing or tracing paper should preferably be of the same dimensions as those on which the article is typed. Photographs should be submitted as clear black and white prints on glossy paper.
All references should be given at the end of the paper. They should be numbered and the numbers should appear in the text at the appropriate places.
A summary of 50 to 200 words should be included.

Reprints

Twenty-five reprints will be supplied free of charge. Additional reprints can be ordered at quoted prices. They must be ordered on order forms which are sent together with the proofs.

Publication

The *Journal of Electroanalytical Chemistry* appears monthly and has six issues per volume and two volumes per year.

Subscription price: £ 12.12.0 or $ 35.00 or Dfl. 126.00 per year; £ 6.6.0 or $ 17.50 or Dfl. 63.00 per volume; postage (per year): 8s, 6d, or $1.25 or Dfl. 4.20.
Additional cost for copies by air mail available on request.
For advertising rates apply to the publishers.

Subscriptions

Subscriptions should be sent to:

ELSEVIER PUBLISHING COMPANY, P.O. Box 211, Amsterdam, The Netherlands.

ALTERNATING CURRENT POLAROGRAPHY WITH MULTI-STEP CHARGE TRANSFER

I. THEORY FOR SYSTEMS WITH REVERSIBLE TWO-STEP CHARGE TRANSFER.

HOYING L. HUNG AND DONALD E. SMITH
Department of Chemistry, Northwestern University, Evanston, Illinois (U.S.A.)
(Received July 9th, 1965)

INTRODUCTION

Studies of electrode reactions involving the transfer of more than one electron per molecule of electroactive species have indicated that multi-step charge transfer schemes represent an important mechanistic category. Among those suggested in the interpretation of experimental results are the mechanisms

$$O + n_1 e \rightleftharpoons Y + n_2 e \rightleftharpoons R \qquad (R1)$$

$$O + n_1 e \rightleftharpoons Y \underset{k_2}{\overset{k_1}{\rightleftharpoons}} Z + n_2 e \rightleftharpoons R \qquad (R2)$$

$$\begin{array}{l} O + n_1 e \rightleftharpoons Y + n_2 e \rightleftharpoons R \\ \qquad\quad k_2 \uparrow\downarrow k_1 \\ \qquad\quad\ \ Z \end{array} \qquad (R3)$$

$$\begin{array}{l} O + n_1 e \rightleftharpoons Y + n_2 e \rightleftharpoons R \\ \uparrow \underline{\qquad k \qquad} | \end{array} \qquad (R4)$$

(*c.f.*, VLČEK[1] for review). Accordingly, numerous theoretical and experimental studies have been devoted to this type of reaction[2-32].

Interest in the applications of a.c. polarography has led us to consider the theory of the a.c. polarographic wave with reactions of this nature. Immediate objectives were to assess on a theoretical basis the power of the a.c. polarographic method in establishing the existence of such mechanisms and in the determination of kinetic and thermodynamic parameters. The present paper is concerned with the theory for the two-step reduction (or oxidation) mechanism represented by reaction (R1) in the limiting case where charge transfer is sufficiently rapid that Nernstian conditions are maintained and faradaic alternating currents are controlled solely by diffusion (the "reversible" case). Of primary concern is the situation where the two charge transfer steps proceed in the same potential range, since the simple theory for the single-step reduction applies when the two steps yield completely resolved waves.

Very recently, equations derived for the fundamental harmonic alternating current were presented by one of us[33] and by HALE[15] without derivation or significant discussion. These brief presentations are supplemented by the present work which amplifies salient aspects of the theory in question, including: (a) the method of derivation; (b) predictions of equations for the fundamental and second harmonic a.c. waves; (c) conditions under which diffusion-controlled two-step and single-step mechanisms are distinguishable; (d) the relative sensitivity of the d.c. and a.c. methods to differences between the two-step and single-step mechanisms; (e) methods of calculating standard potentials for the two steps from a.c. polarographic data.

In a.c. polarography, the number of systems that will obey precisely, equations based on the Nernstian assumption is likely to be small. The importance of such equations lies primarily in their representation of the "ideal" or limiting case. A comparison of predictions for the diffusion-controlled system to theory incorporating contributions due to finite charge transfer kinetics permits a check on the predictions of the latter in the limit of infinite charge transfer rate, and enables quantitative assessment of magnitudes of charge transfer rates required to establish Nernstian behavior. A comparison of predictions for the ideal to experimental results on "real" systems following reaction (R1) allows qualitative evaluation of deviations from pure diffusion control. The theory for the two-step reduction considering the influence of charge transfer kinetics is given elsewhere[34].

THEORY

Assumptions in addition to that of Nernstian behavior are as follows: (a) Fick's law is applicable to each diffusing species independently; (b) each reacting species is soluble either in the solution or electrode phase; (c) adsorption effects are negligible; (d) the potentiostatic approximation for the d.c. potential is accurate, *i.e.*, the scan rate is so slow that the change in d.c. potential is negligible over the life of a single mercury drop; (e) steady state is achieved in the a.c. concentration profile[35]; (f) if existent, coupled chemical reactions exert no kinetic effect on the a.c. wave, *i.e.*, they are so slow that they are essentially inoperative or so rapid that chemical equilibrium is maintained at all times; (g) the stationary plane model is an accurate approximation to the dropping mercury electrode. It has recently been pointed out that the latter assumption may be inaccurate under certain conditions[36]. However, diffusion-controlled systems are expected to obey this approximation reasonably well.

For reaction (R1), the boundary value problem to be solved is represented by eqns. (1)–(12) (a list of notations is given in the Appendix.)

$$\frac{\partial C_O}{\partial t} = D_O \frac{\partial^2 C_O}{\partial x^2} \tag{1}$$

$$\frac{\partial C_Y}{\partial t} = D_Y \frac{\partial^2 C_Y}{\partial x^2} \tag{2}$$

$$\frac{\partial C_R}{\partial t} = D_R \frac{\partial^2 C_R}{\partial x^2} \tag{3}$$

$$t = 0, \text{ any } x; \qquad C_O = C_O^* \tag{4}$$

$$C_Y = C_R = 0 \tag{5}$$

$$t > 0,\ x \to \infty; \qquad C_O \to C_O^* \tag{6}$$

$$C_Y \to C_R \to 0 \tag{7}$$

$$t > 0,\ x = 0; \qquad D_O \frac{\partial C_O}{\partial x} = \frac{i_1(t)}{n_1 FA} \tag{8}$$

$$D_Y \frac{\partial C_Y}{\partial x} = \frac{i_2(t)}{n_2 FA} - \frac{i_1(t)}{n_1 FA} \tag{9}$$

$$D_R \frac{\partial C_R}{\partial x} = -\frac{i_2(t)}{n_2 FA} \tag{10}$$

$$C_O = C_Y \left(\frac{D_Y}{D_O}\right)^{\frac{1}{2}} e^{j_1(t)} \tag{11}$$

$$C_Y = C_R \left(\frac{D_R}{D_Y}\right)^{\frac{1}{2}} e^{j_2(t)} \tag{12}$$

where

$$i_1(t) + i_2(t) = i(t) \tag{13}$$

$$j_i(t) = \frac{n_i F}{RT} [E(t) - E^r_{\frac{1}{2},i}] \tag{14}$$

$$E(t) = E_{d.c.} - \Delta E \sin \omega t \tag{15}$$

$$E^r_{\frac{1}{2},1} = E^0_1 - \frac{RT}{n_1 F} \ln \left(\frac{f_Y}{f_O}\right) \left(\frac{D_O}{D_Y}\right)^{\frac{1}{2}} \tag{16}$$

$$E^r_{\frac{1}{2},2} = E^0_2 - \frac{RT}{n_2 F} \ln \left(\frac{f_R}{f_Y}\right) \left(\frac{D_Y}{D_R}\right)^{\frac{1}{2}} \tag{17}$$

Equations (11) and (12) are statements of the Nernst equation for the two charge-transfer steps expressed in terms of the reversible half-wave potentials for planar diffusion (eqns. (16) and (17)). Derivation of surface concentrations for O, Y and R employing eqns. (1)–(10) and the method of Laplace Transformation has been given by HERMAN AND BARD[16]. The results are:

$$C_{O_{x=0}} = C_O^* - \int_0^t \frac{i_1(t-u)\mathrm{d}u}{n_1 FA(D_O \pi u)^{\frac{1}{2}}} \tag{18}$$

$$C_{Y_{x=0}} = \int_0^t \frac{i_1(t-u)\mathrm{d}u}{n_1 FA(D_Y \pi u)^{\frac{1}{2}}} - \int_0^t \frac{i_2(t-u)\mathrm{d}u}{n_2 FA(D_Y \pi u)^{\frac{1}{2}}} \tag{19}$$

$$C_{R_{x=0}} = \int_0^t \frac{i_2(t-u)\mathrm{d}u}{n_2 FA(D_R \pi u)^{\frac{1}{2}}} \tag{20}$$

Substitution of eqns. (18), (19) and (20) in eqns. (11) and (12) yields a system of two integral equations in two unknowns. Solving for

$$\int_0^t \frac{i_1(t-u)\mathrm{d}u}{(\pi u)^{\frac{1}{2}}}$$

and

$$\int_0^t \frac{i_2(t-u)\mathrm{d}u}{(\pi u)^{\frac{1}{2}}}$$

and introducing the definitions

$$\psi_1(t) = \frac{i_1(t)}{n_1 FAC_O^* D_O^{\frac{1}{2}}} \tag{21}$$

$$\psi_2(t) = \frac{i_2(t)}{n_2 FAC_O^* D_O^{\frac{1}{2}}} \tag{22}$$

yields the expressions (given in the form most convenient for subsequent steps)

$$(1+\mathrm{e}^{-j_2(t)}+\mathrm{e}^{j_1(t)}) \int_0^t \frac{\psi_1(t-u)\mathrm{d}u}{(\pi u)^{\frac{1}{2}}} = 1+\mathrm{e}^{-j_2(t)} \tag{23}$$

$$(1+\mathrm{e}^{-j_2(t)}+\mathrm{e}^{j_1(t)}) \int_0^t \frac{\psi_2(t-u)\mathrm{d}u}{(\pi u)^{\frac{1}{2}}} = \mathrm{e}^{-j_2(t)} \tag{24}$$

Introducing the power series

$$\exp\left[\frac{\pm n_i F\Delta E}{RT} \sin \omega t\right] = \sum_{p=0}^{\infty} (\pm 1)^p \left(\frac{n_i F\Delta E}{RT}\right)^p \frac{(\sin \omega t)^p}{p!} \tag{25}$$

$$\psi_i(t) = \sum_{p=0}^{\infty} \psi_{i,p}(t) \left(\frac{n_i F\Delta E}{RT}\right)^p \tag{26}$$

$$p = 0, 1, 2, 3 \ldots . \tag{27}$$

(where i represents the subscripts 1 and 2) and equating coefficients of equal powers of $n_1 F\Delta E/RT$ yields two systems of integral equations

$$\int_0^t \frac{\psi_{1,p}(t-u)\mathrm{d}u}{(\pi u)^{\frac{1}{2}}} + \sum_{r=0}^{p} \left[\mathrm{e}^{-j_2}\left(\frac{n_2}{n_1}\right) + (-1)^r \mathrm{e}^{j_1}\right] \frac{(\sin \omega t)^r}{r!} \int_0^t \frac{\psi_{1,p-r}(t-u)\mathrm{d}u}{(\pi u)^{\frac{1}{2}}}$$

$$= \mathrm{e}^{-j_2}\left(\frac{n_2}{n_1}\right)^p \frac{(\sin \omega t)^p}{p!} + \delta_{0,p} \tag{28}$$

$$\int_0^t \frac{\psi_{2,p}(t-u)\mathrm{d}u}{(\pi u)^{\frac{1}{2}}} + \sum_{r=0}^{p}\left[\mathrm{e}^{-j_2}+(-1)^r\left(\frac{n_1}{n_2}\right)^r \mathrm{e}^{j_1}\right]\frac{(\sin\omega t)^r}{r!}\int_0^t \frac{\psi_{2,p-r}(t-u)\mathrm{d}u}{(\pi u)^{\frac{1}{2}}}$$

$$= \frac{\mathrm{e}^{-j_2}(\sin\omega t)^p}{p!} \tag{29}$$

where

$$j_i = \frac{n_i F}{RT}(E_{\mathrm{d.c.}} - E^r_{\frac{1}{2},i}) \tag{30}$$

and $\delta_{0,p}$ is a special case of the Kronecker delta[37] defined by

$$\delta_{0,p} = 1 \quad \text{for} \quad p = 0 \tag{31a}$$

$$\delta_{0,p} = 0 \quad \text{for} \quad p \neq 0 \tag{31b}$$

The significance of solutions of eqns. (28) and (29) for various values of p has been discussed at length elsewhere[33,38]. The small amplitude fundamental harmonic faradaic alternating current is represented by the solutions of eqns. (28) and (29) for $p = 1$,

$$(1+\mathrm{e}^{-j_2}+\mathrm{e}^{j_1})\int_0^t \frac{\psi_{1,1}(t-u)\mathrm{d}u}{(\pi u)^{\frac{1}{2}}} + \left(\frac{n_2}{n_1}\mathrm{e}^{-j_2}-\mathrm{e}^{j_1}\right)\sin\omega t\int_0^t \frac{\psi_{1,0}(t-u)\mathrm{d}u}{(\pi u)^{\frac{1}{2}}}$$

$$= \left(\frac{n_2}{n_1}\right)\mathrm{e}^{-j_2}\sin\omega t \tag{32}$$

$$(1+\mathrm{e}^{-j_2}+\mathrm{e}^{j_1})\int_0^t \frac{\psi_{2,1}(t-u)\mathrm{d}u}{(\pi u)^{\frac{1}{2}}} + \left(\mathrm{e}^{-j_2} - \frac{n_1}{n_2}\mathrm{e}^{j_1}\right)\sin\omega t\int_0^t \frac{\psi_{2,0}(t-u)\mathrm{d}u}{(\pi u)^{\frac{1}{2}}}$$

$$= \mathrm{e}^{-j_2}\sin\omega t \tag{33}$$

The relations

$$\int_0^t \frac{\psi_{1,0}(t-u)\mathrm{d}u}{(\pi u)^{\frac{1}{2}}} = \frac{1+\mathrm{e}^{-j_2}}{1+\mathrm{e}^{-j_2}+\mathrm{e}^{j_1}} \tag{34}$$

$$\int_0^t \frac{\psi_{2,0}(t-u)\mathrm{d}u}{(\pi u)^{\frac{1}{2}}} = \frac{\mathrm{e}^{-j_2}}{1+\mathrm{e}^{-j_2}+\mathrm{e}^{j_1}} \tag{35}$$

are provided by the integral equations for $p = 0$. Substitution of eqns. (34) and (35) in eqns. (32) and (33) effects elimination of the integrals in $\psi_{1,0}$ and $\psi_{2,0}$ yielding the results

$$\int_0^t \frac{\psi_{1,1}(t-u)\mathrm{d}u}{(\pi u)^{\frac{1}{2}}} = \frac{\mathrm{e}^{j_1} + \left(\frac{n_1+n_2}{n_1}\right)\mathrm{e}^{j_1}\mathrm{e}^{-j_2}}{(1+\mathrm{e}^{-j_2}+\mathrm{e}^{j_1})^2}\sin\omega t \tag{36}$$

$$\int_0^t \frac{\psi_{2,1}(t-u)\mathrm{d}u}{(\pi u)^{\frac{1}{2}}} = \frac{\mathrm{e}^{-j_2} + \left(\frac{n_1+n_2}{n_2}\right)\mathrm{e}^{j_1}\mathrm{e}^{-j_2}}{(1+\mathrm{e}^{-j_2}+\mathrm{e}^{j_1})^2} \sin \omega t \tag{37}$$

Solution of eqns. (36) and (37) is accomplished as in earlier work[33,38,39], yielding

$$\psi_{1,1}(t) = \frac{\omega^{\frac{1}{2}}\left[\mathrm{e}^{j_1} + \left(\frac{n_1+n_2}{n_1}\right)\mathrm{e}^{j_1}\mathrm{e}^{-j_2}\right]}{(1+\mathrm{e}^{-j_2}+\mathrm{e}^{j_1})^2} \sin\left(\omega t + \frac{\pi}{4}\right) \tag{38}$$

$$\psi_{2,1}(t) = \frac{\omega^{\frac{1}{2}}\left[\mathrm{e}^{-j_2} + \left(\frac{n_1+n_2}{n_2}\right)\mathrm{e}^{j_1}\mathrm{e}^{-j_2}\right]}{(1+\mathrm{e}^{-j_2}+\mathrm{e}^{j_1})^2} \sin\left(\omega t + \frac{\pi}{4}\right) \tag{39}$$

Applying eqns. (13), (21), (22) and (26), one obtains for the fundamental harmonic alternating current component

$$I(\omega t) = \frac{F^2 AC_O^*(\omega D_O)^{\frac{1}{2}} \Delta E[n_1^2\mathrm{e}^{j_1} + n_2^2\mathrm{e}^{-j_2} + (n_1+n_2)^2\mathrm{e}^{(j_1-j_2)}]}{RT(1+\mathrm{e}^{-j_2}+\mathrm{e}^{j_1})^2} \sin\left(\omega t + \frac{\pi}{4}\right) \tag{40}$$

By solving eqns. (27) and (28) in the same manner as above for $p=2$, one obtains for the second harmonic current

$$I(2\omega t) = \frac{\sqrt{2}F^3 AC_O^*(\omega D_O)^{\frac{1}{2}} \Delta E^2}{4R^2T^2} F(E_{\mathrm{d.c.}}) \sin\left(2\omega t - \frac{\pi}{4}\right) \tag{41}$$

where

$$F(E_{\mathrm{d.c.}}) = \frac{1}{(1+\mathrm{e}^{-j_2}+\mathrm{e}^{j_1})^3}\{(1+\mathrm{e}^{-j_2}+\mathrm{e}^{j_1})[n_2^3\mathrm{e}^{-j_2} - n_1^3\mathrm{e}^{j_1} + (n_2^2-n_1^2)(n_1+n_2)\mathrm{e}^{(j_1-j_2)}]$$
$$+ 2(n_1\mathrm{e}^{j_1} - n_2\mathrm{e}^{-j_2})\,[n_1^2\mathrm{e}^{j_1} + n_2^2\mathrm{e}^{-j_2} + (n_1+n_2)^2\mathrm{e}^{(j_1-j_2)}]\} \tag{42}$$

and for the d.c. faradaic rectification component (in the presence of d.c. polarization)

$$I_{\mathrm{d.c.}} = \frac{F^3 AC_O^* D_O^{\frac{1}{2}} \Delta E^2}{4R^2T^2(\pi t)^{\frac{1}{2}}} F(E_{\mathrm{d.c.}}) \tag{43}$$

Examination of the solution to the d.c. wave for this system shows that eqns. (40), (41) and (43) may be written

$$I(\omega t) = -\Delta E(\omega\pi t)^{\frac{1}{2}}\left(\frac{\partial i_{\mathrm{d.c.}}}{\partial E_{\mathrm{d.c.}}}\right) \sin\left(\omega t + \frac{\pi}{4}\right) \tag{44}$$

$$I(2\omega t) = \frac{\sqrt{2}\,\Delta E^2(\omega\pi t)^{\frac{1}{2}}}{4}\left(\frac{\partial^2 i_{\text{d.c.}}}{\partial E^2_{\text{d.c.}}}\right)\sin\left(2\omega t - \frac{\pi}{4}\right) \tag{45}$$

$$I_{\text{d.c.}} = \frac{\Delta E^2}{4}\left(\frac{\partial^2 i_{\text{d.c.}}}{\partial E^2_{\text{d.c.}}}\right) \tag{46}$$

where $\partial i_{\text{d.c.}}/\partial E_{\text{d.c.}}$ is the derivative of the d.c. polarographic wave with respect to potential. Relation (44) was given in an equivalent form by HALE[15].

DISCUSSION

Equation (40) indicates certain similarities and dissimilarities between fundamental harmonic a.c. polarographic waves for diffusion-controlled single-step and two-step mechanisms. For comparison we write the equation for the a.c. wave with the single-step reduction involving (n_1+n_2) electrons:

$$I(\omega t) = \frac{(n_1+n_2)^2 F^2 A C_{\text{O}}^*(\omega D_{\text{O}})^{\frac{1}{2}}\Delta E}{4RT\cosh^2\left(\frac{j_3}{2}\right)}\sin\left(\omega t + \frac{\pi}{4}\right) \tag{47}$$

where

$$j_3 = \frac{(n_1+n_2)F}{RT}(E_{\text{d.c.}} - E^r_{\frac{1}{2},3}) \tag{48}$$

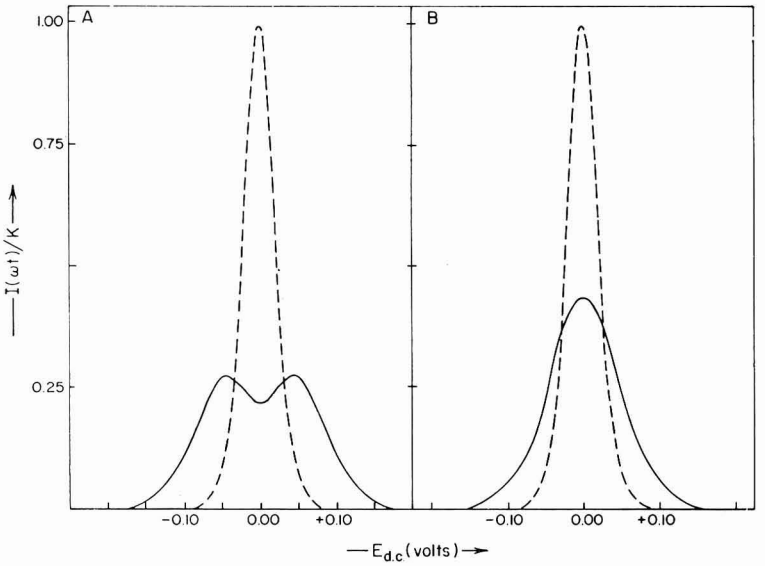

Fig. 1. Fundamental harmonic a.c. polarograms for two-electron transfer. (- - - - -), single-step mechanism, $n = 2$; (———), two-step mechanism, $n_1 = n_2 = 1$; (A), $E^r_{\frac{1}{4},1} - E^r_{\frac{1}{4},2} = 0.10$ V; (B), $E^r_{\frac{1}{4},1} - E^r_{\frac{1}{4},2} = 0.050$ V. $K = (F^2 A C_{\text{O}}^* \Delta E(\omega D_{\text{O}})^{\frac{1}{2}})/RT$.

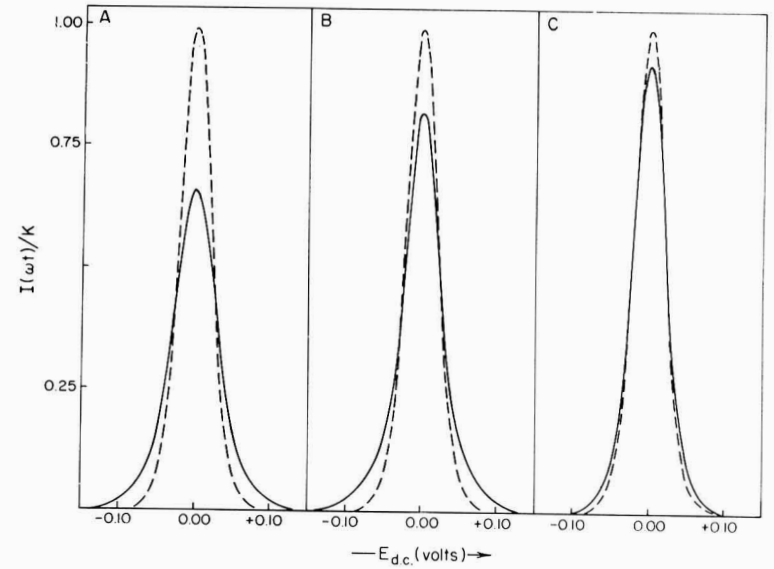

Fig. 2. Fundamental harmonic a.c. polarograms for two-electron transfer. (- - - -), single-step mechanism, $n = 2$; (———), two-step mechanism, $n_1 = n_2 = 1$; (A), $E^r_{\frac{1}{4},1} - E^r_{\frac{1}{4},2} = 0.000$ V; (B), $E^r_{\frac{1}{4},1} - E^r_{\frac{1}{4},2} = -0.050$ V; (C), $E^r_{\frac{1}{4},1} - E^r_{\frac{1}{4},2} = -0.100$ V.

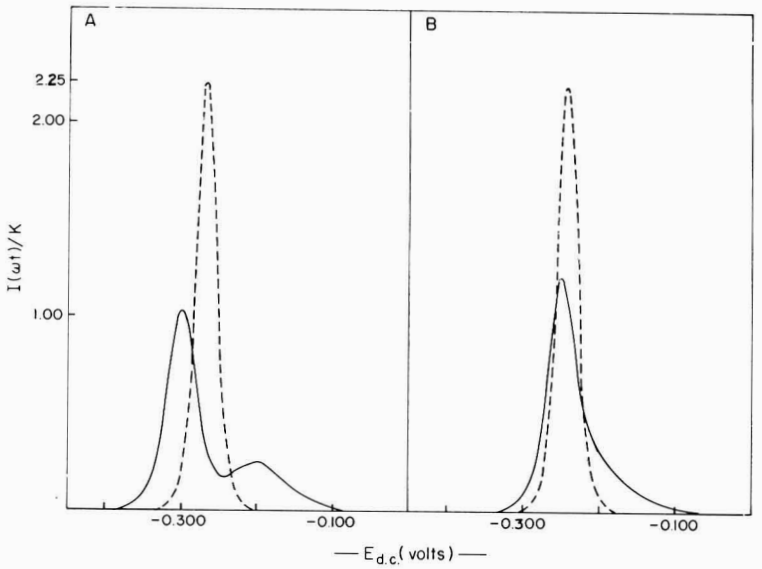

Fig. 3. Fundamental harmonic a.c. polarograms for three-electron transfer. (- - - -), single-step mechanism, $n = 3$; (———), two-step mechanism, $n_2 = 2n_1 = 2$; (A), $E^r_{\frac{1}{4},1} - E^r_{\frac{1}{4},2} = 0.100$ V; (B), $E^r_{\frac{1}{4},1} - E^r_{\frac{1}{4},2} = 0.050$ V.

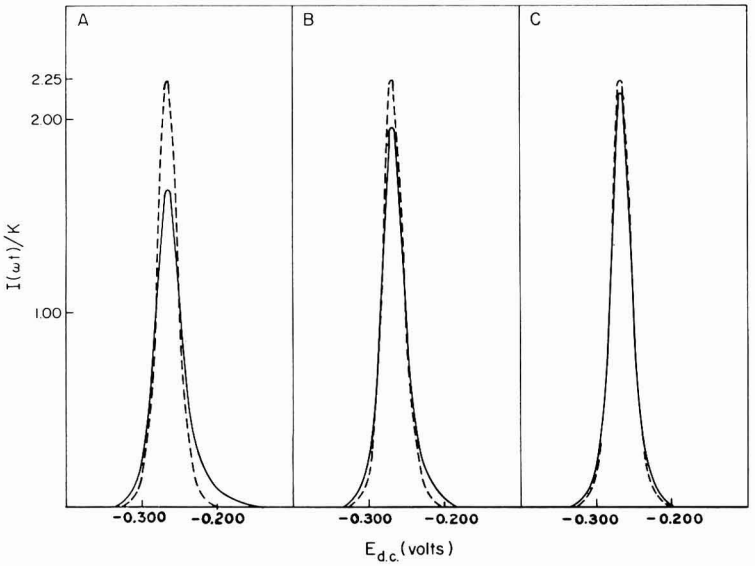

Fig. 4. Fundamental harmonic a.c. polarograms for three-electron transfer. (- - - -), single-step mechanism, $n = 3$; (———), two-step mechanism, $n_2 = 2n_1 = 2$; (A), $E^r_{\frac{1}{2},1} - E^r_{\frac{1}{2},2} = 0.000$ V; (B), $E^r_{\frac{1}{2},1} - E^r_{\frac{1}{2},2} = -0.050$ V; (C), $E^r_{\frac{1}{2},1} - E^r_{\frac{1}{2},2} = -0.100$ V.

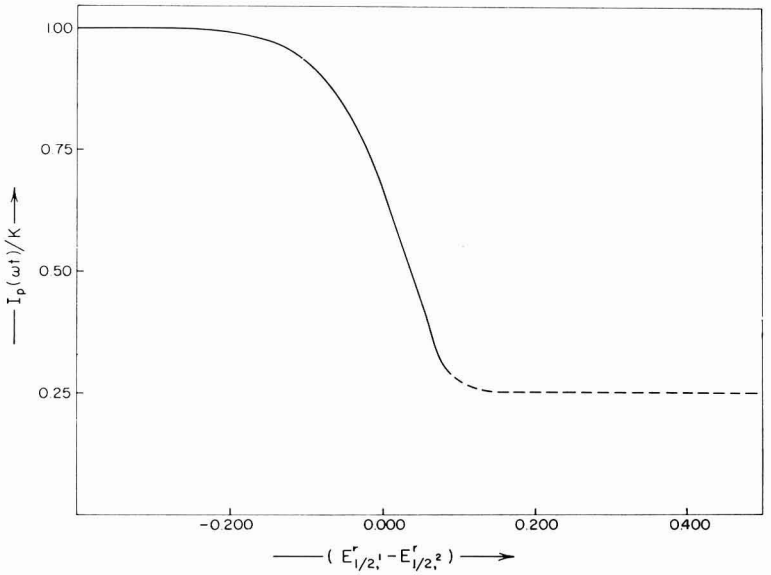

Fig. 5. Variation of peak fundamental harmonic alternating current with $E^r_{\frac{1}{2},1} - E^r_{\frac{1}{2},2}$, for $n_1 = n_2 = 1$. (———), single peak region: (- - - -), double peak region.

$$E^r_{\frac{1}{2},3} = E^0_3 - \frac{RT}{(n_1+n_2)F} \ln\left(\frac{f_R}{f_O}\right)\left(\frac{D_O}{D_R}\right)^{\frac{1}{2}} \tag{49}$$

E^0_3 is the standard redox potential for the O–R couple. Similarities lie in the dependence on the parameters F, $A\,C_O^*$, ΔE, R, T, D_O, ω, and in the facts that phase angles are predicted to be 45° and that the shape of the a.c. wave is directly related to the derivative of the d.c. wave with both mechanistic schemes. Disparities between the two cases, providing the basis for distinction, are found in the potential dependence and magnitudes of the a.c. polarographic wave. With the two-step mechanism, these latter characteristics are profoundly influenced by the parameters $(E^r_{\frac{1}{2},1}-E^r_{\frac{1}{2},2})$ and n_1/n_2, as one would expect. Figures 1–4 illustrate the nature of the a.c. polarographic wave predicted by eqn. (40) for $n_1=n_2=1$ and $n_2=2n_1=2$ with various values of $E^r_{\frac{1}{2},1}-E^r_{\frac{1}{2},2}$. A.c. polarographic waves predicted for the single-step transfer of n_1+n_2 electrons are included in these figures for comparison. Figure 5 illustrates the influence of the parameter $E^r_{\frac{1}{2},1}-E^r_{\frac{1}{2},2}$ on the peak current for $n_1=n_2=1$. The qualitative aspects of the predictions illustrated in Figs. 1–5 are as expected. When the half-wave potentials (*i.e.*, the standard redox potentials) of the O–Y and Y–R couples are comparable ($E^r_{\frac{1}{2},1}-E^r_{\frac{1}{2},2}\sim\pm 50$ mV) the waves are notably wider than predicted for single-step transfer of n_1+n_2 electrons. If $E^r_{\frac{1}{2},1}$ is sufficiently more positive than $E^r_{\frac{1}{2},2}$, two resolved peaks can be observed. In the limit when $E^r_{\frac{1}{2},1}\gg E^r_{\frac{1}{2},2}$ one finds for $E_{\text{d.e.}}$ in the vicinity of $E^r_{\frac{1}{2},1}$

$$j_2 \gg j_1 \tag{50}$$

$$e^{-j_2} \ll e^{j_1} \tag{51}$$

so that

$$I(\omega t) = \frac{n_1^2 F^2 A C_O^*(\omega D_O)^{\frac{1}{2}}\Delta E}{4RT\cosh^2\left(\frac{j_1}{2}\right)} \sin\left(\omega t + \frac{\pi}{4}\right) \tag{52}$$

and when $E_{\text{d.c.}}$ is in the vicinity of $E^r_{\frac{1}{2},2}$

$$e^{-j_2} \gg e^{j_1} \tag{53}$$

and

$$I(\omega t) = \frac{n_2^2 F^2 A C_O^*(\omega D_O)^{\frac{1}{2}}\Delta E}{4RT\cosh^2\left(\frac{j_2}{2}\right)} \sin\left(\omega t + \frac{\pi}{4}\right) \tag{54}$$

Thus, when $E^r_{\frac{1}{2},1}$ becomes much more positive than $E^r_{\frac{1}{2},2}$, eqn. 40 predicts two completely resolved a.c. polarographic waves, each obeying the equation for single-step reversible waves of n_1 and n_2 electrons, respectively. This obviously anticipated prediction is of interest primarily in so far as it serves as a convenient check on the validity of eqn. (40). The figures show also that as $E^r_{\frac{1}{2},2}$ becomes more positive than $E^r_{\frac{1}{2},1}$, the two-step a.c. wave becomes larger and narrower, approaching the prediction for the single-step mechanism. That the predictions for the two cases converge in the limit of $E^r_{\frac{1}{2},1}\ll E^r_{\frac{1}{2},2}$ is seen readily by examination of eqn. (40). Rearrangement of eqn. (40) yields

$$I(\omega t) = \frac{F^2 AC_O^*(\omega D_O)^{\frac{1}{2}} \Delta E[n_1^2 e^{j_2} + n_2^2 e^{-j_1} + (n_1+n_2)^2]}{RT[e^{-(j_1+j_2)} + e^{-j_1} + 1][e^{(j_1+j_2)} + e^{j_2} + 1]} \sin\left(\omega t + \frac{\pi}{4}\right) \quad (55)$$

When $E^r_{\frac{1}{2},1} \ll E^r_{\frac{1}{2},2}$, the a.c. wave appears at values of $E_{d.c.}$ intermediate and well-removed from these half-wave potentials so that

$$e^{j_2}, e^{-j_1} \ll 1 \quad (56)$$

This leads to the result

$$I(\omega t) = \frac{(n_1+n_2)^2 F^2 AC_O^*(\omega D_O)^{\frac{1}{2}} \Delta E}{4RT \cosh^2\left(\frac{j_1+j_2}{2}\right)} \sin\left(\omega t + \frac{\pi}{4}\right) \quad (57)$$

One notes that

$$j_1 + j_2 = \frac{(n_1+n_2)F}{RT}\left[E_{d.c.} - \left(\frac{n_1 E^r_{\frac{1}{2},1} + n_2 E^r_{\frac{1}{2},2}}{n_1+n_2}\right)\right] \quad (58)$$

and that combination of the Nernst equations for the O–Y and Y–R couples yields a relationship between E^0_1, E^0_2 and the standard potential for the O–R couple, E^0_3:

$$E^0_3 = \frac{n_1 E^0_1 + n_2 E^0_2}{n_1+n_2} \quad (59)$$

so that

$$E^r_{\frac{1}{2},3} = \frac{n_1 E^r_{\frac{1}{2},1} + n_2 E^r_{\frac{1}{2},2}}{n_1+n_2} \quad (60)$$

Comparison of eqns. (48), (58) and (60) leads to the conclusion that

$$j_1 + j_2 = j_3 \quad (61)$$

Thus, eqn. (57) is identical to eqn. (47) leading to the expected conclusion that diffusion-controlled single-step and two-step mechanisms cannot be distinguished experimentally when the second reduction step proceeds at much more positive potentials than the first step. It is instructive to recognize that this behavior is a direct consequence of the fact that the charge transfer processes under consideration are thermodynamically controlled, *i.e.*, the Nernst equation is obeyed. When $E^r_{\frac{1}{2},1} \ll E^r_{\frac{1}{2},2}$, the Nernstian surface concentration of species Y is essentially zero at all potentials encompassed by the a.c. wave (this is not the case with other combinations of $E^r_{\frac{1}{2},1}$ and $E^r_{\frac{1}{2},2}$). Thus, under these conditions, both the single-step and two-step mechanisms involve the same initial and final states so distinction between mechanisms on the basis of data manifesting only the thermodynamic aspects of charge transfer is not possible. On the other hand, if charge transfer kinetics influence the a.c. process, one might expect that distinction between the mechanisms should be possible, even when $E^r_{\frac{1}{2},1} \ll E^r_{\frac{1}{2},2}$. It is shown elsewhere[34] that theory predicts this to be the case.

It would be of interest to obtain expressions for the values of $E_{d.c.}$ corresponding to the maxima and minima of the a.c. wave with a two-step mechanism, by dif-

ferentiation of eqn. (40) with respect to $E_{d.c.}$. This operation yields cumbersome algebraic forms for the general case. However, the special case where $n_1 = n_2$ will be considered because it yields readily to mathematical treatment and because it includes the most likely encountered experimental situation; $n_1 = n_2 = 1$. For $n_1 = n_2 = n$, setting the derivative of eqn. (40) with respect to $E_{d.c.}$ equal to zero yields three solutions corresponding to

$$E_{d.c.} = \frac{E^r_{\frac{1}{2},1} + E^r_{\frac{1}{2},2}}{2} \tag{62}$$

$$E_{d.c.} = \frac{RT}{nF} \ln \left\{ \frac{1 - 8e^{(\delta_2 - \delta_1)} \pm [(8e^{(\delta_2 - \delta_1)} - 1)^2 - 4e^{(\delta_2 - \delta_1)}]^{\frac{1}{2}}}{2e^{-\delta_1}} \right\} \tag{63}$$

where

$$\delta_i = \frac{nFE^r_{\frac{1}{2},i}}{RT} \tag{64}$$

The solution corresponding to eqn. (62) is applicable for any combination of values for $E^r_{\frac{1}{2},1}$ and $E^r_{\frac{1}{2},2}$, while eqn. (63) yields real solutions only when

$$(8e^{(\delta_2 - \delta_1)} - 1)^2 \geq 4e^{(\delta_2 - \delta_1)} \tag{65}$$

which is equivalent to the statement

$$E^r_{\frac{1}{2},1} - E^r_{\frac{1}{2},2} \geq \frac{0.0712}{n} \tag{66}$$

It is apparent that eqn. (66) represents the mathematical condition for the appearance of two resolved peaks in the a.c. wave. When it is obeyed, three real solutions exist, with those of eqn. (63) corresponding to maxima and eqn. (62) giving the minima. When eqn. (66) is not obeyed, one real solution exists corresponding to a maximum at the potential given by eqn. (62).

If it is established that a two-step reversible charge transfer is taking place, determination of the reversible half-wave potentials and standard potentials for the two steps from a.c. polarographic data can be accomplished readily. Obviously, analysis of data is simplest when $n_1 = n_2$. In this situation, eqns. (62) and (63) can be employed to calculate $E^r_{\frac{1}{2},1}$ and $E^r_{\frac{1}{2},2}$ if two peaks are observed on the a.c. wave. The moderate complexity of eqn. (63) suggests the advisability of constructing a working curve of the difference in peak potentials ("peak separation") *vs.* $E^r_{\frac{1}{2},1} - E^r_{\frac{1}{2},2}$ based on eqn. (63) to facilitate data evaluation. From the experimental value of peak separation, the working curve yields $E^r_{\frac{1}{2},1} - E^r_{\frac{1}{2},2}$. The information necessary to calculate $E^r_{\frac{1}{2},1}$ and $E^r_{\frac{1}{2},2}$ is completed by determining $E^r_{\frac{1}{2},1} + E^r_{\frac{1}{2},2}$ from eqn. (62) and the observed potential of the minimum. If only a single peak is observed, eqn. (62) is still employed to obtain $E^r_{\frac{1}{2},1} + E^r_{\frac{1}{2},2}$ from the peak potential. A working curve of the half-width of the wave *vs.* $E^r_{\frac{1}{2},1} - E^r_{\frac{1}{2},2}$ may be employed to determine the difference in the half-wave potentials (it is readily shown that the half-width is a function of $E^r_{\frac{1}{2},1} - E^r_{\frac{1}{2},2}$). Alternatively, the working curve corresponding to Fig. 5 may be employed.

When $n_1 \neq n_2$, the problem of determining $E^r_{\frac{1}{2},1}$ and $E^r_{\frac{1}{2},2}$, while more compli-

cated, remains readily solved despite implications to the contrary by HALE[15]. As when $n_1 = n_2$, one can base the determination of the reversible half-wave potentials on the peak separation and potential of the minimum when two peaks are observed, and on peak potential and half-width or magnitude of the wave when only one peak is observed. Construction of working curves of these parameters *versus* an appropriate function of the reversible half-wave potentials will facilitate their calculation. Unlike the foregoing case, when $n_1 \neq n_2$ a single working curve will not suffice to define unambiguously the variation of the parameters of interest with variation of $E^r_{\frac{1}{2},1} - E^r_{\frac{1}{2},2}$ (or $E^r_{\frac{1}{2},1} + E^r_{\frac{1}{2},2}$). For each parameter such as peak potential, half-width of wave, etc., and for each combination of n_1 and n_2, one may construct a series of working curves of the parameter *vs.* $E^r_{\frac{1}{2},1}$ corresponding to different values of $E^r_{\frac{1}{2},2}$, or *vice-versa*. The availability of such sets of working curves then permits unambiguous determination of $E^r_{\frac{1}{2},1}$ and $E^r_{\frac{1}{2},2}$. For example, if one employs the peak potential and half-width of the a.c. wave as basis for data analysis, the experimentally observed values of these parameters each define a curve of $E^r_{\frac{1}{2},1}$ *vs.* $E^r_{\frac{1}{2},2}$ (*i.e.*, the curves defined by the intersections of the sets of working curves of peak potential and half-width *vs.* $E^r_{\frac{1}{2},1}$, with the experimental values of peak potential and half-width). The intersection of these curves corresponds to the correct values of $E^r_{\frac{1}{2},1}$ and $E^r_{\frac{1}{2},2}$. The foregoing approach is likely not the only possible method and may not be the simplest. It is presented primarily to show that $E^r_{\frac{1}{2},1}$ and $E^r_{\frac{1}{2},2}$ can be determined from a.c. polarographic data with an orderly procedure (as opposed to trial-and-error curve fitting), even when $n_1 \neq n_2$. Construction of such working curves can be accomplished relatively easily with the aid of high-speed digital computers.

Once $E^r_{\frac{1}{2},1}$ and $E^r_{\frac{1}{2},2}$ are determined, the corresponding standard potentials may be calculated in the usual manner with the aid of eqns. (16) and (17). In most situations, knowledge of the individual diffusion and activity coefficients, which are often difficultly determined, will not be necessary since the logarithmic term is usually

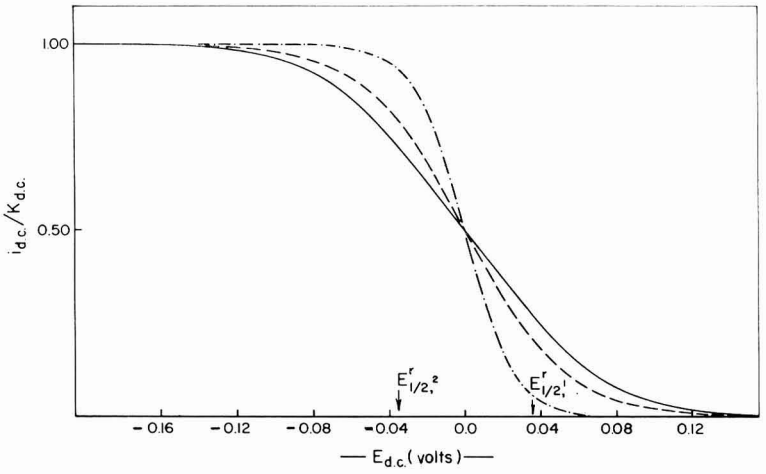

Fig. 6. Calculated d.c. polarograms. (- - - -), single-step mechanism, $n = 1$; (·····), single-step mechanism, $n = 2$; (———), two-step mechanism, $n_1 = n_2 = 1$, $E^r_{\frac{1}{2},1} - E^r_{\frac{1}{2},2} = 0.070$ V. $K_{d.c.} = nFAC_0^* D_0^{\frac{1}{2}}/(\pi t)^{\frac{1}{2}}$.

very small and the reversible half-wave potentials may be taken as the standard potentials.

It is of interest to examine the relative sensitivity of the a.c. and d.c. polarographic methods to the presence of the diffusion-controlled two-step mechanism. The direct correspondence between the shape of the d.c. and a.c. waves manifested in eqns. (44) and (45) indicates that the same information should be obtainable with

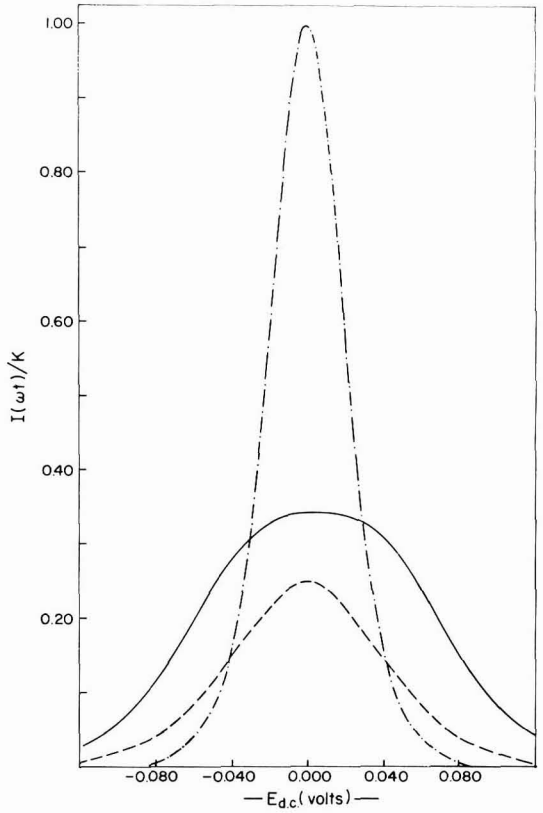

Fig. 7. Calculated fundamental harmonic a.c. polarograms. Notation as Fig. 6, except for K which is given in Fig. 1.

either method so that differences in utility will be small. The only apparent distinction is found in the well-known principle that derivative read-out is somewhat more sensitive than direct read-out to small differences in the original signal. This suggests that the a.c. polarographic method, representing derivative read-out, will be somewhat more sensitive to differences between the one-step and two-step mechanisms. Of course, the same can be said for derivative d.c. polarography[40,41]. The advantages derived from derivative response are illustrated in Figs. 6–8 which show d.c., fundamental harmonic a.c. and second harmonic a.c. polarograms for a two-step mechanism, with the single-step diffusion-controlled waves included for comparison. The sensitivity to the difference in mechanism is seen to increase with the order of the

harmonic. On the other hand, some forms of data analysis will show little or no difference between the a.c. and d.c. methods. One example is found in the comparison of the effect of the two-step mechanism on the classical plot of log $(i_d-i)/i$ *vs.* $E_{d.c.}$ from the d.c. polarogram and on an analogous plot from the a.c. polarogram[33] of

$$\log\left\{\left[\frac{I_p(\omega t)}{I(\omega t)}\right]^{\frac{1}{2}}+\left[\frac{I_p(\omega t)-I(\omega t)}{I(\omega t)}\right]^{\frac{1}{2}}\right\}$$

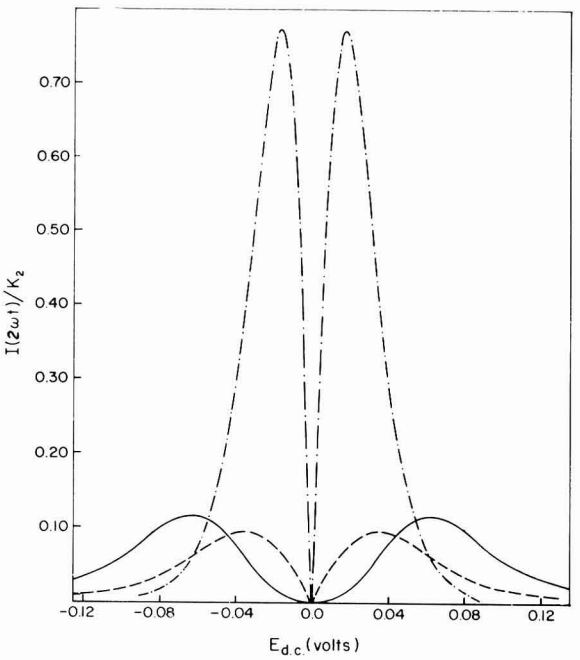

Fig. 8. Calculated second harmonic a.c. polarograms.

$$K_2=\frac{\sqrt{2}\,F^3AC_0^*(\omega D_0)^{\frac{1}{2}}\Delta E^2}{4R^2T^2}$$

Remaining notation as Fig. 6.

vs. $E_{d.c.}$. For diffusion-controlled single-step processes, the a.c. plot yields a straight line of slope 0.1182/n V (at 25°) as opposed to the well-known slope of 0.0591/n V obtained from the d.c. plot. For the case in which $n_1=n_2=n$, the two-step mechanism will yield points lying between lines of slope 0.0591/n and 0.0591/2n for the d.c. plot, and between lines of slope 0.1182/n and 0.1182/2n with the a.c. plot. It is seen that the range of possible variation in these linear plots with variation in $E^r_{\frac{1}{2},1}$ and $E^r_{\frac{1}{2},2}$ is greater for the a.c. plot on an absolute basis, while there is no difference on a relative basis. Thus, there is little difference in the qualitative appearance of these plots for any given combination of $E^r_{\frac{1}{2},1}$ and $E^r_{\frac{1}{2},2}$. This is illustrated in Fig. 9. Note that the ordinate is compressed by a factor of 2 in the a.c. plot.

The foregoing differences in sensitivity to variation in mechanism, while

existent, are sufficiently small that they are not particularly noteworthy. However, such an observation applies only to Nernstian systems. The a.c. polarographic method has much more to offer in the study of systems where charge transfer kinetics influence the response of the system. It is in such cases that the use of the a.c. method will most likely attract more interest.

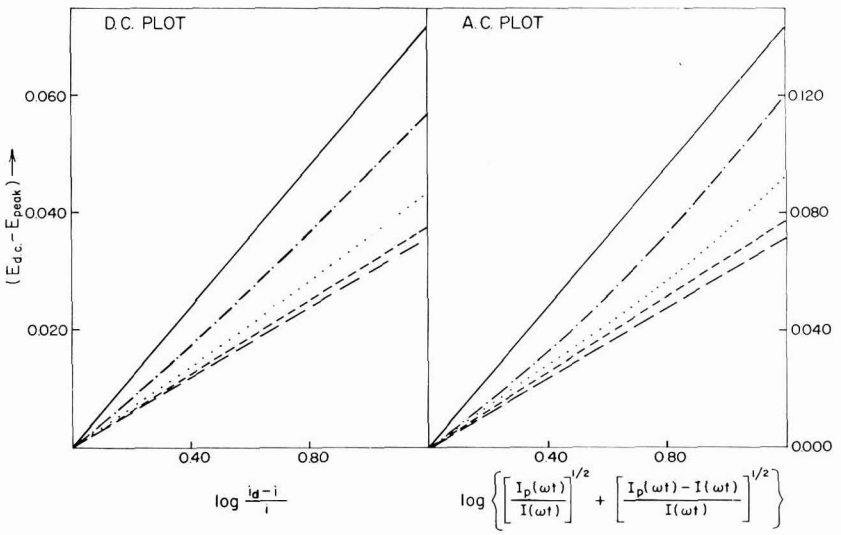

Fig. 9. A.c. and d.c. polarographic current–potential plots. (———), single-step mechanism, $n = 1$; (— —), single-step mechanism, $n = 2$; (·····), two-step mechanism, $E^r_{\frac{1}{4},1} - E^r_{\frac{1}{4},2} = 0.000$; (. . . .), two-step mechanism, $E^r_{\frac{1}{4},1} - E^r_{\frac{1}{4},2} = -0.050$; (– – – –), two-step mechanism, $E^r_{\frac{1}{4},1} - E^r_{\frac{1}{4},2} = -0.100$.

ACKNOWLEDGEMENT

The authors are indebted to the National Science Foundation for support of this work and to the Northwestern University Computing Center for generous donation of computer time.

SUMMARY

A theory is given for the a.c. polarographic wave with two-step charge transfer in which the overall electrode process is controlled kinetically solely by diffusion (the "reversible" or "Nernstian" case). Topics discussed are: (a) a method of derivation applicable to fundamental and higher harmonic alternating currents; (b) predictions of equations; (c) conditions under which diffusion-controlled two-step and single-step mechanisms are distinguishable; (d) the relative sensitivity of d.c. and a.c. methods to differences between single-step and two-step mechanisms; (e) methods of calculating standard potentials from a.c. polarographic data.

APPENDIX

Notation definitions

C_i	= concentration of species i.
C_i^*	= initial concentration of species i.
$C_{i_{x=0}}$	= surface concentration of species i.
D_i	= diffusion coefficient of species i.
f_i	= activity coefficient of species i.
x	= distance from electrode surface.
t	= time.
u	= dummy variable of integration.
ω	= angular frequency.
F	= Faraday's constant.
T	= absolute temperature.
R	= ideal gas constant.
A	= electrode area.
n_1, n_2	= number of electrons transferred in first and second reduction steps, respectively.
E_1^0, E_2^0, E_3^0	= standard redox potentials in European convention for O–Y, Y–R and O–R couples, respectively.
$E_{\frac{1}{2},1}^r$, $E_{\frac{1}{2},2}^r$, $E_{\frac{1}{2},3}^r$	= reversible half-wave potentials (planar diffusion) corresponding to O–Y, Y–R and O–R couples, respectively.
$E(t)$	= instantaneous value of applied potential.
$E_{d.c.}$	= d.c. component of applied potential.
ΔE	= amplitude of applied alternating potential.
$i(t)$	= total faradaic current.
$i_1(t)$, $i_2(t)$	= faradaic current due to first and second reduction steps, respectively.
$I(\omega t)$	= fundamental harmonic faradaic alternating current.
$I_p(\omega t)$	= peak fundamental harmonic faradaic alternating current.
$I(2\omega t)$	= second harmonic faradaic alternating current.
$i_{d.c.}$	= "normal" d.c. faradaic current (d.c. polarographic current).
$I_{d.c.}$	= d.c. faradaic rectification component.

REFERENCES

1 A. A. VLČEK, *Progress in Inorganic Chemistry*, Vol. 5, edited by F. A. COTTON, Interscience, New York, 1963, pp. 211–384.
2 T. BERZINS AND P. DELAHAY, *J. Am. Chem. Soc.*, 75 (1953) 5716.
3 H. A. LAITINEN AND S. WAWZONEK, *J. Am. Chem. Soc.*, 64 (1942) 1765.
4 K. J. VETTER AND G. THIEMKE, *Z. Elektrochem.*, 64 (1960) 805.
5 D. M. MOHILNER, *J. Phys. Chem.*, 68 (1964) 623.
6 K. J. VETTER, *Z. Naturforsch.*, 79 (1952) 328; 89 (1953) 823.
7 R. M. HURD, *J. Electrochem. Soc.*, 109 (1962) 327.
8 H. MAUSER, *Z. Elektrochem.*, 62 (1958) 419.
9 A. C. RIDDIFORD, *J. Chem. Soc.*, (1960) 1175.
10 R. BRDIČKA, *Z. Elektrochem.*, 47 (1941) 314.
11 O. H. MÜLLER, *Ann. N. Y. Acad. Sci.*, 40 (1940) 91.
12 T. BERZINS AND P. DELAHAY, *J. Am. Chem. Soc.*, 75 (1953) 4205.
13 A. C. TESTA AND W. H. REINMUTH, *Anal. Chem.*, 33 (1961) 1320.
14 J. M. HALE, *J. Electroanal. Chem.*, 8 (1964) 181.

15 J. M. HALE, *J. Electroanal. Chem.*, 8 (1964) 408.
16 H. B. HERMAN AND A. J. BARD, *Anal. Chem.*, 36 (1964) 971.
17 D. G. PETERS AND J. J. LINGANE, *J. Electroanal. Chem.*, 2 (1961) 249.
18 H. HURWITZ, *J. Electroanal. Chem.*, 2 (1961) 328.
19 R. W. MURRAY AND C. N. REILLEY, *J. Electroanal. Chem.*, 3 (1962) 182.
20 P. DELAHAY, *New Instrumental Methods in Electrochemistry*, Interscience, New York, 1954.
21 Y. P. GOKHSTEIN AND A. Y. GOKHSTEIN, *Advances in Polarography*, Vol. 2, edited by I. S. LONGMUIR, Pergamon, New York, 1960, pp. 465–481.
22 J. KOUTECKÝ, *Proc. Intern. Polarog. Cong., Prague*, 1 (1951) 826.
23 M. SMUTEK, *Collection Czech. Chem. Commun.*, 18 (1953) 171.
24 M. G. EVANS AND N. S. HUSH, *J. Chim. Phys.*, 49 (1952) C159.
25 K. EBATA, *Tohoku Univ. Science Reports*, 47 (1964) 191.
26 O. DRAČKA, *Collection Czech. Chem. Commun.*, 28 (1963) 3194.
27 I. TACHI AND M. SENDA, *Advances in Polarography*, Vol. 2, edited by I. S. LONGMUIR, Pergamon, New York, 1960, pp. 454–464.
28 A. C. TESTA AND W. H. REINMUTH, *J. Am. Chem. Soc.*, 83 (1961) 784.
29 G. S. ALBERTS AND I. SHAIN, *Anal. Chem.*, 35 (1963) 1859.
30 L. HOLLECK AND R. SCHINDLER, *Z. Elektrochem.*, 60 (1956) 1138.
31 M. SUZUKI, *Mem. Coll. Agr. Kyoto Univ.*, 67 (1954).
32 R. S. NICHOLSON AND I. SHAIN, *Anal. Chem.*, 37 (1965) 178, 190.
33 D. E. SMITH, *Advances in Electroanalytical Chemistry*, Vol. 1, edited by A. J. BARD, M. Dekker, Inc., New York, in press.
34 H. L. HUNG AND D. E. SMITH, *J. Electroanal. Chem.*, 11 (1966) 425.
35 P. DELAHAY, *Advances in Electrochemistry and Electrochemical Engineering*, Vol. 1, edited by P. DELAHAY AND C. W. TOBIAS, Interscience, New York, 1961, chap. 5.
36 J. R. DELMASTRO AND D. E. SMITH, *J. Electroanal. Chem.*, 9 (1965) 192.
37 L. I. SCHIFF, *Quantum Mechanics*, McGraw-Hill, New York, 1955, p. 45.
38 H. MATSUDA, *Z. Elektrochem.*, 61 (1958) 977.
39 D. E. SMITH, *Anal. Chem.*, 35 (1963) 602.
40 W. B. SCHAAP AND P. S. MCKINNEY, *Anal. Chem.*, 36 (1964) 29.
41 M. T. KELLEY, H. C. JONES AND D. J. FISHER, *Anal. Chem.*, 31 (1959) 1475; 32 (1960) 1262.

A GENERAL EQUATION FOR THE DESCRIPTION OF REDOX TITRATION CURVES

JAMES A. GOLDMAN
Department of Chemistry, Polytechnic Institute of Brooklyn, N.Y. (U.S.A.)
(Received July 16th, 1965)

There has been recently[1,2] a re-investigation of the properties of equations used for the representation of the potential change occurring during the progress of a redox titration. BISHOP[1] proposed a method which took into account the reaction deficiency and thereby permitted a rigorous calculation of the potential during the entire course of a titration. As he emphasized, the results of such a method of calculation show explicitly that the entire titration curve is a continuous monotonically changing function of the fraction titrated although the usual procedure[3,4] is one in which the potential before the equivalence point is calculated from the Nernst expression for the reductant system, whereas after the equivalence point, the Nernst expression for the oxidant (used as the titrant) is employed; at the equivalence point a separate equation is required[2-6]. NIGHTINGALE[7] has presented some rigorously derived expressions for the concentration variation of species present in a redox system as a function of potential, but no explicit comparison was made between his results and the common procedure for the calculation of a redox titration curve.

It is shown here that for all except inhomogeneous[2,5] reactions, it is possible to derive an equation describing the entire redox titration curve. The resulting equation is then compared with the more commonly used expressions.

THE DERIVATION OF THE GENERAL EQUATION

Let us consider the following two reversible redox systems:

$$a\mathrm{Ox}_1 + n_1\varepsilon = c\mathrm{Red}_1 \tag{1}$$

$$d\mathrm{Ox}_2 + n_2\varepsilon = b\mathrm{Red}_2 \tag{2}$$

for which the respective Nernst expressions are

$$E = E_1^{0\prime} - \frac{RT}{n_1 F} \ln \frac{[\mathrm{Red}_1]^c}{[\mathrm{Ox}_1]^a} \tag{3}$$

and

$$E = E_2^{0\prime} - \frac{RT}{n_2 F} \ln \frac{[\mathrm{Red}_2]^b}{[\mathrm{Ox}_2]^d} \tag{4}$$

where $E^{0\prime}$ represents the formal potential of the indicated couple, R, T and F have their usual significance, and the concentrations of all species are expressed in moles l^{-1}.

If we consider the titration of Red_2 with Ox_1 as the titrant, then the chemical equation representing the titration reaction is

$$ax Ox_1 + by Red_2 = cx Red_1 + dy Ox_2 \tag{5}$$

where[1,2] $n_1 x = n_2 y$. From eqn. (5) it is readily seen that throughout the entire course of the titration

$$[Red_1] = \frac{cx}{dy}[Ox_2] \tag{6}$$

The equivalence point may be defined in the following manner:

$$C_1^0 q = \frac{ax}{by} C_2^0 V^0 \tag{7}$$

where C_2^0 is the initial stoichiometric (analytical) molar concentration of Red_2 and C_1^0 is the stoichiometric molar concentration of the titrant; q is the volume (ml) of titrant necessary to reach the equivalence point in the titration of V^0 ml of solution originally containing Red_2.

The application of material balance considerations to the species involved in each couple is accomplished by the following equations (where V is the volume of titrant added):

$$\frac{C_1^0 V}{V^0 + V} = [Ox_1] + \frac{a}{c}[Red_1] \tag{8}$$

and

$$\frac{C_2^0 V^0}{V^0 + V} = [Red_2] + \frac{b}{d}[Ox_2] \tag{9}$$

which may be rewritten as

$$\frac{C_1^0 V}{V^0 + V} = [Red_1]\left\{\frac{[Ox_1]}{[Red_1]} + \frac{a}{c}\right\} \tag{10}$$

and

$$\frac{C_2^0 V^0}{V^0 + V} = [Ox_2]\left\{\frac{[Red_2]}{[Ox_2]} + \frac{b}{d}\right\} \tag{11}$$

Division of eqn. (10) by eqn. (11), accompanied by appropriate substitution of eqn. (6) yields

$$\frac{C_1^0 V}{C_2^0 V^0} = \frac{cx}{dy}\,\frac{\dfrac{a}{c} + \dfrac{[Ox_1]}{[Red_1]}}{\dfrac{b}{c} + \dfrac{[Red_2]}{[Ox_2]}} \tag{12}$$

Now, from eqn. (7) it is evident that $C_1^0/C_2^0 V^0 = (ax/by)/q$, and by definition the fraction titrated, f, is equal to V/q, so that eqn. (12) may be rewritten as

$$f = \frac{bc}{ad}\,\frac{\dfrac{a}{c} + \dfrac{[Ox_1]}{[Red_1]}}{\dfrac{b}{d} + \dfrac{[Red_2]}{[Ox_2]}}$$

from which it may be verified that at $f=1$, $[Ox_1]=(ax/by)[Red_2]$, as is required by the stoichiometry of eqn. (5).

To obtain f as a function of the potential, it is now only necessary to substitute, by use of the Nernst equation, expressions for the indicated concentration ratios. To obtain $[Red_1]/[Ox_1]$ from eqn. (3), it is obvious that the only requirement is $a=c$, and, similarly, to obtain $[Red_2]/[Ox_2]$, it is only necessary that $b=d$. In this case then, $ad=bc$ so that the potential at the equivalence point will be independent of the concentrations of any species participating in the reaction[5]. Nevertheless, when $ad=bc$ it is possible that this is so because $a=b$ and $c=d$. In this situation, however, it will be impossible, using the present procedure, to obtain the required ratios as a function only of potential.

Therefore for situations where $a=c$, and $b=d$, eqn. (12) becomes

$$f = \frac{1 + \dfrac{[Ox_1]}{[Red_1]}}{1 + \dfrac{[Red_2]}{[Ox_2]}} \tag{13}$$

and eqns. (3) and (4) may be written as

$$E = E_1^{0'} - \frac{aRT}{n_1 F} \ln \frac{[Red_1]}{[Ox_1]}$$

and

$$E = E_2^{0'} - \frac{bRT}{n_2 F} \ln \frac{[Red_2]}{[Ox_2]}$$

which are the Nernst expressions for the corresponding half-reactions

$$Ox_1 + \frac{n_1}{a}\varepsilon = Red_1$$

$$Ox_2 + \frac{n_2}{b}\varepsilon = Red_2$$

so that for convenience we may make the following transformations: $n_1/a \rightarrow n_1$ and $n_2/b \rightarrow n_2$; then the formulation of the chemical equation representing the titration may be expressed as

$$n_2 Ox_1 + n_1 Red_2 = n_2 Red_1 + n_1 Ox_2 \tag{14}$$

According to BISHOP's categories[2] this would be the representation for homogeneous and symmetrical reactions.

Solution of the rewritten (subsequent to the above-mentioned transformation) Nernst expressions for the required concentration ratios and substitution of these into eqn. (13) yields

$$f = \frac{1 + \exp\left[\dfrac{n_1 F}{RT}(E - E_1^{0'})\right]}{1 + \exp\left[\dfrac{-n_2 F}{RT}(E - E_2^{0'})\right]} \tag{15}$$

By setting $f=1$, we obtain the equivalence point potential, E^*

$$E^* = \frac{n_1 E_1^{0'} + n_2 E_2^{0'}}{n_1 + n_2} \tag{16}$$

as expected[2-6].

The relationship between the equilibrium constant for the reaction represented by eqn. (14) and the formal potentials is

$$\Delta E^{0'} = E_1^{0'} - E_2^{0'} = \frac{RT}{n_1 n_2 F} \ln K \tag{17}$$

Let us consider the quantity $E - E_1^{0'}$. By addition and subtraction of E^* we may rewrite $E - E_1^{0'}$ as $(E - E^*) + (E^* - E_1^{0'})$. It is easily shown by use of eqn. (16) that $(E^* - E_1^{0'}) = -[n_2/(n_1 + n_2)]\,\Delta E^{0'}$. Thus

$$E - E_1^{0'} = (E - E^*) - [n_2/(n_1 + n_2)]\,\Delta E^{0'}$$

and it may be similarly shown that

$$E - E_2^{0'} = (E - E^*) + [n_1/(n_1 + n_2)]\,\Delta E^{0'}$$

Therefore it is convenient to rewrite eqn. (15) as

$$f = \frac{1 + [\exp(-n\delta)]\ [\exp(n_1\psi)]}{1 + [\exp(-n\delta)]\ [\exp(-n_2\psi)]} \tag{18}$$

where $\psi = (F/RT)\,(E - E^*)$, $\delta = (F/RT)\,\Delta E^{0'}$, and $n = n_1 n_2/(n_1 + n_2)$. If we express $\exp(-n\delta)$ by k, then eqn. (18) may be more simply written as

$$f = \frac{1 + k\exp(n_1\psi)}{1 + k\exp(-n_2\psi)} \tag{19}$$

The value of k, determined only by the value of n and K, remains constant throughout the course of any particular titration. It is readily seen that at $f=1$, $\psi=0$.

Therefore, either from eqn. (15) or (19), it is possible, *during the entire course of the titration*, to calculate f as a function of E by use of a single continuous equation. The general validity of the principle that it is always possible to make a rigorous calculation of a titration curve by considering the concentration (or in this case, the potential) as the independent variable and f as the dependent one has been recently reiterated[8] and is now once again explicitly demonstrated for a case where *until now no expression has been presented.*

DISCUSSION

It is of interest to compare the commonly used expressions with those obtainable from eqns. (15) or (19).

Let us first investigate the value of f at which $E = E_2^{0'}$. Using either eqn. (15) or (19) we obtain

$$f = \frac{1}{2} + \frac{1}{2}\exp(-n_1\delta) \quad \text{at } E = E_2^{0'} \tag{20}$$

which shows that f *is never exactly equal* to $\frac{1}{2}$ at $E = E_2^{0'}$ and that the actual value of f at this point is always greater than $\frac{1}{2}$.

Similarly, we obtain

$$f = \frac{2}{1+\exp(-n_2\delta)} \quad \text{at } E = E_1^{0'} \tag{21}$$

so that the value of f at this point is *always less* than 2. These statements are true *even* for symmetrical reactions. For given values of n_1 and n_2, the larger the value of δ, *i.e.*, the larger the difference between the two formal potentials, the smaller is the magnitude of the exponential term in eqns. (20) and (21), and the more nearly do the values of f correspond to those predicted by simple theory[4]. Values of f calculated by the use of eqns. (20) and (21), are presented in Table 1.

TABLE 1

VALUES OF f AT $E = E_2^{0'}$ AND AT $E = E_1^{0'}$ (AT 25°)

$p\Delta E^{0'}$ (mV)	f at $E = E_2^{0'}$	f at $E = E_1^{0'}$
50	0.5715	1.866
100	0.5102	1.980
150	0.5015	1.997
200	0.5002	1.9996
250	0.50003	1.99994
300	0.500004	1.999991

The first column lists values of $p\Delta E^{0'}$ where p represents the number of electrons, and $\Delta E^{0'}$ is the difference in formal potentials, $(F/RT)\Delta E^{0'} = \delta$. The second and third columns list the values of f at $E = E_2^{0'}$ and $E = E_1^{0'}$, respectively. If $p = 1$, then the values of f pertain to the values of $\Delta E^{0'}$ listed in the first column. If $p = 2$, then for $\Delta E^{0'} = 50$, the second entry in the first column must be used, *viz.*, that for $p\Delta E^{0'} = 100$ mV.

The relationship between eqn. (15) and those expressions commonly used for the calculation of E is not immediately evident and is, therefore, worthy of consideration.

For values of $f < 1$, *i.e.*, prior to equivalence, it is convenient to solve eqn. (15) for the quantity $(E - E_2^{0'})$, anticipating that the exponential term in the numerator will be small compared to unity.

Thus eqn. (15) may be rewritten as

$$E - E_2^{0'} = -\frac{RT}{n_2F} \ln \left\{ \frac{1-f}{f} + \frac{1}{f} \exp\left[\frac{n_1 F}{RT} (E - E_1^{0'}) \right] \right\}$$

Making use of the relationship: $E - E_1^{0'} = (E - E_2^{0'}) + (E_2^{0'} - E_1^{0'}) = (E - E_2^{0'}) - \Delta E^{0'}$, we may then write

$$E - E_2^{0'} = -\frac{RT}{n_2F} \ln \left\{ \frac{1-f}{f} + \frac{1}{f}\left[\exp(-n_1\delta)\right] \left[\exp \frac{n_1F}{RT}(E - E_2^{0'}) \right] \right\} \tag{22}$$

This expression is mathematically exact and is rigorously derived from eqn. (15) but it shows more clearly the relationship between the common form and the exact one. Equation (22) may serve for the calculation of the true value of $E - E_2^{0'}$ by successive approximations by first assuming that $E - E_2^{0'} = -(RT/n_2F) \ln \{(1-f)/f\}$ and then using the value obtained to re-evaluate the argument of the logarithm. However, this

is a tedious process because even at $f=0.98$, the calculated values converge slowly. At 30° (2.30 $RT/F=60.2$ mV), for $\Delta E^{0\prime}=200$ mV, the first approximation yields a value for $E-E_2^{0\prime}$ of 101.8 mV which when resubstituted into eqn. (22), yields a value of 81.4. Using the average (in order to increase the rate of convergence) of these two values, namely 91.6, a value of 86.4 is obtained for the left-hand side of eqn. (22). The average of this and the immediately antecedent value is 89.0, which upon substitution into eqn. (22) leads to $E-E_2^{0\prime}=87.5$. Using the value of 88.2 ($=\frac{1}{2}$ [87.5 + 89.0)), we obtain 87.9 which averaged with 88.2 is 88.0. With this value, eqn. (22) yields a value of 87.97 or 88.0 mV, as found by BISHOP[1]. The number of calculations is considerably increased if an average of two successive values is not used. Indeed, the nearer the value of f is to unity, the greater is the necessity to do this. For example at $f=0.9999$, the first approximation leads to a value of 240.8 mV which when resubmitted into eqn. (22) yields a value of −40.8 mV. Now fortuitously, the average of these two consecutively calculated values is 100.0 mV, which is the true value[1]. However, if the value −40.8 mV is used in eqn. (22) the left-hand side gives −22.5 mV which will then yield a value of 222.5 mV, so that convergence to 100 mV is very slow. Yet it is interesting to note that again the average of these two consecutively calculated values is also 100.0. Nevertheless, there is really no need to use the method of successive approximations when there is readily available an equation relating f to E, *i.e.*, eqn. (15) or (19), by which f may be easily calculated for each value of E.

It should be noted that BISHOP's formulation[1], where the reaction deficiency must be calculated, involves the solution of a quadratic equation even for a symmetrical ($n_1=n_2$) reaction, whereas for a homogeneous reaction his equation is of the fifth order and must be solved by successive approximations. However, by use of the equations presented here it is no more difficult to calculate f as a function of E for homogeneous than for symmetrical reactions. BISHOP's[1] method can be applied to inhomogeneous equations but then the equation used to determine the reaction deficiency will be always greater than third order. It should be emphasized that eqns. (15) and (19) apply to all redox reactions (represented by eqn. (14)) except inhomogeneous ones.

For $f>1$, we may derive an equation analogous to eqn. (22):

$$E-E_1^{0\prime} = \frac{RT}{n_1 F} \ln \left\{(f-1)+f \exp\left[\frac{-n_2 F}{RT}(E-E_2^{0\prime})\right]\right\}$$

which may be rewritten as

$$E-E_1^{0\prime} = \frac{RT}{n_1 F} \ln \left\{(f-1)+f\left[\exp(-n_2\delta)\right]\left[\exp \frac{-n_2 F}{RT}(E-E_1^{0\prime})\right]\right\} \qquad (23)$$

since $E-E_2^{0\prime}$ may be expressed as $(E-E_1^{0\prime})+(E_1^{0\prime}-E_2^{0\prime})$ or, therefore, as $(E-E_1^{0\prime})+\Delta E^{0\prime}$. Equation (23) may be used as a basis for calculation by the method of successive approximations for the portion of the curve subsequent to the equivalence point.

SUMMARY

An equation is presented for the description of the entire titration curve obtained in homogeneous and symmetrical redox reactions. This equation permits the

rigorous calculation of the progress of the titration from the corresponding value of the potential. The form of the equation is investigated in detail at some points of interest. Also discussed, is the relationship between the exact form of the equation and the commonly used equations.

REFERENCES

1 E. BISHOP, *Anal. Chim. Acta*, 26 (1962) 397.
2 E. BISHOP, *Anal. Chim. Acta*, 27 (1962) 253.
3 E. BISHOP, *Theory and Principles of Titrimetric Analysis*, Vol. IB, *Comprehensive Analytical Chemistry*, edited by C. L. WILSON AND D. W. WILSON, Elsevier, Amsterdam, 1960.
4 I. M. KOLTHOFF AND N. H. FURMAN, *Potentiometric Titrations*, Wiley, New York, 1931, chap. III.
5 U. A. TH. BRINKMAN, *Chem. Weekblad*, 59 (1963) 9.
6 A. J. BARD AND S. H. SIMONSEN, *J. Chem. Educ.*, 37 (1960) 364.
7 E. R. NIGHTINGALE, Jr., *Anal. Chem.*, 30 (1958) 267.
8 J. A. GOLDMAN AND L. MEITES, *Anal. Chim. Acta*, 30 (1964) 28.

SPONTANEOUS VOLTAMMETRY AND VOLTAMMETRIC TITRATIONS

YECHESKEL ISRAEL AND AVRAHAM VROMEN
Israel Mining Industries, Institute for Research and Development, Haifa
(Received June 5th, 1965)

Direct voltammetric determinations, with the dropping mercury electrode at a constant applied voltage, have been previously described for Cu(II)[1], Ag(I)[2] and Hg(II)[3]. In the work presented here, similar determinations using a cell without an external applied voltage, by short-circuiting the two electrodes in the cell are described. The voltage of a cell, E_{cell}, at zero current and ignoring liquid-junction potential, is given by*

$$E_{cell} = E_c - E_a \qquad \text{(a)}$$

where E_c and E_a are, respectively, the cathode and anode potentials. For the cell to be spontaneous, the free energy of the cell has to be negative, or E_{cell} is positive. If the working electrode for a reversible system is the cathode, then from eqn. (a), E_c must be positive, or the cathode reaction should take place at a more positive potential than the potential of the reference electrode (Fig. 1, curve a). Similarly, when the working electrode is the anode, the reaction should occur at a more negative potential than that of the reference electrode (Fig. 1, curve b). At equilibrium, the voltage of such a cell (ignoring iR drop) is zero. The potential of the large non-polarizable reference electrode remains unchanged, while the small working electrode is easily

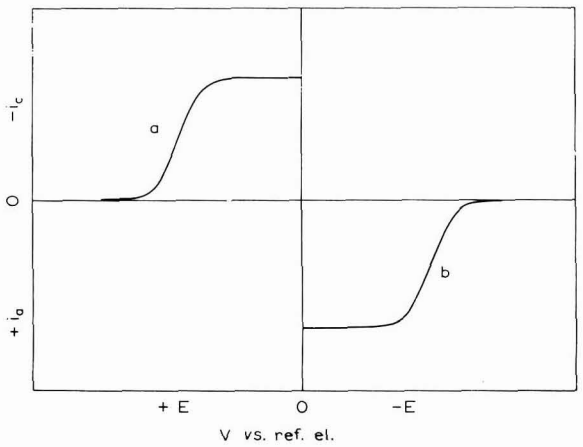

Fig. 1. Schematic voltammograms of substances determinable at zero applied voltage: (a), reducible; (b), oxidizable.

* Conforming with the conventions established by I.U.P.A.C. at its 1953 meeting in Stockholm.

polarized to the potential of the reference electrode, or

$$(E_{\text{w.e.}})_{\text{eq}} = E_{\text{ref}} = E^0{}_{O,R} - \frac{RT}{nF} \ln \left[\frac{(a_R)_{x=0}}{(a_O)_{x=0}}\right]_{\text{eq}} \qquad \text{(b)}$$

where $E^0{}_{O,R}$ is the standard potential of the redox couple at the working electrode, w.e. (which is a dropping-mercury electrode or a rotating-platinum electrode), $(a_R)_{x=0}$ and $(a_O)_{x=0}$ are, respectively, the activities of the reductant and oxidant at the electrode surface, and the subscript, eq, denotes equilibrium conditions. The current flowing through the cell under these conditions, corresponds to the potential of the reference electrode. If this potential is located at the plateau of the limiting current of the voltammogram of an active constituent, a current-measuring device will indicate a value proportional to its concentration. The determination of an irreversible active constituent is also possible when the current–potential curves simulate the voltammograms obtained in Figs. 1a and 1b, at the potential of the reference electrodes in use, the waves become diffusion-controlled (or the rate of electron-transfer at the electrodes is fast enough not to be a determining factor). This method is rapid and involves the simplest instrumental set-up. It has the following advantages over the "internal electrolysis" method[4]:

(1) Equilibrium is attained instantaneously on the surface of the small electrode and stoichiometric bulk reduction is avoided.

(2) The current which has a constant value is measured instead of the total quantity of electricity (or gravimetric measurement).

The application of direct voltammetric determinations for Hg(II), Ag(I), cyanide and EDTA ions was investigated. Special attention was devoted to voltammetric titrations at zero applied voltage with the D.M.E. (except for the case of titration of ferrous ion with permanganate where R.P.E. was used). KOLTHOFF AND HARRIS[5] applied this principle to the titration of mercaptans in ammoniacal medium with silver nitrate using a mercury–mercuric iodide–potassium iodide reference electrode (−0.23 V *vs.* S.C.E.). RINGBOM AND WILKMAN[6] titrated aluminum with fluoride ion with ferric iron as the indicator, and using the S.C.E. as a reference electrode at zero applied voltage. EWING[7], HARRIS[8] and MEITES[9] have listed a number of reference electrodes in the range +0.4 to −1 V *vs.* S.C.E., that can be used for the above titrations. In principle, most amperometric titration methods can be performed at zero applied voltage by a proper choice of the reference electrode. However, only titrations at positive enough potentials, where oxygen does not interfere, were chosen to further speed and simplify the procedures. Titrations were usually performed between a titrated sample and a titrant where one produces an anodic current and the other a cathodic current or *vice versa* at zero applied voltage. The instantaneous current, before the end-point, was not the result of direct compensation of anodic and cathodic currents, such as described by KOLTHOFF AND MILLER[10] and by LINGANE[11], but due to the following chemical processes:

(1) Direct complexation, such as the titration of Hg(II) with ethylenediaminetetraacetic acid and *vice versa*.

(2) Indirect complexation, such as the titration of Ag(I) with ethylenediaminetetraacetic acid.

(3) Oxidation–reduction, such as the titration of ferrous ion with permanganate ion.

(4) Precipitation, such as the titration of cyanide ion with Ag(I).

It will be shown that to obtain a stoichiometric end-point, the compensation of current, due to the titrated constituent and the titrant before and up to the end-point, should occur *via* chemical reaction in the bulk of solution. If the chemical reaction occurs, however, at the surface of the electrode (such as the indirect titration in case 2) stoichiometry is not observed, and the end-point depends on the ratio of the diffusion current constants.

EXPERIMENTAL

The cell used for direct measurements and titrations consisted of three separate round-mouthed 100-ml beakers with two agar–potassium chloride bridges (or agar–potassium nitrate, when chloride ions were undesirable)[12] serving as the conducting media between the beakers. One of the beakers contained the reference electrode having one of the following compositions:

	Approximate potential (V vs. N.H.E.)
Hg/Hg_2Cl_2 (satd.), KCl (satd.) (S.C.E.)	+0.25
Hg/Hg_2Cl_2 (satd.), KCl (1.5 *F*)	+0.26
Hg/Hg_2Cl_2 (satd.), KCl (0.016 *F*), KNO_3 (2.0 *F*)	+0.40
Hg/Hg_2SO_4 (satd.), K_2SO_4 (satd.)	+0.65

The second beaker contained saturated potassium chloride solution (or saturated potassium nitrate solution when chloride ions were undesirable). The third beaker had a D.M.E. (or R.P.E.) immersed in the solution of interest. The cell was thermostatted at a temperature of $25 \pm 0.05°$ for direct voltammetric determinations, but titrations were performed at room temperature. The cell was short-circuited through a Hartmann–Braun galvanometer model HLM 3 with five sensitivity stages. Each scale division equalled 0.005 μA at the highest sensitivity; other scale divisions were: 0.05, 0.5, 5.0 and 50 μA/scale division. The average of maximum and minimum readings of the galvanometer deflections was corrected for the average reading of the blank for direct determinations, while for the various titrations these readings were also corrected for dilutions, multiplying by $(V_0+V_t)/V_0$, where V_0 is the initial volume of the titrated sample and V_t the volume of titrant added to the titration cell. A Radiometer Type PO4 Polariter (pen-recording polarograph) was used for preliminary investigations to determine the most suitable conditions for direct determinations and titrations. When required, the pH of solutions was checked and regulated using a Radiometer Model 22 pH meter. A locally constructed R.P.E. rotating at a speed of 400 rev./min. was used, similar to the arrangement suggested by KOLTHOFF AND HARRIS[5].

Analytical-grade reagents were employed and stock solutions of the following reagents were prepared and standardized:

(1) Silver nitrate, 0.1000 *F*, standardized against a standard 0.1000 *F* solution of sodium chloride (Titrisol Merck).

(2) Disodium salt of ethylenediaminetetraacetic acid (EDTA or Y^{-4}), 0.01000 F, standardized against a standard solution of Zn(II) in the presence of Eriochrome Black indicator or a standard solution of Ca(II) in the presence of Murexide indicator.

(3) Mercuric chloride, 0.02010 F, standardized by adding excess of a standard solution of EDTA and back-titrating the excess with a standard solution of Zn(II)[13].

(4) Potassium cyanide, 0.0996 F, standardized by the addition of an excess of a standard solution of Ni(II) and back-titration with a standard solution of EDTA[13].

(5) Ferrous ammonium sulfate, 0.00991 F, standardized with a standard solution of permanganate.

(6) Potassium permanganate, 0.02000 F, standardized by the arsenious oxide and the oxalate methods.

Fresh dilutions of stock solutions were made immediately before determinations. A McIlvaine buffer was used and sodium citrate–citric acid buffer solutions were prepared by adding 0.1 F citric acid to a 0.1 F solution of sodium citrate to the desired pH. Similarly, trisodium phosphate–disodium phosphate buffer solutions were prepared by adding 0.1 F trisodium phosphate solution to 0.1 F disodium phosphate solution to the desired pH.

RESULTS AND DISCUSSION

I. Direct voltammetric determination

(a) Determination of Hg(II). To determine mercuric ion in a non-complexing medium, a 0.2 F solution of potassium nitrate was chosen as a supporting electrolyte since KOLTHOFF AND MILLER[14] have described the reduction of mercuric chloride at the D.M.E. in this solution as supporting electrolyte. The mercuric chloride in the vicinity of the dropping electrode is quantitatively converted into calomel according to the expression:

$$HgCl_2 + Hg \rightarrow Hg_2Cl_2 \qquad (1)$$

and the reduction wave is due to the reduction of calomel:

$$Hg_2Cl_2 + 2\,e \rightarrow Hg + 2\,Cl^- \qquad (2)$$

The apparent half-wave potential (H.W.P.) of the reduction step was shifted to more negative potentials as the concentration of mercuric chloride was increased, but the limiting-current plateau was already developed for all the concentrations in Table 1, using agar–KNO_3 bridges and Hg/Hg_2Cl_2 (satd.), KCl (1.5 F) reference electrode. The wave had a large maximum, which was not suppressed satisfactorily by gelatin or Triton X-100. It was suppressed by methylene blue but the wave was then affected by the reduction of methylene blue at the D.M.E. at fairly positive potentials[13]. Methyl red (0.0005%), first suggested by KOLTHOFF AND MILLER[14], was an effective maximum suppressor. The results obtained in this medium in the range $1 \cdot 10^{-5}$–$4 \cdot 10^{-3}$ M of $HgCl_2$ are summarized in Table 1. The dependence on concentration is shown to be satisfactory and the mean deviation for this concentration range was better than $\pm 0.8\%$. Under similar conditions, satisfactory results were also obtained using 0.2 F potassium sulfate and 0.0005% methyl red base solution, but the results are not reported.

TABLE 1

DIRECT DETERMINATION OF MERCURIC ION USING 0.2 F KNO_3 AND 0.0005% METHYL RED SUPPORTING ELECTROLYTE

Concn. (M)	*μA**	*μA (corr.)*	*μA/mM*
blank	0.05175 (anodic)	—	—
$1 \cdot 10^{-5}$	0.02815	0.0799	7.990
$2 \cdot 10^{-5}$	0.1000	0.1518	7.590
$5 \cdot 10^{-5}$	0.3273	0.3791	7.582
$1 \cdot 10^{-4}$	0.7213	0.7730	7.730
$2 \cdot 10^{-4}$	1.440	1.492	7.459
$5 \cdot 10^{-4}$	3.715	3.768	7.534
$1 \cdot 10^{-3}$	7.675	7.727	7.727
$2 \cdot 10^{-3}$	15.18	15.23	7.614
$4 \cdot 10^{-3}$	30.44	30.49	7.623

Agar–potassium nitrate bridges and Hg/Hg_2Cl_2 (satd.), KCl (1.5 F) reference electrode
$m^{2/3}t^{1/6} = 1.834$ mg$^{2/3}$ sec$^{-1/2}$
$i_d/c = 7.610 \pm 0.055$ μA/mM

$$I = \frac{7.610}{1.834} = 4.150 \pm 0.030\ \mu\Lambda\ \mathrm{m}M^{-1}\ \mathrm{mg}^{-2/3}\ \mathrm{sec}^{1/2}$$

* Average of two readings

(b) Determination of Ag(I). In non-complexing media, Ag(I) oxidizes metallic mercury to mercurous ion at the surface of the mercury electrode. This reaction may proceed considerably in spite of the smallness of the difference between the standard potentials of Ag^+/Ag and Hg_2^{2+}/Hg couples ($E^0_{Ag^+,Ag} = 0.799$ and $E^0_{Hg_2^{2+},Hg} = 0.792$ V *vs.* N.H.E.). This is due to the favourable initial composition of both couples and the reduction of mercurous ion alone or together with silver ion in non-complexing media at the dropping electrode surface. 0.2 F potassium sulfate containing 0.0005% methyl red base solution was used and measurements were made against Hg/Hg_2Cl_2 (satd.), KCl (1.5 F) reference electrode with agar–KNO_3 bridges. The results are

TABLE 2

DIRECT DETERMINATION OF Ag(I) ION USING 0.2 F K_2SO_4 AND 0.0005% METHYL RED SUPPORTING ELECTROLYTE

Concn. (M)	*Reading (μA)*	*i_d (μA)*	*i_d/C (μA/mM)*
blank	0.0360	—	—
$1 \cdot 10^{-5}$	0.0830	0.0470	(4.700)
$2 \cdot 10^{-5}$	0.1130	0.0770	3.850
$5 \cdot 10^{-5}$	0.2540	0.2180	4.360
$1 \cdot 10^{-4}$	0.4425	0.4065	4.065
$2 \cdot 10^{-4}$	0.8630	0.8270	4.135
$5 \cdot 10^{-4}$	2.050	2.014	4.028
$1 \cdot 10^{-3}$	4.146	4.110	4.110
$2 \cdot 10^{-3}$	8.486	8.450	4.225
$5 \cdot 10^{-3}$	21.52	21.48	4.296

Agar–potassium nitrate bridges and Hg/Hg_2Cl_2 (satd.), KCl (1.5 F) reference electrode
$m^{2/3}t^{1/6} = 1.826$ mg$^{2/3}$ sec$^{-1/2}$
$i_d/C = 4.134 \pm 0.121$ μA/mM (excluding $1 \cdot 10^{-5}$ M)
$I = 2.264 \pm 0.066$ μA mM^{-1} mg$^{-2/3}$ sec$^{1/2}$

summarized in Table 2, and show the dependence of current measurements on the concentration of Ag(I) for the range $1 \cdot 10^{-5}$–$5 \cdot 10^{-3}$ M. A mean deviation of better than $\pm 3\%$ was obtained (excluding only $1 \cdot 10^{-5}$ M Ag^+).

(c) Determination of cyanide ion. Cyanide ion depolarizes the D.M.E. to produce an anodic wave:

$$Hg + 2\,CN^- \rightarrow Hg(CN)_2 + 2\,e \tag{3}$$

KOLTHOFF AND MILLER[14] suggested the determination of cyanide ion in air-free solutions that contained sodium hydroxide to prevent loss of hydrocyanic acid by volatilization. However, the use of this base solution would have necessitated the employment of a more negative reference electrode than the S.C.E. and the de-aeration of the sample, in order to prevent the interference of the hydroxyl-ion oxidation wave of mercury—which is very high at the potential of the S.C.E. at high pH. Therefore, a base solution of lower pH but alkaline enough to prevent considerable loss of hydrocyanic acid, was thought to be more suitable for our purposes. The available concentration of free hydrocyanic acid from various concentrations of cyanide ion can be calculated on the basis of acid–base considerations. The reaction is given by

$$CN^- + H_2O \rightleftharpoons HCN + OH^-; \quad K_b = 2 \cdot 10^{-5} \tag{4}$$

$$K_b = \frac{[HCN]\,[OH^-]}{[CN^-]} \tag{c}$$

and in non-buffered solutions

$$K_b = \frac{[HCN]^2}{C^0_{CN^-} - [HCN]} \tag{d}$$

where $C_{CN^-}{}^0$ is the initial concentration of cyanide ion. The available concentration of hydrocyanic acid is calculated using eqn. (e)

$$[HCN] = \frac{-K_b + \sqrt{K_b^2 + 4\,K_b C_{CN^-}{}^0}}{2} \tag{e}$$

and the results are given in Table 3 for various concentrations of cyanide ion. It is clear that at low concentrations of cyanide ion such as 10^{-5} F, the bulk of cyanide ion is converted to hydrocyanic acid.

TABLE 3

CALCULATED CONCENTRATIONS OF FREE HYDROCYANIC ACID OF VARIOUS CONCENTRATIONS OF NON-BUFFERED CYANIDE SOLUTIONS

$C^0_{CN^-}$ (*F*)	[*HCN*] (*M*)
10^{-2}	$4.4 \cdot 10^{-4}$
10^{-3}	$1.31 \cdot 10^{-4}$
10^{-4}	$3.57 \cdot 10^{-5}$
10^{-5}	$7.30 \cdot 10^{-6}$

It is advantageous to determine cyanide ion in buffered solutions, since the ratio

[HCN] : [CN$^-$] is constant for various initial concentrations of cyanide ion at a specific pH:

$$\frac{[HCN]}{[CN^-]} = \frac{K_b}{[OH^-]} \qquad (e')$$

At a high pH the ratio becomes very small. For example at pH = 7, the ratio [HCN] : [CN$^-$] = 200, while at pH = 11 it is only 0.02. The available free hydroxyl-ion concentration is also not very high at pH = 11, and therefore a buffer solution of disodium phosphate–trisodium phosphate of pH *ca.* 11 was chosen for these determinations. Although the results obtained indicated that the direct current readings were proportional to concentrations, in the limited range given in Table 4, however, the mean deviation was *ca.* ±5%, and the accuracy obtained in a wider range of concentrations was even less satisfactory.

TABLE 4

DETERMINATION OF CYANIDE ION IN TRISODIUM PHOSPHATE–DISODIUM PHOSPHATE BUFFER OF pH 10.8

Concn. *(M)*	*Readings* *(μA)*	i_d *(μA)*	i_d/C *(μA/mM)*
blank	0.075	—	—
$2.00 \cdot 10^{-4}$	0.725	0.650	3.250
$3.50 \cdot 10^{-4}$	1.325	1.250	3.570
$5.00 \cdot 10^{-4}$	1.780	1.705	3.410
$7.00 \cdot 10^{-4}$	2.360	2.285	3.264
$8.00 \cdot 10^{-4}$	2.650	2.575	3.219
$1.00 \cdot 10^{-3}$	3.200	3.125	3.125
$1.20 \cdot 10^{-3}$	3.640	3.515	2.979
$1.40 \cdot 10^{-3}$	4.250	4.115	2.978

$i_d/C = 3.223 \pm 0.150\ \mu A\ mM^{-1}$

(d) Determination of EDTA. Although EDTA is not active at the R.P.E., it produces an anodic wave at the D.M.E., due to the oxidation of mercury

$$Hg + Y^{4-} \rightarrow HgY^{2-} + 2\,e \qquad (5)$$

MATYSKA, DOLEZAL AND ROUBALOVA[16] studied the polarographic behaviour of EDTA as a function of pH and found that the wave height did not change in the pH range 3–8, but decreased somewhat in the range 8–11. In this investigation, the half-wave potential of the oxidation step of EDTA, in citric acid–sodium citrate buffer of pH 7.5, was found to be *ca.* +0.05 V *vs.* S.C.E. for 10^{-3} *M* solution. Direct measurements of current against Hg/Hg_2Cl_2 (satd.), KCl (0.016 *F*), KNO_3 (2.0 *F*) reference electrode, indicated proportionality with concentration of EDTA, but the accuracy was very poor due to the narrow plateau of the diffusion current.

II. Voltammetric titrations

(a) Direct complexation titrations; Hg(II)–EDTA system. ROUBALOVA AND DOLEZAL[17] and CHARLOT *et al.*[18] have described the titration of EDTA with Hg(II) and *vice versa*. In the present work, titrations were performed in sodium citrate–citric acid buffer (total 0.1 *F*) of pH 7–8 against Hg/Hg_2Cl_2 (satd.), KCl (0.016 *F*),

KNO_3 (2.0 F) reference electrode, a potential that corresponds to the anodic diffusion current plateau of EDTA in this medium. This potential is also located at the diffusion current plateau of the cathodic wave of Hg(II). The volume at the end-point is expected to occur at a 1 : 1 molar ratio at the point of intersection of the titration curve with the zero current. The reaction before the end-point is:

$$Y^{4-} + Hg^{2+} \rightarrow HgY^{2-} \qquad (6)$$

An anodic or cathodic wave is produced depending on the reagent in excess. At the end-point, corresponding to a 1 : 1 molar ratio of EDTA and Hg(II), the only active constituent is HgY^{2-} (assuming species Y^{4-} and Hg^{2+} to be negligible or compensating each other) which is not reducible at the chosen potential; therefore no current flows through the cell. After the end-point, the excess of the titrant is the active

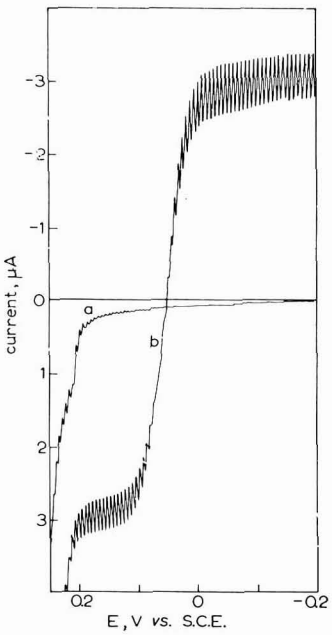

Fig. 2. Polarograms of sodium citrate–citric acid buffer (0.1 F total) pH 7.4. (a), alone; (b), $1.00 \cdot 10^{-3}$ M in EDTA and $5.05 \cdot 10^{-3}$ M in $HgCl_2$. Polarogram (b) displays approx. equal anodic and cathodic waves.

constituent and produces an anodic or cathodic current. Figure 2 is a polarogram of a solution 10^{-3} M in EDTA and $5 \cdot 10^{-4}$ M in Hg(II) using 0.1 F total concentration of sodium citrate–citric acid supporting electrolyte at pH 7.4. Figure 3a is obtained by titrating Hg(II) with EDTA under these conditions, while Fig. 3b is obtained by titrating EDTA with Hg(II); both yield satisfactory results indicating a 1 : 1 ratio. In Fig. 3a, some deviation from linearity was obtained before the end-point, but this did not seriously affect the location of the end-point.

(b) Indirect complexation titration; Ag(I) with EDTA. The titration of EDTA with Ag(I) cannot be performed using the R.P.E. due to the absence of any interaction

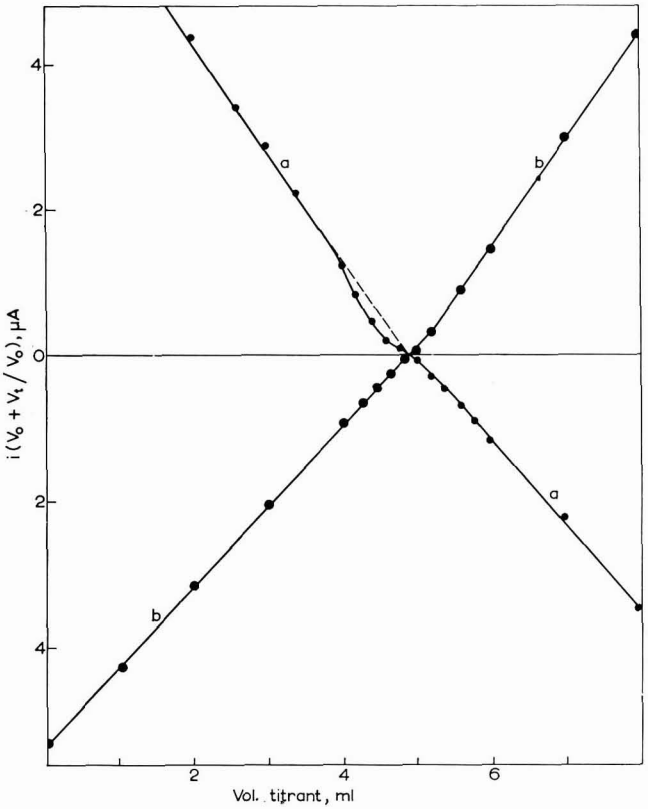

Fig. 3. Direct complexometric titrations with the D.M.E., using Hg/Hg_2Cl_2 (satd.), KCl (0.016 F), KNO_3 (2.0 F) and agar–potassium nitrate bridges in sodium citrate–citric acid buffer (0.1 F total) pH 7.5. (a), titration of 50 ml $1.01 \cdot 10^{-3}$ M $HgCl_2$ with $1.00 \cdot 10^{-2}$ M EDTA, vol. at end-point, 4.94 ml; (b), titration of 50 ml $1.00 \cdot 10^{-3}$ M EDTA with $1.01 \cdot 10^{-2}$ M $HgCl_2$, vol. at end-point, 4.96 ml.

between them, both in the bulk of solution and at the electrode surface. It can be carried out, however, using the D.M.E. and applying a potential corresponding to the plateau of the diffusion current of the anodic wave of EDTA. In this instance, the zero current does not correspond to the stoichiometric end-point and the results are similar to the case of compensation of currents described by KOLTHOFF AND MILLER[10] and by LINGANE[11], where the following relationship holds at the end-point when the current is zero:

$$n_1 V_1 C_1 D_1^{\frac{1}{2}} = n_2 V_2 C_2 D_2^{\frac{1}{2}} \qquad \text{(f)}$$

n_1 and n_2 are the number of electrons or atoms of the titrated sample and the titrant used, respectively, to account for stoichiometry of reactions at the electrode surface. V_1 is the volume of the titrated sample and V_2 the volume of the titrant at the end-point. C_1, C_2, D_1 and D_2 are the concentrations and the diffusion coefficients of the titrated sample and the titrant, respectively.

However, this titration does not represent merely a direct compensation of anodic and cathodic currents, since the following chemical reactions occur at the surface of the electrode during this titration:

$$2\,Ag^{+} + x\,Hg \rightarrow Hg_2^{2+} + Ag(Hg_{(x-2)}) \tag{7}$$

$$Hg_2^{2+} \rightleftharpoons Hg^{2+} + Hg \tag{8}$$

$$Hg^{2+} + Y^{4-} \rightarrow HgY^{2-} \tag{9}$$

The equilibrium constant in reaction (8) was reported by KOLTHOFF AND MILLER to be approximately 0.01[14], or in favour of the formation of Hg(I), but due to the presence of EDTA, reaction (9) shifts the equilibrium in (8) to the right. This view is supported by the chemical reaction between mercurous chloride and EDTA, where the dissolution of mercurous chloride and the formation of grey metallic mercury occur instantaneously. As these reactions take place at the surface of the electrode, the immediate neighbourhood of the electrode is depleted and both Ag(I) and EDTA will diffuse from the bulk of solution to the electrode surface, hence the dependence on $D^{\frac{1}{2}}$. Figure 4 is the titration curve of Ag(I) in sodium citrate–citric acid buffer (total 0.1 *F*) at pH 7, using Hg/Hg_2Cl_2 (satd.), KCl (0.016 *F*), KNO_3 (2.0 *F*) reference electrode. The molar ratio at zero current in this titration was 1 : 1.32, EDTA to Ag(I), while the ratio of the diffusion current constants in the same medium was 1 : 1.38.

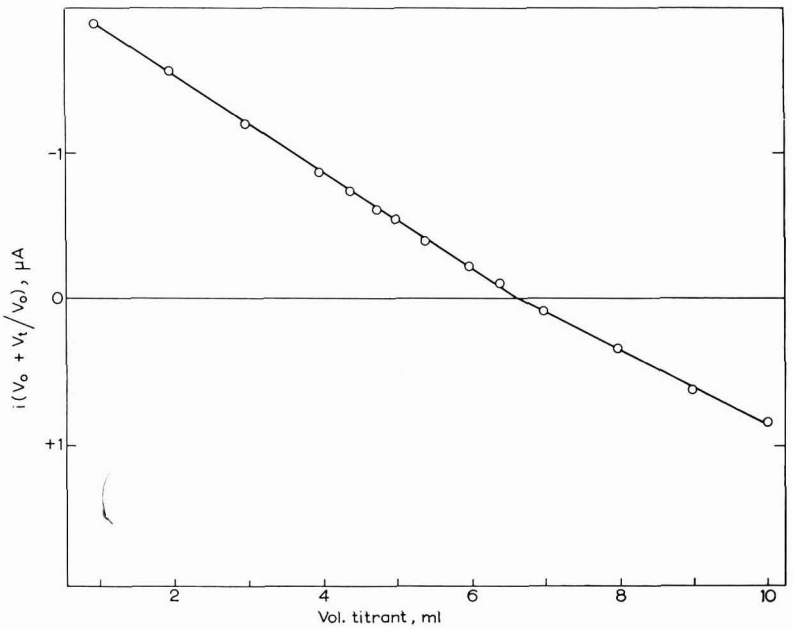

Fig. 4. Indirect complexometric titration with the D.M.E., of 50 ml $1.00 \cdot 10^{-3}$ *M* $AgNO_3$ with $5.00 \cdot 10^{-3}$ *M* EDTA, using Hg/Hg_2Cl_2 (satd.), KCl (0.016 *F*), KNO_3 (2.0 *F*) and agar–potassium nitrate bridges in sodium citrate–citric acid buffer pH 7; vol. at end-point, 6.60 ml.

(c) Oxidation–reduction titration; ferrous ion with permanganate. The titration of ferrous ion in 0.3 F sulfuric acid with permanganate was performed at the R.P.E., using Hg/Hg_2SO_4 (satd.), K_2SO_4 (satd.) reference electrode. The titration curve is different from those obtained previously, since this potential is located at the foot of the ferric–ferrous reduction and oxidation waves; thus a negligible contribution is obtained from either one before the end-point. Permanganate ion is reducible at the R.P.E. at this potential, therefore it contributes a large current after the end-point. Excellent accuracy was obtained in titrating 50-ml solutions of $5 \cdot 10^{-4}$ and $1 \cdot 10^{-3}$ M acid solutions of ferrous ion with $2 \cdot 10^{-3}$ M permanganate (Figs. 5a and 5b).

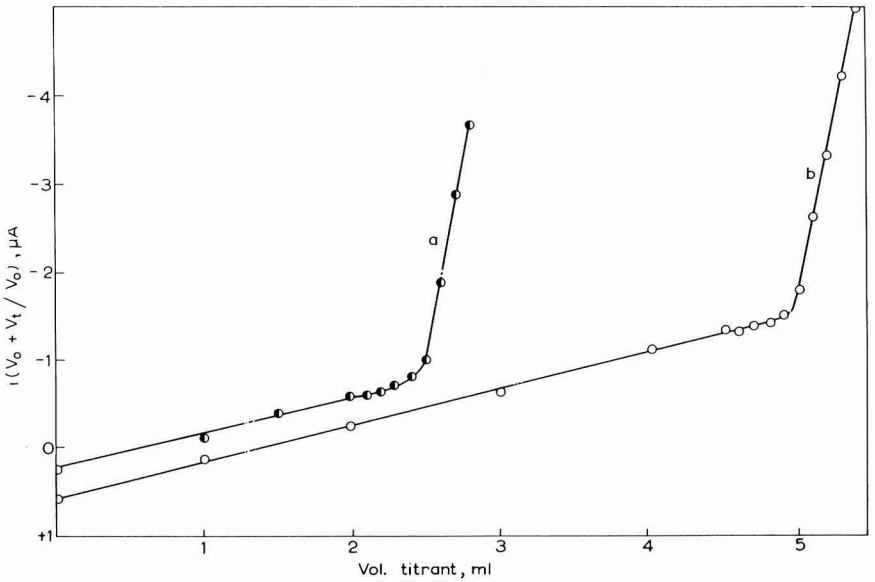

Fig. 5. Oxidation–reduction titration with the R.P.E., of ferrous ammonium sulfate in 0.3 F H_2SO_4 titrated with $2.00 \cdot 10^{-3}$ M $KMnO_4$. (a), 50 ml of $4.955 \cdot 10^{-4}$ M Fe^{2+}, vol. at end-point, 2.48 ml; (b), 50 ml of $9.91 \cdot 10^{-4}$ M Fe^{2+}, vol. at end-point, 4.96 ml.

(d) Precipitation titration; cyanide ion with Ag(I). LAITINEN, JENNINGS AND PARKS[19] worked out the amperometric titration of cyanide with silver ion to the argentocyanide complex formation, using the R.P.E. In this work, the D.M.E. was used and the titration was carried out to the formation of the silver cyanide precipitate, $Ag\,[Ag(CN)_2]$. The reactions occurring in the bulk of solution are:

$$2\,CN^- + Ag^+ \rightarrow Ag(CN)_2^- \qquad (10)$$

$$Ag(CN)_2^- + Ag^+ \rightarrow Ag\,[Ag(CN)_2] \qquad (11)$$

The end-point is expected to occur at a 1 : 1 molar ratio.

Figure 6a is the titration curve of cyanide ion with Ag(I) at zero applied voltage *vs.* the S.C.E. in Na_3PO_4–Na_2HPO_4 buffer (0.1 F total) of pH 10.8. The volume at the end-point is obtained at the intersection of sections 1 and 2 of the curve and agrees well with the expected value. Section 1 represents the current produced due to the

solubility of Ag_2O ($K_{sp} = 2.6 \times 10^{-8}$) formed by the addition of excess Ag(I) after the end-point. A comparison with Fig. 6b, where the titration was performed at pH 6.8—at which no precipitation of silver oxide occurs—supports this view. The end-point in the latter determination is the intersection of the curve with the zero current

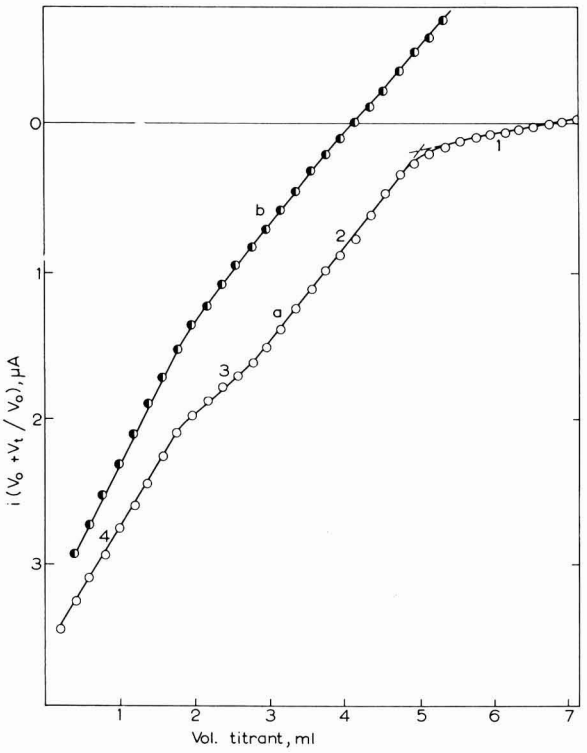

Fig. 6. Precipitation titration with the D.M.E., of 25 ml $9.96 \cdot 10^{-4}$ *M* KCN with $5.00 \cdot 10^{-3}$ *M* $AgNO_3$: (a), in trisodium phosphate–disodium phosphate buffer (0.1 *F* total) pH 10.8, vol. at end-point, 5.02 ml Ag^+; (b), in McIlvaine buffer pH 6.8, vol. at end-point, 4.14 ml Ag^+.

reading. The result obtained was low (by about 16%), which is mainly due to the volatility of hydrocyanic acid formed at this pH (see above). Section 4 in Fig. 6a is the resultant of both the removal of cyanide ion by the formation of argentocyanide complex in eqn. (10) and the reaction of argentocyanide complex at the D.M.E. mentioned by LARGE AND PRZYBLOWICZ[20]

$$Hg + 2\ Ag(CN)_2^- \rightarrow Hg(CN)_2 + 2\ Ag + 2\ CN^- \qquad (12)$$

The net effect is—the removal of cyanide ion follows a molar ratio of 1 : 1 cyanide ion to Ag(I). Section 2 in Fig. 6a evidently corresponds to the conversion of argentocyanide complex to silver cyanide precipitate as in eqn. (11). Section 3 displays the slow change of current at 40–60% titration and does not appear in Fig. 6b. The difference between Figs. 6a and 6b may give an indication of the effect of pH on the species formed.

KOLTHOFF AND STOCK[21] reported the formation of hydroxyargentocyanide complex $Ag_{(CN)}{}^{(OH)-}$ in the presence of strong alkali according to the following reaction:

$$Ag^+ + 2\ OH^- + Ag(CN)_2^- \rightleftharpoons 2\ Ag_{(CN)}{}^{(OH)-};\quad K = 3.4 \pm 0.8 \times 10^6 \tag{13}$$

$$K = \frac{[Ag_{(CN)}{}^{(OH)-}]^2}{[Ag^+]\,[OH^-]^2[Ag(CN)_2^-]} \tag{g}$$

The decomposition of $Ag_{(CN)}{}^{(OH)-}$ is given by

$$Ag_{(CN)}{}^{(OH)-} \rightleftharpoons Ag^+ + OH^- + CN^-;\quad K_d = 6 \cdot 10^{-14} \tag{14}$$

$$K_d = \frac{[Ag^+]\,[OH^-]\,[CN^-]}{[Ag_{(CN)}{}^{(OH)-}]} \tag{h}$$

Multiplying (g) and (h) and rearranging the product of multiplication:

$$\frac{[Ag_{(CN)}{}^{(OH)-}]}{[Ag(CN)_2^-]} = 2 \cdot 10^{-7}\frac{[OH^-]}{[CN^-]} \tag{i}$$

This indicates that the formation of $Ag_{(CN)}{}^{(OH)-}$ is negligibly small at pH 10.8 at concentrations of cyanide ions corresponding to a 40% titration. SHINOZUKA AND STOCK[22] reported that the addition of Ag(I) to cyanide ion, especially without powerful auxiliary stirring, probably causes local separation of silver oxide which redissolves slowly, at low concentrations of cyanide ion, in the region of the equivalence point. Section 4 may be accounted for, if either hydroxyargentocyanide complex or silver oxide precipitates form locally, followed by a slow transformation to equilibrium composition.

ACKNOWLEDGEMENT

The helpful suggestions of Professor LOUIS MEITES, Department of Chemistry, Polytechnic Institute of Brooklyn, Brooklyn, N.Y., are gratefully acknowledged. We thank Mr. VICTOR SOFER for performing part of the experimental work and also the directors of Israel Mining Industries for permission to publish this work.

SUMMARY

The theoretical and practical principles of direct spontaneous voltammetry and spontaneous voltammetric titrations were discussed and the direct determinations of Hg(II), Ag(I), cyanide ion and EDTA were investigated. The spontaneous titrations investigated were: (i) direct complexation, such as the titrations involving Hg(II)–EDTA system; (ii) indirect complexation, such as the titration of Ag(I) with EDTA; (iii) oxidation–reduction, such as the titration of ferrous ion with permanganate, and (iv) precipitation, such as the titration of cyanide ion with Ag(I). The mechanism of electrode reactions at the D.M.E. in the titration of Ag(I) with EDTA was explained. In this instance, the end-point of the titration, obtained by the intersection of the titration curve with the zero current, does not correspond to the stoichiometric end-point but to the ratio of the diffusion current constants of the

species involved. This is true for all cases where the reaction between the active constituents occurs at the electrode surface. A stoichiometric end-point is obtained only when the active constituents react in the bulk of the solution.

REFERENCES

1 Y. ISRAEL, *Bull. Res. Council Israel*, 6A (1957) 184.
2 Y. ISRAEL AND A. VROMEN, *Anal. Chem.*, 31 (1959) 1470.
3 Y. ISRAEL, *Anal. Chem.*, 31 (1959) 1473.
4 A. SCHLEICHER, *Elektroanalytische Schnellmethoden*, F. Enke, Stuttgart, 1947.
5 I. M. KOLTHOFF AND W. E. HARRIS, *Ind. Eng. Chem., Anal. Edn.*, 18 (1946) 161.
6 A. RINGBOM AND B. WILKMAN, *Acta Chem. Scand.*, 3 (1949) 22.
7 G. W. EWING, *Instrumental Methods of Chemical Analysis*, McGraw-Hill Inc., New York, 1954, p. 77.
8 W. E. HARRIS, *J. Chem. Educ.*, 35 (1958) 408.
9 L. MEITES AND H. C. THOMAS, *Advanced Analytical Chemistry*, McGraw-Hill Inc., New York, 1958, p. 410.
10 I. M. KOLTHOFF AND C. S. MILLER, *J. Am. Chem., Soc.*, 62 (1940) 2171.
11 J. J. LINGANE, *J. Am. Chem. Soc.*, 65 (1943) 866.
12 L. MEITES, *Polarographic Techniques*, Interscience Publishers Inc., New York, 1955, pp. 21–22.
13 F. J. WELCHER, *The Analytical Uses of Ethylene Diamine Tetraacetic Acid*, Van Nostrand Inc., Princeton, 1957, p. 164; p. 255.
14 I. M. KOLTHOFF AND C. S. MILLER, *J. Am. Chem. Soc.*, 63 (1941) 2732.
15 G. W. C. MILNER, *The Principles and Applications of Polarography and other Electroanalytical Processes*, Longmans, Green and Co., London, 1956, p. 595.
16 B. MATYSKA, J. DOLEZAL AND D. ROUBALOVA, *Chem. Listy*, 49 (1955) 1012; *Collection Czech. Chem. Commun.*, 21 (1956) 107.
17 D. ROUBALOVA AND J. DOLEZAL, *Chemist-Analyst*, 49 (1960) 76.
18 G. CHARLOT, J. BADOZ-LAMBLING AND B. TREMILLON, *Electrochemical Reactions. The Electrochemical Methods of Analysis*, Elsevier Publishing Co., Amsterdam, 1962, p. 211.
19 H. A. LAITINEN, W. P. JENNINGS AND T. D. PARKS, *Ind. Eng. Chem., Anal. Edn.*, 18 (1946) 574.
20 R. F. LARGE AND E. P. PRZYBLOWICZ, *Anal. Chem.*, 36 (1964) 1648.
21 I. M. KOLTHOFF AND J. T. STOCK, *J. Am. Chem. Soc.*, 78 (1956) 2081.
22 F. SHINOZUKA AND J. T. STOCK, *Anal. Chem.*, 34 (1962) 926.

A SIMPLE DEVICE* FOR TAST-POLAROGRAPHY USING KNOCK-OFF ELECTRODES

P. O. KANE

Imperial Chemical Industries Limited, Mond Division, Research Department, The Heath, Runcorn (England)

(Received June 23rd, 1965)

INTRODUCTION

The technique of, and a circuit for, d.c. Tast-polarography were first described by KRONENBERGER *et al.*[1]. Principles and applications of KRONENBERGER's polarograph have been reviewed by KANE[2], and circuits suitable for recording of Tast-polarograms have also been described by NASH[3], and YASUMORI[4]. In all these circuits, however, extensive modification of the polarograph circuitry is involved, making adaptation of an existing polarograph for Tast-operation difficult. The device described here is extremely simple in operation. It does not involve any alteration in the polarograph polarising circuit and only a simple alteration in the circuit of the polarograph recording potentiometer. This device has been used for a.c. polarography and could probably be used in a square-wave polarograph.

PRINCIPLE AND CONSTRUCTION

The overall principle of the device is to knock off the mercury drop mechanically by means of a cam rotating at a constant speed and to render the pen-motor of the potentiometric recorder inoperative for all but a fixed, reproducible part of the enforced drop-life by means of a switch operated by a second cam mounted on the same shaft as the knock-off cam.

Figs. 1a and 1b show two photographs of the device, which, for convenience, is mounted on a modified Cambridge Instrument Co. Polarograph stand.

(i) Knock-off

The arm holding the dropping electrode capillary is modified to enable it to pivot freely about its mounting point, and a spring holds the arm against a pre-set stop. A shaft carrying two cams, A and B, is mounted in the horizontal plane and is driven by a synchronous motor, the period of rotation of which must be less than the shortest natural drop-life of the dropping electrode. In the apparatus described here, a Honeywell recorder chart motor of period 1.5 sec/rev. was used. Once per revolution of the cam-shaft, cam A, the shape of which can be seen in Fig. 1a, bears upon a nylon roller mounted on the electrode arm causing the arm to swivel gently a few degrees about its pivot against the spring tension until, when the cam step is reached, it is

* This device is the subject of a provisional patent application.

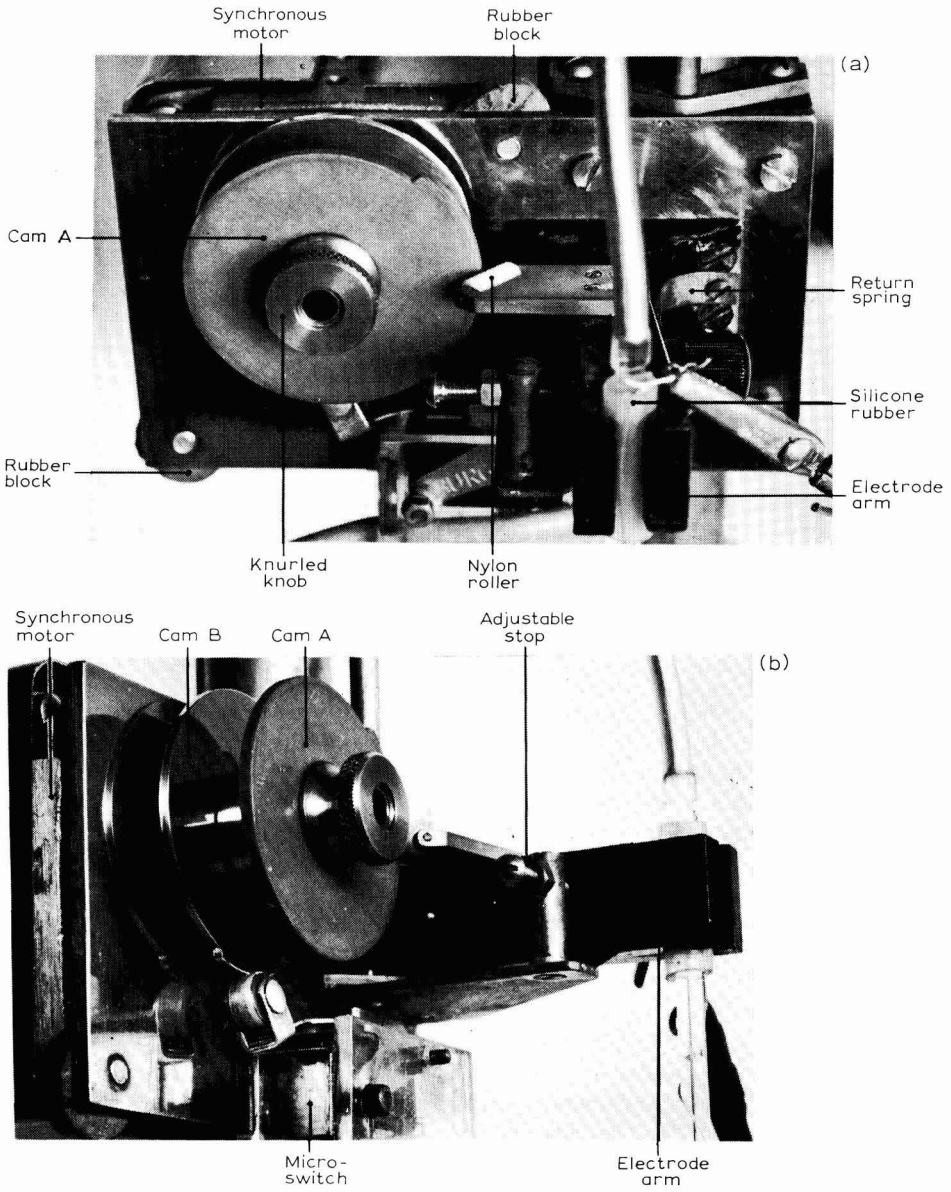

Fig. 1. Photographs of device for knock-off electrode and Tast-operation.

returned sharply by the spring to the stop. This sharp movement knocks off the mercury drop, thus giving an enforced drop-time equal to the period of rotation of the cam-shaft.

(ii) Tast-operation

In order that it may respond to input signals, the servo-motor of a potentio-

metric recorder requires a corresponding signal from the output of the servo-amplifier and also excitation of its a.c. mains coil. In the Tinsley polarograph[3], Tast-operation is achieved by reducing the gain of the servo-amplifier considerably for all but a pre-selected part of the drop-life. In the present device, the a.c. mains excitation is switched off for all but a pre-selected part of the drop-life. This is achieved by inserting a micro-switch into this circuit of the recorder. This micro-switch, normally open, is closed once per revolution of the electrode knock-off cam-shaft by cam B (the shape of which can be seen in Fig. 1b). Thus, over a short, fixed, reproducible part of the enforced drop-life, the recorder-pen motor operates normally and for the remainder of that drop-life and part of the next, it indicates a constant current corresponding to the current when the switch closed previously. The size of the fraction of drop-life in which Tast-operation occurs is governed by the length of the raised portion of cam B. For a 1.5-sec enforced drop-time, two interchangeable cams giving Tast operation periods of 0.3 and 0.15 sec were found to provide sufficient flexibility.

The Tast interval, that is, the time elapsing between the start of drop-life and the end of the Tast operation, can be altered by altering the angle between the cams, A and B, on the cam-shaft.

This device has so far only been used with a Bristol Dynamaster potentiometric recorder, but, presumably, could be used in conjunction with any high-speed recorder of this general type.

SETTING-UP PROCEDURE

It is first necessary to ensure that the mercury drops of the electrode are knocked-off consistently. With the cam-shaft rotating and the electrode dipping into a suitable electrolyte, such as 0.1 *M* hydrochloric acid, the position of the stop is adjusted so that cam A does not touch the nylon roller and the mercury drops fall freely. The position of the stop is then slowly adjusted until the position is established of consistent knock-off at minimum movement of the arm by cam A. At this point the stop is locked by a lock-nut. The next requirement is (for analytical purposes) to set the Tast interval near the end of drop-life so that maximum sensitivity and minimum oscillation is obtained. The knurled screw on the end of the cam-shaft is loosened and cam A is set manually so that it is almost in contact with the nylon roller. Then, without moving cam A, cam B is rotated so that its trailing edge is just clear of the micro-switch roller in the direction of rotation of the cam-shaft. The knurled knob on the cam-shaft is then tightened to prevent movement of cam A relative to cam B. For other settings of the Tast interval when required, cam A or cam B can be marked with an angular scale to permit setting to any time value within the drop-life.

In initial trials of the device it was found that high-frequency mechanical vibration was transmitted from the motor to the mercury drop. This was minimised by mounting the motor on rubber blocks and the capillary in a soft silicone rubber tube.

POLAROGRAPH

The polarograms reproduced here were obtained with a simple laboratory-constructed polarograph fitted with rectilinear counter-current. The device has also

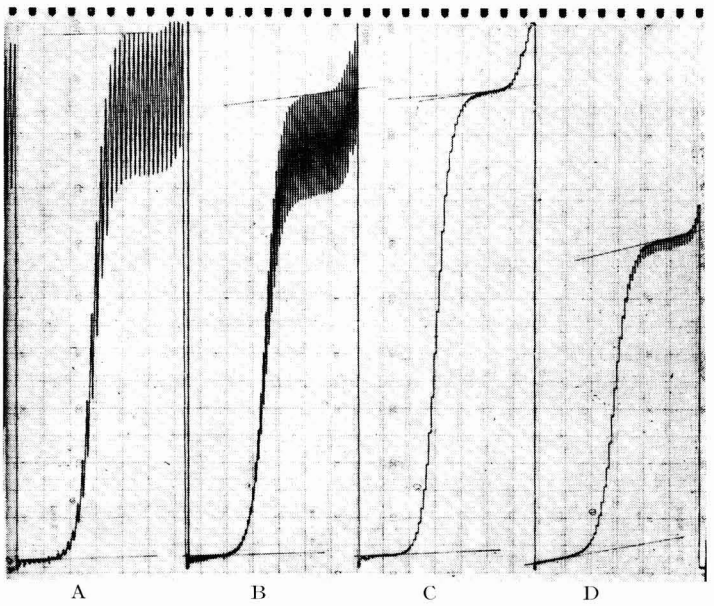

Fig. 2. Polarograms of 2.5 m*M* Paraquat in borax–potassium chloride buffer containing 50% v/v methanol. (A), Freely dropping electrode, undamped operation (t = 2.7 sec); (B), knock-off electrode, undamped operation (t = 1.5 sec); (C), knock-off electrode, Tast operation (t = 1.5 sec, Tast interval = 1.5 sec); (D), knock-off electrode, Tast operation (t = 1.5 sec, Tast interval = 0.15 sec).

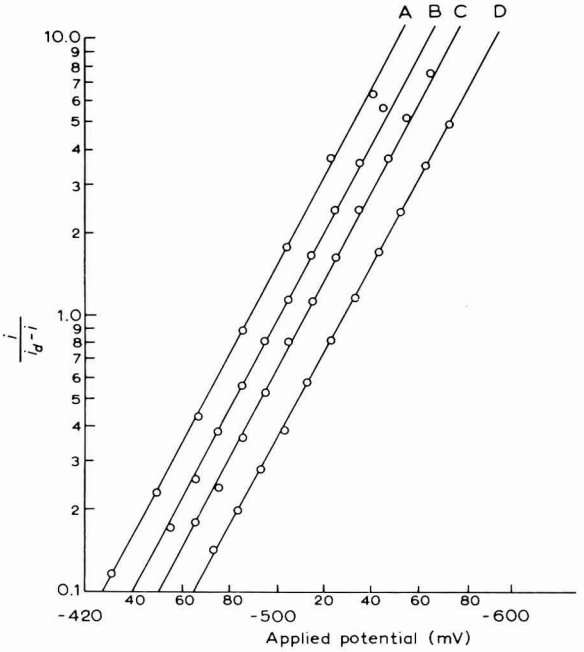

Fig. 3. Log plots of the waves of Fig. 2. (A), free drop; (B), knock-off (t = 1.5 sec); (C), Tast (t = 1.5 sec); (D), Tast (t = 0.15 sec). Potential scale correct for (A) is shifted 10 mV for each successive curve.

been used with a Cambridge G.P. polarograph operating on d.c. and, in conjunction with a Univector unit, on a.c. polarography.

TYPICAL POLAROGRAMS

In order to be certain that the Tast device did not introduce any distortion of polarograms, a compound that gave a well-defined wave was first investigated. The system chosen was N,N′-dimethyl-4,4′-dipyridylium dichloride (Paraquat), which has been found to yield two thermodynamically-reversible waves each of one electron/molecule in solvents containing a high concentration of methanol to suppress adsorption phenomena. For the purpose of testing the Tast device, only the first wave was investigated, the sensitivity being chosen to give approximately full-scale recorder deflection for this wave with a freely dropping electrode (drop time *ca.* 2.7 sec). Figure 2 shows polarograms of 2.5 m*M* Paraquat in a buffer containing 0.05 *M* borax and 0.05 *M* potassium chloride in 50% v/v methanol–water. An internal silver wire anode was used to minimise *iR* losses.

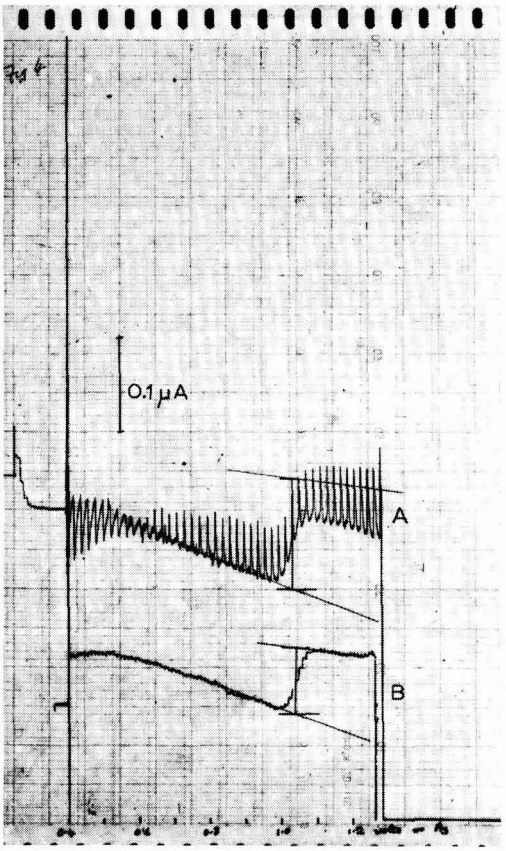

Fig. 4. Polarograms of 0.01 m*M* zinc ions in 0.1 *M* potassium chloride. (A), Undamped operation (t = 2.7 sec); (B), Tast operation (t = 1.5 sec, Tast interval = 1.3 sec).

The graphs of log $[i/(i_d-i)]$ *vs.* applied voltage, shown in Fig. 3, for the four polarograms of Fig. 2 have slopes of 63, 63, 63 and 64 mV; the identity of these slopes clearly shows that, as required, there is no perceptible distortion of the polarogram even at very short Tast intervals. The total spread of half-wave potential of the four polarograms was only 9 mV which is within the limits of error of the instrument.

A second application, shown in Fig. 4, is the determination of a fairly low concentration of a depolariser (0.01 m*M* Zn^{2+}) under conditions in which capacity and diffusion currents produce oscillations in opposite directions and of comparable magnitude. This problem has been discussed previously by the author[2] in some detail. Figure 4A is an undamped polarogram, with counter-current, of 0.01 m*M* Zn^{2+} in 0.1 *M* potassium chloride, on which tangents corresponding to capacity and diffusion current envelope at the end of drop-life have been added. The much greater ease of evaluation of the Tast-polarogram, Fig. 4B, is quite evident.

CONCLUSIONS

The data of Figs. 2, 3 and 4 show that the simple device described here provides an inexpensive method of adapting a recording polarograph for Tast-polarography. It is limited to polarographs employing a potentiometric recorder, but, since the Tast-operation is independent of the polarising unit, this device can be applied to polarographs other than the classical. It has for example, been used for a.c. polarography.

SUMMARY

A simple method of converting an existing polarograph for Tast-polarography is described. It is based on the use of a mechanical knock-off electrode and concomitant mechanical switching of the servo-motor of the polarograph recording potentiometer. Typical polarograms show that this device gives greater legibility than normal undamped operation without the distortion usually associated with heavy damping.

REFERENCES

1 K. KRONENBERGER, H. STREHLOW AND A. W. ELBEL, *Polarograph. Ber.*, 5 (1957) 62.
2 P. O. KANE, *J. Polarog. Soc.*, 8 (1962) 10.
3 L. F. NASH, Brit. Patent 850, 078, 28/9/1960.
4 Y. YASUMORI, *Japan Analyst*, 7 (1958) 354.

POLARISATION PHENOMENA MANIFESTED BY Pb–Sb ALLOYS AT LOW CURRENT DENSITIES

E. M. KHAIRY*, A. A. ABDUL AZIM AND K. M. EL-SOBKI
Laboratory of Electrochemistry, N.R.C., Cairo (Egypt)
(Received June 23rd, 1965)

INTRODUCTION

Antimony has proved to be indispensable in the production of grids in lead–acid cells. The influence of antimony on the cell reactions has been the subject of many investigations[1–4]. Studies on the electrochemical behaviour of Pb–Sb alloys have been almost exclusively confined to acid solutions. In a previous study[5] we have demonstrated the effect of antimony inclusions on the pH–potential relationship for lead. In the present work, polarisation phenomena encountered with Pb–Sb alloys are investigated in a variety of electrolytes at relatively low current densities.

EXPERIMENTAL

Three Pb–Sb alloys containing 8, 11 and 49.3% Sb, respectively, were used. Galvanostatic anodic, and occasionally cathodic, polarisation experiments were conducted at relatively low current densities (5–300 μA/cm^2) to investigate the electrode reactions, operating in various media under conditions of low overvoltage. Charging and decay potential–time curves were plotted over prolonged periods.

The electrolytic cell had two compartments separated by a fine-porosity sintered-glass disc. Prior to use, the electrodes were polished by rubbing with very fine emery paper and cloth, thoroughly washed with redistilled water, and then with the electrolyte. The counter electrode was a platinum wire.

Experiments at lower current densities were made in several electrolytes including 3 *M* and 0.1 *M* NaCl, 0.05 *M* borax and 0.05 *M* Na_2CO_3. Before measurements dissolved oxygen was removed from the electrolyte by passing a stream of purified nitrogen.

RESULTS AND DISCUSSION

Behaviour in sodium chloride solution

In Fig. 1 are shown the charging and decay curves obtained on anodic polarisation of Pb–Sb alloys containing 11% Sb (alloy II) and 49% Sb (alloy III) in 0.1 *M* NaCl. The polarising current densities were 20 and 300 μA/cm^2. It can be seen that the potential, after a rapid rise, tends to attain a steady value. The anode potential acquired by alloy II agrees closely at the higher current density with the calculated

* Chemistry Department, Faculty of Science, Cairo University, Cairo (Egypt).

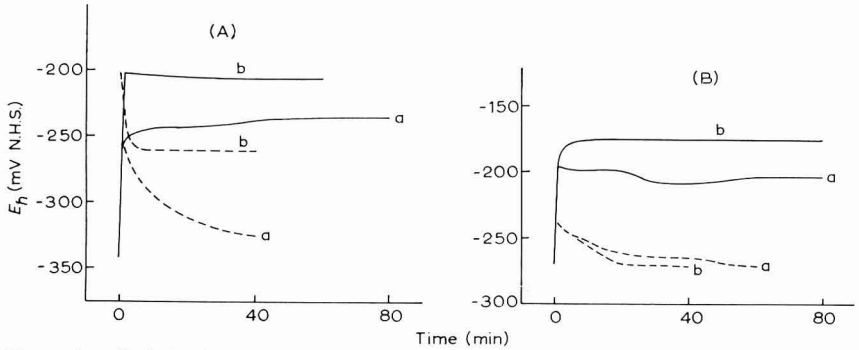

Fig. 1. Anodic behaviour of alloys II (A) and III (B) in 0.1 *M* NaCl. (a), 20; (b), 300 μA/cm^2. (——), charging curves; (– – – –), decay curves.

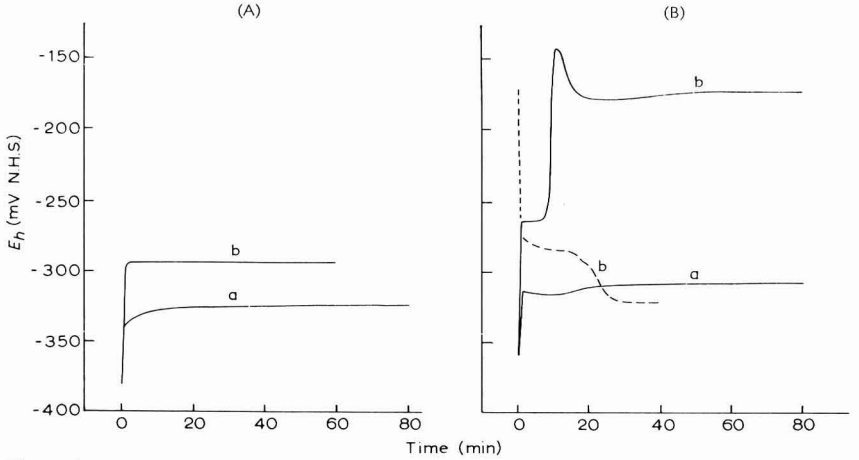

Fig. 2. Anodic behaviour of alloys II (A) and III (B) in 3 *M* NaCl. (a), 20; (b), 300 μA/cm^2.

value for the reversible Pb/$PbCl_2$ couple at the prevailing Cl^- ion activity; at the lower current density, it attains a value ~ 30 mV lower. Alloy III, on the other hand, approaches closely the reversible Pb/$PbCl_2$ potential at the lower current density of 20 μA/cm^2, but shifts 20 mV in the positive direction at 300 μA/cm^2.

In 3 *M* NaCl, alloy II behaves very much the same as in the 0.1 *M* solution in so far as the reversible Pb/$PbCl_2$ potential is only approached at the higher current density (Fig. 2A). Alloy III, on the other hand, behaves somewhat differently at the higher current density as can be seen from Fig. 2B. The anodic curve obtained at 300 μA/cm^2 passes through an arrest at -0.265 V, after which the potential rises very rapidly to a sharp peak of amplitude about 35 mV. It then increases slowly to attain a steady value of -0.175 V, which is slightly higher than the calculated value for the Pb/PbO system, *viz.* -0.185 V. At the lower current density, however, alloy III behaves in a similar way to alloy II, showing a difference of only 20 mV from the calculated Pb/$PbCl_2$ potential.

The above results indicate that the two alloys undergo a continuous corrosion process at, or slightly below, the Pb/$PbCl_2$ potential. This process is associated with the deposition of a $PbCl_2$ layer through metallic dissolution with subsequent inter-

action with Cl^- ions diffusing to the surface. The characteristics of such corrosion layers *i.e.*, the mode of thickening, type of conduction and attainment of protective nature, are determined by several factors including current density, polarisation period, chloride ion activity and antimony content of the alloy. Thus, at the lower chloride ion concentration and lower antimony content (alloy II), the solubility product of $PbCl_2$ is satisfied only at the higher applied current density, where the corrosion potential is consistent with the calculated one. At a current density as low as 20 $\mu A/cm^2$, the corrosion process is apparently inadequate to furnish sufficient Pb^{2+} ion to deposit $PbCl_2$; the anode potential lies below the $Pb/PbCl_2$ value and the decay potential approximates to the initial open circuit value. It is apparent that the anodically-formed $PbCl_2$ layer is dissolved away in solution on switching off the current, since the product of the bulk concentrations of Pb^{2+} and Cl^- ions after decay of polarisation lies below the solubility product of $PbCl_2$ ($1.6 \cdot 10^{-5}$). With alloy III (49.3% Sb), however, the potential attained at 300 $\mu A/cm^2$ lies mid-way between the calculated $Pb/PbCl_2$ and Pb/PbO potentials. It is quite likely that the resulting potential is determined by the fraction of current used for both chloride and oxide formation. The heterogenity of composition and electrical properties of the films anodically formed on lead in sodium chloride solutions, have been described by some authors[6] indicating that the corrosion of lead is apparently increased when antimony is present in considerable proportion. The double layer is furnished with sufficient Pb^{2+} ions to allow the simultaneous deposition of $PbCl_2$ and PbO at an appropriate current density, or of $PbCl_2$ alone at lower current density (20 $\mu A/cm^2$).

At the higher chloride ion concentration (3 *M*), particularly at small current densities (20 $\mu A/cm^2$), the emerging Pb^{2+} ions are partially complexed giving $PbCl_4^{2-}$ ions. The formation of a stable $PbCl_2$ film on the metal surface cannot therefore take place, and the anode potential lies below the reversible $Pb/PbCl_2$ value. At the appropriate current density (300 $\mu A/cm^2$), however, the double layer may be furnished with sufficient Pb^{2+} ions to establish a $PbCl_2$ layer which, being porous, thickens at a more or less constant potential (*cf.* Fig. 2A with alloy II). In the presence of higher proportions of antimony, as in alloy III, it seems that the corrosion process is enhanced and the effective current density operating on the lead part of the surface is progressively increased so that a slightly porous $PbCl_2$ layer is formed. The anodic process would then be governed by the diffusion of metal ions from the metal/layer interface through the layer to the layer/solution interface. This process is presumably associated with considerable overvoltage, and hence the potential jump observed. The mean film thickness calculated from the coulombs consumed and using the reported value[7] of 5.89 for the specific gravity of $PbCl_2$, amounts to about $4 \cdot 10^{-5}$ cm. It has been assumed, for simplicity, that the $PbCl_2$ film covers the whole surface. This value is of the same order of magnitude as the values reported by KOCH[8] ($8 \cdot 10^{-5}$ cm) and by FEITKNECHT AND GAUMANN[9] (10^{-4} cm) for the passivating $PbSO_4$ film formed on the surface of lead in sulphuric acid. When the surface film attains this thickness, the anode potential jumps to a more positive value at which another electro-chemical process takes place. Under such conditions and because of the pronounced effective current density operating in the pores of the film, OH^- ions diffuse into the pores and react with the clean metal parts forming PbO.

$$Pb + 2\,OH^- = PbO + H_2O + 2\,e$$

During the period of oxide nuclei formation associated with the potential peak observed, the electronic current is conducted across the compact lead chloride layer, a process involving resistance polarisation. Once oxide channels are built within the pores, the conduction of electrons takes place across these channels at a lower polarisation, and the anode potential approaches the Pb/PbO potential. The resistance of the lead chloride film primarily formed on the electrode surface, may be concluded from the overshoot of potential transient above the potential of PbO formation. The observed overshoot amounts to 35 mV which corresponds, at a current density of 0.3 mA/cm^2 to a resistance of $\sim 117\ \Omega$. This value gives a value of $2.9 \cdot 10^6\ \Omega$ cm for the specific resistance of $PbCl_2$ and demonstrates its insulating character under these conditions.

Oxidised electrodes allowed to rest on open circuit, exhibit the phenomenon of self-discharge. When the polarising current was switched off, the electrode potential fell rapidly to that of Pb/$PbCl_2$. The following reaction scheme is suggested:

$$Pb = Pb^{2+} + 2\,e$$
$$PbO + 2\,H^+ + 2\,e = Pb + H_2O$$

and

$$Pb + 2\,Cl^- + H_2O = PbCl_2 + 2\,OH^-$$

Along the potential halt, the process of self-discharge is expressed as:

$$PbCl_2 + 2\,e = Pb + 2\,Cl^-$$

and the electrons are given by:

$$Pb = Pb^{2+} + 2e$$

This latter reaction takes place in the fissures in the $PbCl_2$ layer. The final, more negative, potential value which is ultimately attained by the electrode indicates a small concentration of Pb^{2+} which accords with the tendency of these ions, as does $PbCl_2$, to be complexed in the presence of an excess of chloride ions. In 0.1 *M* solution, on the other hand, the potential on open circuit remains in the vicinity of the Pb/$PbCl_2$ value provided that the electrode has been pre-anodised at a sufficiently high current density.

Comparison of the behaviour of Pb–Sb alloys in concentrated sodium chloride and in sulphuric acid leads to the conclusion that the mechanism of oxide formation is almost the same, although the oxide formed in the former case is PbO. The stability of this oxide which was derived in sulphuric acid[10], may be assumed to be similar in neutral media.

Behaviour in 0.05 M borax

Fig. 3 illustrates the characteristic curves for the anodic polarisation of the three Pb–Sb alloys in 0.05 *M* borax solution at a current density of 35 μA/cm^2. Before anodisation was started, the sample was usually cathodised for 30–60 min until hydrogen evolution. The electrode potential at first rises very rapidly from the hydrogen evolution value which is the starting point of the curves; this rapid rise is followed by an arrest at about -0.400 V. Another shorter but well-defined stage occurs at -0.220 V, after which the potential jumps towards oxygen evolution, supposedly associated with the attainment of passivity. The decay curves obtained with alloys II and III exhibit, during the fall of potential towards a steady open-

circuit value, a stage of slow decay, whereas with alloy I the decay occurs sharply.

The above results may be explained on the premise that when Pb–Sb electrodes become passive under appropriate conditions, anodic polarisation curves show two arrests prior to oxygen evolution. The first step may be attributed to the formation of a salt layer, most probably lead metaborate[11]. An arrest occurring at the same

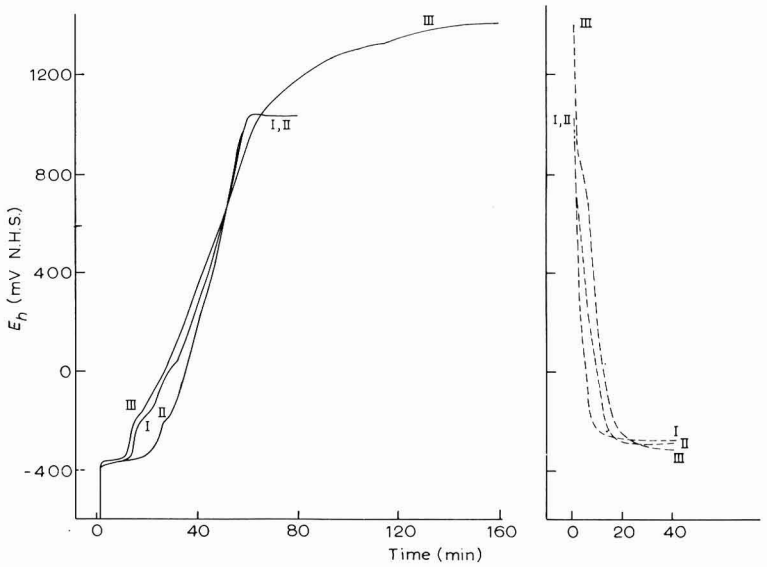

Fig. 3. Anodic behaviour of alloys I, II and III in 0.05 *M* borax at 35 μA/cm^2; (left), charging curves; (right), decay curves.

potential, could be reproduced with a spectroscopically pure lead sample. Once a protecting layer is formed, there is a sharp rise in potential to more positive values. Consequently, the anodic process comprises the direct oxidation of lead in the available pores of the salt layer and/or the transformation of lead metaborate to PbO, during which process the potential approximates to the Pb/PbO value. When a passivating film is established, the potential jumps to the oxygen evolution value, which is considerably higher on alloy III than on alloy II owing to greater overpotential.

The anodic decay curves reveal that the corrosion process occurring during oxygen evolution, *viz.*, the formation of PbO_2, is enhanced by the presence of antimony in the alloy. This is demonstrated by the breaks observed on these curves, which correspond to the partial reduction of PbO_2. The reduction product is most probably Pb_3O_4, which is then rapidly transformed into PbO whereupon the electrode acquires the Pb/PbO potential.

The curves obtained at 35 μA/cm^2 do not, however, fully explain the effect of the antimony content on the behaviour of the alloys. To obtain further insight regarding the role of antimony, polarisation experiments were conducted at a current density as low as 5 μA/cm^2 (Fig. 4). The charging curves obtained with alloys I, II and III each have three main potential arrests. The first one simulates that observed at the higher current density (35 μA/cm^2) and corresponds to the Pb/Pb metaborate

as well as to the Sb/Sb_2O_3 potential. The rise of potential associated with the completion of this stage is a criterion of a protecting layer established on the anode surface. It is supposed that a layer of metaborate is established on the lead surface, and antimony trioxide is deposited on the antimony surface and thus assumes a protec-

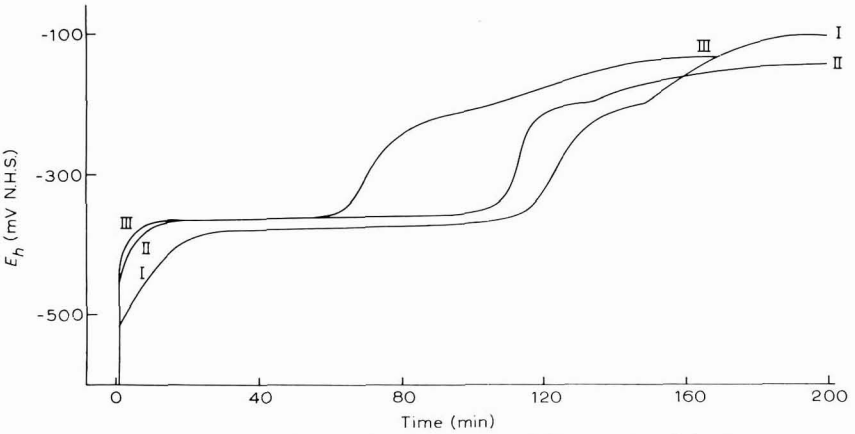

Fig. 4. Anodic behaviour of alloys I, II and III in 0.05 *M* borax at 5 μA/cm^2.

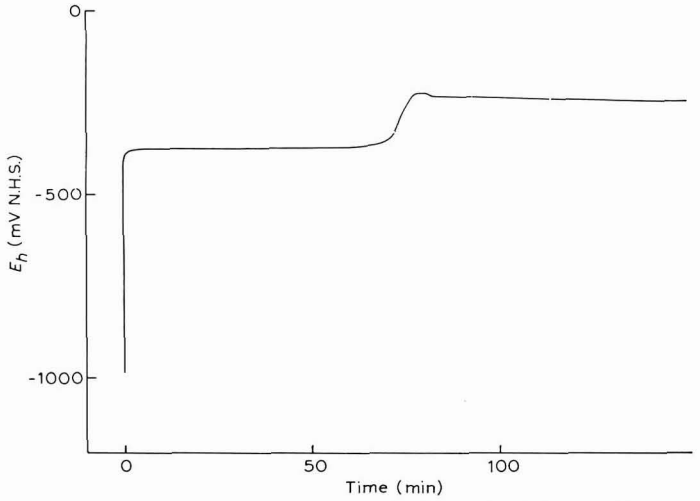

Fig. 5. Anodic behaviour of spectroscopically pure lead in 0.05 *M* borax at 5 μA/cm^2.

tive nature. The process is apparently enhanced by a greater proportion of antimony in the alloy. The anode potential then shifts to a more positive value at which another electrochemical process takes place which is most probably the formation of PbO, either by the interaction of OH^- ions with the clean metal parts in the salt layer, and/or the chemical transformation of metaborate into oxide. This view is substantiated by the second arrest observed on the polarisation curves, which lies near the reversible Pb/PbO potential. The lead surface becomes progressively passivated and the potential shifts of the Sb/Sb_2O_5 value[12], owing to the anodic oxidation of Sb_2O_3.

Anodic polarisation of spectroscopically pure lead under the same conditions revealed a rapid rise of potential, from a first arrest associated with the formation of PbO crystal nuclei. This is followed by a sharp decrease to a value close to the reversible Pb/PbO couple, supposedly after PbO channels have been established within the pores of the salt layer (Fig. 5).

The potential discharge transients observed during cathodic polarisation at 35 μA/cm^2 of electrodes (alloys I and III) pre-anodised for 1 h at 1 mA/cm^2 until oxygen evolution, are shown in Fig. 6. The potential of alloy III (49% Sb) drops from the

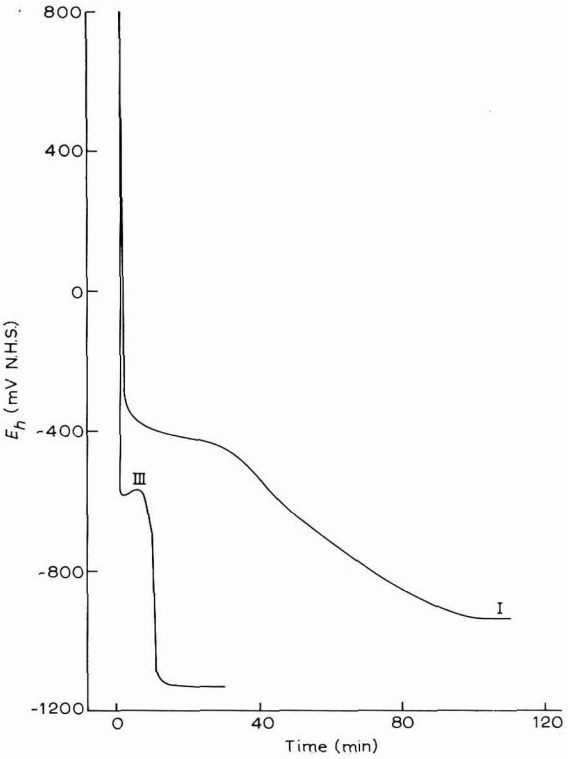

Fig. 6. Cathodic polarisation of alloys I and III in 0.05 M borax at 35 μA/cm^2.

oxygen evolution value to a minimum; it then recovers to a plateau and drops thereafter to the hydrogen evolution potential. The cathodic curve of alloy I does not show a minimum; the potential arrest (−0.42 V) is more prolonged and the hydrogen evolution potential value is approached more gradually than in the former case.

The potential arrest on the cathodic reduction curve obtained with alloy I corresponds to the reduction of PbO since it starts at a potential close to the reversible Pb/PbO value (−0.29 V). It seems, however, that the complete reduction is subject to certain overvoltage as shown by the slow change of potential with time and the more negative potential at which the arrest occurs. The behaviour of alloy III demonstrates the greater overvoltage associated with the reduction of lead oxide as revealed by the more negative reduction potential. This may be ascribed to a higher

effective current density operating at the lead surface of the alloy, owing to its much greater antimony content. The more negative hydrogen evolution potential observed with alloy III than with alloy I may be similarly explained. The effect of increase of current density on the reduction transient can be observed when pure lead is cathodically polarised, after being anodically pre-treated in the above way.

Behaviour in 0.05 M sodium carbonate

The anodic charging and decay curves for the polarisation of the three alloys at 90 μA/cm^2 in 0.05 M Na_2CO_3 are shown in Fig. 7. The cathodic curves obtained at the same current density with pre-anodised electrodes are shown in Fig. 7B. The

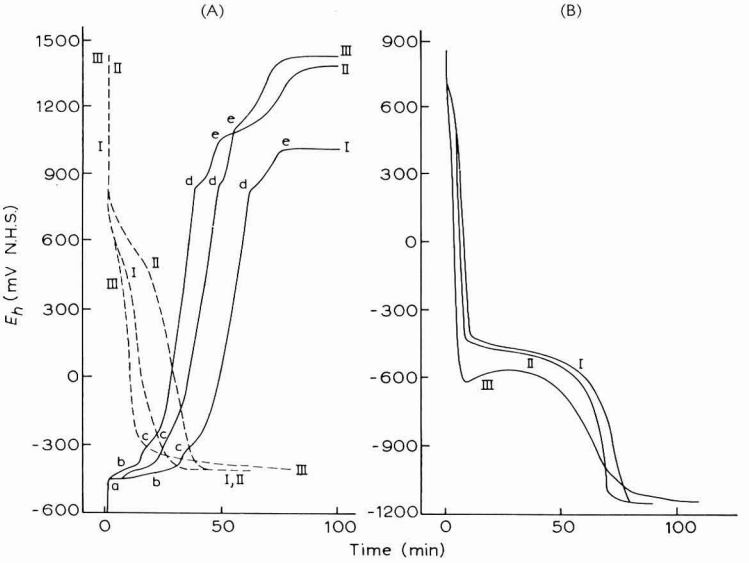

Fig. 7. (A), Anodic charging (—) and decay (---) curves; (B), cathodic polarisation; of alloys I, II and III in 0.05 M Na_2CO_3 at 90 μA/cm^2.

anodic curves indicate that on switching on the anodic current, the electrodes being cathodically pre-polarised, the potential rises rapidly to acquire a more or less steady value (stage a) at about −0.46 V, a value closely comparable with the potential of the Pb/$PbCO_3$ couple at the prevailing CO_3^{2-} concentration. The curves then pass through another stage (b), of gradual change of potential with time. These curves approach the Pb/PbO potential, indicating the transformation of $PbCO_3$ into oxide. In this way, the surface of lead is protected and the antimony surface becomes subsequently oxidised probably forming Sb_2O_5 (stage c). The anode surface is thus rendered decidedly inhibited and the potential jumps to more positive values, towards another electrochemical process. Hydroxyl ions may react with the surface PbO transforming it to Pb_3O_4 (stage d), and then to PbO_2 (stage e).

$$3\,PbO + 2\,OH^- = Pb_3O_4 + H_2O + 2\,e$$

$$Pb_3O_4 + 4\,OH^- = 3\,PbO_2 + 2\,H_2O + 4\,e$$

It seems that alloy I (8% Sb) attains the latter state under the conditions described with a protecting PbO_2 layer established on its surface. Alloys II and III,

on the other hand, attain the oxygen evolution potential at still more positive values. The higher oxidation states of lead, and the oxygen evolution potentials, are invariably subject to overvoltage effects.

Self-decay and cathodic discharge experiments support the above views. Thus, when the anodic current is switched off, the anode potential falls rapidly to a stage of gradual decrease with time occurring within the regions of PbO_2/Pb_3O_4, and Pb_3O_4/PbO potentials, respectively. This extends for different periods according to the alloy used, and may be ascribed to reduction of surface lead oxides into PbO. Once the process is complete, the decay potential falls rapidly to approach the reversible Pb/PbO value. These observations agree fairly well with those reported by JONES *et al.*[13] for pure lead in sodium hydroxide. Potential–time curves obtained on cathodic polarisation of pre-anodised electrodes (Fig. 7B) show arrests corresponding to the reactions $PbO_2 \rightarrow Pb_3O_4 \rightarrow PbO$ and then of $PbO \rightarrow Pb$. The reduction period corresponding to the latter process is smaller the greater the antimony content. The cathodic potential then falls to the hydrogen evolution potential which is subject to overpotential.

SUMMARY

A continuous anodic corrosion process occurs in 0.1 *M* NaCl at the surface of Pb–Sb alloys [11% Sb (alloy II) and 49.3% Sb (alloy III)] at low current densities. This is associated at an appropriate current density, or in presence of considerable amounts of Sb (alloy III), with the deposition of $PbCl_2$. In 3 *M* NaCl, a corrosion layer is deposited only at a higher current density (300 $\mu A/cm^2$), followed, in the case of alloy III, by the deposition of PbO within the pores; the specific resistance of the $PbCl_2$ film calculated from the potential–time curve amounts to $2.9 \cdot 10^6$ Ω cm.

Pb–Sb alloys [8% Sb (alloy I) and 49.3% Sb (alloy III)], pre-cathodised until hydrogen evolution, are readily passivated in 0.05 *M* borax. Arrests corresponding to different corrosion products including lead borate, Sb_2O_3, PbO and PbO_2 have been distinguished, the amount of the latter increasing with increase in antimony content. Similar results are obtained in 0.05 *M* Na_2CO_3; the first corrosion product seems to be $PbCO_3$. Self-decay and cathodic discharge experiments support these findings.

REFERENCES

1 D. W. JONES, *J. Soc. Chem. Ind.*, 47 (1928) 151–7 T.
2 G. ÖSTERHELD AND A. PORTMANN, *Helv. Chim. Acta*, 24 (1941) 389–97.
3 V. P. MASHOVETS AND A. Z. LAYANDRES, *Zh. Prikl. Khim.*, 21 (1948) 441–7.
4 P. RUETSCHI AND B. D. CAHAN, *J. Electrochem. Soc.*, 105 (1958) 369–77.
5 E. M. KHAIRY, A. A. ABDUL AZIM AND K. M. EL-SOBKI, submitted for publication.
6 E. MULLER AND K. SCHWABE, *Z. Elektrochem.*, 40 (1955) 862.
7 J. W. MELLOR, *A. Comprehensive Treatise on Inorganic Chemistry*, Vol. VII, Longmans–Green, New York, 1947, p. 708.
8 D. F. A. KOCH, *Electrochim. Acta*, 1 (1959) 32.
9 W. FEITKNECHT AND A. GAUMANN, *J. Chim. Phys.*, 49 (1952) C135.
10 P. RUETSCHI AND B. D. CAHAN, *J. Electrochem. Soc.*, 104 (1957) 406.
11 J. W. MELLOR, *A Comprehensive Treatise on Inorganic Chemistry*, Vol. V, Longmans–Green, New York, 1946, p. 106.
12 S.E.S. EL WAKKAD AND A. HICKLING, *J. Phys. Chem.*, 57 (1953) 203.
13 P. JONES, H. R. THIRSK AND W. F. K. WYNNE-JONES, *Trans. Faraday Soc.*, 52 (1956) 1003.

CATHODE-RAY POLAROGRAPHIC STUDY OF YTTERBIUM AND EUROPIUM AND THEIR DETERMINATION IN MONAZITE

V. T. ATHAVALE, R. G. DHANESHWAR AND C. S. PADMANABHA IYER
Analytical Division, Atomic Energy Establishment, Trombay, Bombay (India)
(Received June 9th, 1965)

It should be easy to estimate, polarographically, europium, ytterbium and samarium in rare-earth mixtures because of their easy reduction from the tri- to divalent state. The estimation of europium in ores, using 0.1 *M* ammonium chloride as supporting electrolyte has been reported[1]. LAITINEN AND TAIBEL[2] report that ytterbium gives irregular waves in the same supporting electrolyte. Polarographic data for the rare earths in various supporting electrolytes is not complete and there is a need for a study of the polarography of ytterbium.

The analysis of ytterbium in monazite ores does not appear to have been reported[3–5]. The analysis of the yttrium group of the rare earths has been reported but in the separation only part and not the whole of the ytterbium may be present.

This paper reports on the search for a suitable base electrolyte for the polarography of europium and ytterbium in a mixture and the application to the determination of both these elements in monazite ore.

EXPERIMENTAL

Apparatus

A cathode ray polarograph (Model K 1000, Southern Instruments Ltd., England) was used. All peak-potential values were taken against a mercury-pool anode using the delayed-trace method. An electronically operated thermostat was used to keep the temperature constant at $30 \pm 0.1°$.

Chemicals

Appropriate weighed quantities of europium oxide and ytterbium oxide (Stanley Mathews, high purity) were dissolved in a few millilitres of hydrochloric acid and the solutions made up to 100 ml to give a metal concentration of 900 μg/ml. Subsequent dilutions were made from these solutions.

Hydrazine hydrate: concentrated ammonia solution was added to hydrazine sulphate (B.D.H., L.R.) and the ammonium sulphate formed was filtered. The filtrate was evaporated on a water bath to remove excess ammonia and the solution made up to a known volume. An aliquot was taken for titration against potassium iodate in hydrochloric acid medium to determine the molarity. The solutions of the molarity were prepared by dilution of this stock solution.

Acetate buffer solution (0.2 *M* with respect to acetate) was prepared from AnalaR ammonium acetate and acetic acid in the usual manner.

The other chemicals were hydrazine hydrochloride (Merck, fine chemical) and AnalaR-grade sulphuric acid and oxalic acid.

RESULTS AND DISCUSSION

Because of the close proximity of the ytterbium and hydrogen waves, d.c. polarography did not yield good results. The work described has therefore been carried out with a cathode-ray polarograph only.

Different supporting electrolytes were tried to find out if good peaks for europium and ytterbium could be obtained in the same supporting electrolyte (Table 1). Europium, but not ytterbium, gave a peak in 0.1 *M* EDTA at pH 4.5 and

TABLE 1

EUROPIUM AND YTTERBIUM PEAKS IN VARIOUS SUPPORTING ELECTROLYTES

Total concn. of Eu and Yb is $0.59 \cdot 10^{-3}$ *M* and $0.52 \cdot 10^{-3}$ *M*, respectively.

No.	*Supporting electrolyte*	*Peak potential against Hg pool anode (V)*		*Peak current (μA)*	
		Eu	*Yb*	*Eu*	*Yb*
1.	0.1 *M* EDTA	−1.20	No wave	4.1	Nil
2.	0.1 *M* phthalate	−0.84	No wave	4.4	Nil
3.	0.017 *M* acetate	−0.95	−1.50	5.25	6.8

TABLE 2

EFFECT OF VARYING ACETATE CONCENTRATION ON EUROPIUM AND YTTERBIUM PEAKS

1 ml of Yb or Eu soln. (1 ml = 900 μg) + appropriate quantities of acetate buffer soln. were made up to 10 ml. Peak current for Yb is calculated the same way as i_d on d.c. polarograph.

Supporting electrolyte (ml)	*Peak voltage vs. Hg pool (V) Eu*	*Peak current Eu (μA)*	$E_{\frac{1}{4}}$ *Yb (V)*	*Peak current Yb (μA)*
1	−0.96	6.2	−1.5	6.8
2	−1.02	6.6	−1.62	7.0
4	−1.1	5.2	−1.67	6.4
6	−1.13	5.2	−1.70	5.2

in phthalate buffer supporting electrolyte. In acetate buffer, however, both europium and ytterbium yielded good peaks. Acetate buffer was therefore chosen as a suitable supporting electrolyte for further work.

From the results given in Table 2, it can be seen that for both elements, the current increases slightly with increasing concentration of the supporting electrolyte and then drops again after an optimum value is reached, while the peak potentials are shifted slightly to the negative side. Europium gives an "S"-shaped wave below a concentration of 2 ml of acetate buffer/10 ml of solution and a peak at 2 ml, but the peak broadens above this concentration. With ytterbium, an "S"-shaped wave

precedes the hydrogen wave. However, on increasing the acetate concentration above 2 ml, the two waves tend to merge; 2 ml of the acetate buffer in a total volume of 10 ml was found to be most suitable, and was used for further work.

Effect of hydrazine on ytterbium curves

During our work (to be published) on the polarography of uranium, it was observed that hydrazine stabilised U(V) ions to a certain extent. Hydrazine was therefore tried as a constituent of the supporting electrolyte for europium and ytterbium.

Hydrazine alone was not a useful supporting electrolyte. On the addition of hydrazine to acetate supporting electrolyte, an irregular hydrazine peak was obtained at about −0.90 V. Since europium has a similar reduction potential in this region, no further studies were carried out with europium in mixed acetate–hydrazine media.

Ytterbium reduction was studied in 0.5 g hydrazine and acetate medium and an increase in current was observed in this medium compared to the acetate medium alone. Various hydrazine salts, *e.g.*, sulphate, chloride, hydrate, were tried and it was found that for the same amount of hydrazine the increase in current is the same, irrespective of the nature of the salt. The hydrazine salt solution must be freshly prepared because the ytterbium peak disappeared in a two-days-old hydrazine solution mixed with freshly prepared acetate. Ammonium acetate buffer solution with hydrazine, gave sharper curves for ytterbium than did sodium acetate buffer with hydrazine.

Effect of pH on ytterbium curves in hydrazine–acetate medium

The pH was adjusted by means of hydrochloric acid or ammonia. No ytterbium curve was observed at pH 4 (Table 3). At pH 5, an "S"-shaped curve was obtained,

TABLE 3

CHANGE OF CURRENT AND POTENTIAL WITH PH

900 μg/ml Yb, 2 ml acetate buffer soln. and 0.5 g hydrazine, as sulphate, were made up to 10 ml after appropriate pH adjustment.

pH	*Current (μA)*	*Potential (vs. Hg-pool anode)*
4	No wave	—
5	8.0	−1.50
6	7.2	−1.55
7	6.4	−1.60

which changed to a peak at pH 6–7. The resolution between ytterbium and hydrogen curves is better at higher pH.

The current decrease and the reduction potential shifts to the negative side from pH 5–7. Hydrogen ions help the process of disproportionation[2] and this explains the decreasing current with increasing pH.

Effect of changing hydrazine concentration at pH 5.0

The hydrazine concentration was changed from 0.1 to 0.6 g in a 10-ml solution

containing 900 μg ytterbium and 2.0 ml acetate buffer solution (Table 4). The peak current rises with increasing hydrazine concentration and levels off at 0.5 g; since above 0.6 g of hydrazine, the ytterbium curve tends to merge with the hydrogen peak, 0.5 g hydrazine was taken to be the optimum concentration.

TABLE 4

EFFECT OF VARYING QUANTITIES OF HYDRAZINE ON YTTERBIUM CURVES

Amount of hydrazine (g)	*Potential (vs. Hg pool anode)*	*Current (μA)*
Nil	−1.50	6.3
0.1	−1.55	6.8
0.2	−1.53	6.4
0.3	−1.51	8.4
0.5	−1.51	8.8
0.6	−1.51	8.8

TABLE 5

DETERMINATION OF EUROPIUM AND YTTERBIUM IN MONAZITE SAND

Element determined	*Supporting electrolyte*	*Addition (%)*	*Found (%)*	*Recovery*
Yb	Acetate only	Nil	0.32; 0.32	
Yb	Acetate only	0.12 (500 μg Yb)	0.44	100%
Yb	Acetate only	0.24 (1000 μg Yb)	0.56	100%
Yb	Acetate + hydrazine	Nil	0.33; 0.33; 0.33; 0.31; 0.33	
Eu	Acetate only	Nil	0.0166 (mean of 3 values)	

It was not possible to make a detailed study of the reason for increase in current, because of the close proximity of the ytterbium and hydrogen curves. A similar effect was noted in the case of uranyl ion, and the results will be reported later.

Linearity of current for various ytterbium concentrations

Linearity was observed from 1–1000 μg/ml of ytterbium or europium in acetate buffer medium. Linearity was also tested for the same ytterbium concentration range in hydrazine (0.5 g)–acetate buffer medium. For 900 μg of ytterbium, a higher current (*ca.* 40%) was obtained in the mixed medium compared to the acetate medium. This increase was obtained for all concentrations of ytterbium and a very good linearity was obtained in the mixed medium.

Effect of other rare earths

Cerium(IV) is reported to give a wave in acetate medium[6]. Cerous salts were found not to interfere in the ytterbium estimation. Samarium did not give a wave in acetate medium but in the presence of large quantities of samarium (5 : 1), the ytterbium

wave was ill-formed. However, even for very high concentrations of samarium, ytterbium can be estimated by using the derivative circuit of the cathode-ray polarograph. Europium and ytterbium waves were taken in the presence of large quantities of other rare earths and these were found not to interfere.

Estimation of europium and ytterbium in monazite

1 g of monazite was decomposed by 2.5 ml of sulphuric acid (conc.). The insolubles were filtered off and the solution was made up to 50 ml. From an aliquot equivalent to 0.4 g monazite, rare earths were precipitated as oxalates and ignited to oxides. The oxide was dissolved in 5 ml of hydrochloric acid with the addition of a few drops of hydrogen peroxide. Cerium is in the cerous state in chloride medium and will not interfere in the estimation. The solution was evaporated to dryness and the polarogram taken, after the addition of acetate buffer solution, for the estimation of europium and ytterbium. The ytterbium estimation was carried out in the presence of hydrazine using the method of standard addition. The mean value of ytterbium in monazite was found to be 0.32% and that of europium, 0.0166% (Table 5). This value for europium is in reasonably good agreement with the previously reported value of 0.016%[1].

The estimations in acetate medium were carried out on a 0.4-g monazite sample. In the presence of hydrazine, however, a sample weight of 0.2 g is sufficient.

SUMMARY

Of the various electrolytes investigated, acetate buffer was found to be a suitable supporting electrolyte for the simultaneous determination of ytterbium and europium. The addition of hydrazine to the acetate buffer gave an irregular hydrazine reduction wave at −0.90 V and the analysis of europium in the mixed supporting electrolyte medium was not feasible. The ytterbium wave was found to increase as a result of the addition of hydrazine to the acetate buffer. The effect of variation in concentration of hydrazine, pH etc., was studied for ytterbium. None of the other rare earths interfered. Ytterbium and europium were determined in monazite sand.

REFERENCES

1 V. T. ATHAVALE, R. G. DHANESHWAR AND M. M. MEHTA, *Anal. Chim. Acta*, 23 (1960) 71.
2 H. A. LAITINEN AND W. A. TAIBEL, *Ind. Eng. Chem., Anal. Ed.*, 13 (1947) 1.
3 *Dana's System of Mineralogy*, edited by C. PALACHE, H. BERMAN AND C. FRONDEL, Vol. II, John Wiley and Sons Inc., New York, 7th ed., 1951, p. 694.
4 S. I. JOHNSTONE, *Minerals for Chemical and Applied Industries*, Chapman and Hall Ltd., London, 1954, p. 523.
5 D. N. WADIA, *Symposium on Rare Metals*, Atomic Energy Establishment, Trombay, and the Indian Institute of Metals, Bombay, 1957, p. 1.
6 O. P. AGARWAL AND R. C. KAPOOR, *Talanta*, 10 (1963) 316.

A STUDY OF TRANSFERENCE AND SOLVATION PHENOMENA OF HYDROCHLORIC ACID IN WATER–DIOXANE SOLVENTS

JAMES R. BARD AND EDWARD S. AMIS
University of Arkansas, Fayetteville, Arkansas (U.S.A.)
JAMES O. WEAR
Sandia Laboratory, Albuquerque, New Mexico (U.S.A.)
(Received May 25th, 1965)

In this contribution to the series of investigations, the transport and solvation phenomena of the ions of hydrochloric acid in water–dioxane solvents have been observed. The transference numbers of hydrochloric acid in water–dioxane solvents had been previously measured[1], but no solvation data were available that could be compared with the water–ethanol system[2] to further the understanding of solvation theory. It was hoped also that the dioxane would break up the Grotthus-type conductance and allow the actual measurement of the movement and solvation of the hydrogen ion. Solvation data could not be taken in solvents with more dioxane than 85 wt % because the water–dioxane–HCl system separates into two layers[3a,3b].

EXPERIMENTAL

The hydrochloric acid was prepared by bubbling hydrogen chloride gas through either water or dioxane. The hydrogen chloride gas was prepared in a generator from Fisher Certified Reagent-Grade sodium chloride and reagent sulfuric acid. The dioxane was Fisher Certified Reagent-Grade. The inert reference substance, α-methyl-D-glucoside, was prepared by Nutritional Biochemical Corporation. The silver wire and all other chemicals were of reagent quality. A Hittorf transference measurement with the use of an inert reference substance was the method for the determination of the transport and solvation data. This is the same method as has been described previously[4].

TREATMENT OF DATA

The symbols used in this paper are the same as were used in the lithium chloride study[4].

The Hittorf transference number of the cation and anion, respectively, and the grams of solvent transferred per faraday of electricity were calculated, as already described[5,6], using the following equations:

$$t_c = \left(\frac{P_s^m}{100 - P_s^m} - \frac{P_s^m}{100 - P_s^a}\right) \frac{W(100 - P_s^a) A_{Ag}}{100 W_{Ag} M_s} \qquad (1)$$

$$t_a = 1 = t_c \tag{2}$$

$$\Delta G_{sol}{}^F = \left(\alpha_a \frac{d_m}{d_a} - \alpha_m \frac{(1-f_s{}^a)}{(1-f_s{}^m)}\right) \frac{W'}{F\alpha_m} \tag{3}$$

The data for Figs. 1 and 2 are tabulated in Table 1. Figures 1 and 2, respectively, give the cation transference numbers and the grams of solvent transferred from

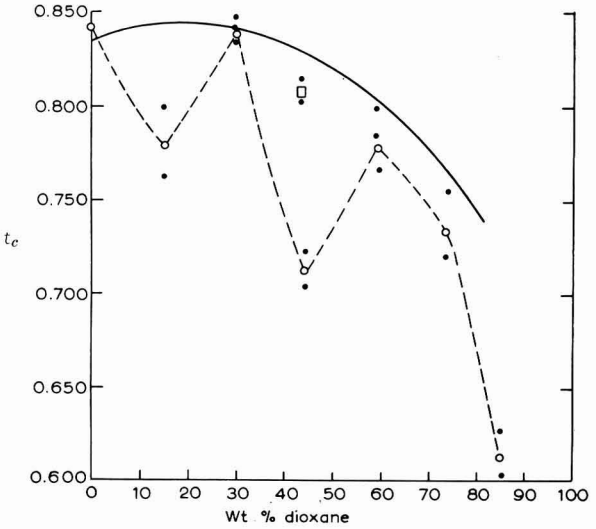

Fig. 1. Smooth curve of HARNED AND DREBY.
Cation transference number at 0.19 moles HCl/1000 g of soln. plotted against wt% dioxane in the solvent at 25°. (○), with sugar; (□), without sugar.

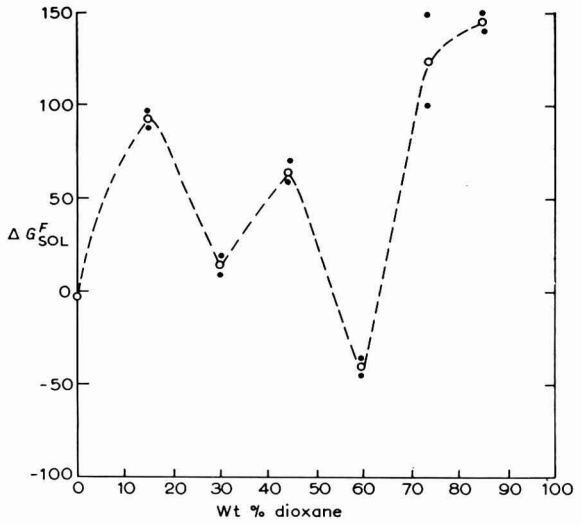

Fig. 2. Calc. grams of solvent transferred from anode to cathode/faraday of electricity at 0.19 moles of HCl/1000 g of soln. plotted against wt% dioxane in the solvent at 25°.

TABLE 1

HITTORF TRANSFERENCE NUMBERS AND GRAMS OF SOLVENT TRANSPORTED FROM THE ANODE TO THE

Wt % dioxane	*15.1*	*15.1*	*15.1*	*30.0*	*30.0*	*30.6*	*43.9*
Concn. HCl (moles/ 1000 g of soln.)	*0.189*	*0.190*	*0.195*	*0.213*	*0.213*	*0.225*	*0.194*
α_m	10.411	10.579	—	6.714	6.714	—	—
α_a	10.438	10.599	—	6.719	6.717	—	—
Ag_1	0.50128	0.37248	0.86910	0.82223	0.82602	0.95848	0.80280
Ag_2	0.50185	0.37244	0.86962	0.81736	0.82606	0.95849	0.80290
$F \cdot 10^{-3}$	4.65	3.45	8.06	7.60	7.66	8.88	7.44
W	212.3672	210.4803	209.7466	215.4285	215.4463	215.2667	213.2272
$C_a{}^x$	0.172	0.177	0.166	0.183	0.183	0.191	—
t_c	0.779	0.799	0.759	0.845	0.836	0.833	0.809
t_a	0.221	0.201	0.241	0.155	0.164	0.167	0.191
d_m	1.01967	1.01986	—	1.02786	1.02786	—	—
d_a	1.01953	1.01978	—	1.02694	1.02676	—	—
$\Delta G_{sol}{}^F$	96.55	90.94	—	16.8	12.5	—	—

the anode to the cathode per faraday plotted *vs.* wt % dioxane in the solvent at a hydrochloric acid concentration of 0.19 mole/1000 g of solution.

In Fig. 1, our data are compared with the smoothed curve of the data of HARNED AND DREBY[1], which were taken by e.m.f. measurements (there is some question whether e.m.f. and Hittorf numbers are the same). All the water–dioxane points fall below this smoother curve. Also, at 45 wt % dioxane there is a large difference between t_c measured with the inert reference substance present and t_c measured in the absence of the inert reference substance. This indicates that α-methyl-D-glucoside is reacting in some way with the ions of hydrochloric acid.

In pure water, our value of the transference number in 0.19 mole of hydrochloric acid/1000 g of solution extrapolates to within about 6 parts in 835, or to within 0.7 % of the accepted value of HARNED AND DREBY. Actually, HARNED AND DREBY rounded off their values of transference number, giving more weight to the values obtained at concentrations above 0.03 *M*. Their smoothed values were from curves showing maxima and minima, and which in some cases showed considerable variation from the smoothed curve.

The value of t_c at 45 wt % dioxane without α-methyl-D-glucoside and the values at 60 and 74 wt % dioxane appear to lie on a curve similar to the smoothed curve and within a few per-cent of it. This indicates that, at concentrations of dioxane higher than 60 wt %, α-methyl-D-glucoside has little or no effect on the mobility of the ions. The value of t_c at 85 wt % dioxane appears to be too low when compared to the termination of the smoothed curve at 82 wt % dioxane. However, since in this region, the breaking up, by the large excess of dioxane present, of the hydrogen-bonded water chains could rapidly eliminate the possibility of Grotthus conductance, t_c could decrease rapidly as indicated.

Since, in water–ethanol, no effect of α-methyl-D-glucoside on t_c was observed, it is hard to explain the effect of the sugar on t_c in certain regions of solvent composition. It cannot be a hydrolysis or any chemical reaction with the hydrogen or chloride

CATHODE FOR HCl SOLUTE AT 25°

43.9	*44.5*	*44.5*	*59.1*	*59.1*	*73.8*	*73.8*	*85.0*	*85.0*
0.194	*0.191*	*0.191*	*0.193*	*0.193*	*0.191*	*0.191*	*0.256*	*0.256*
—	10.628	10.628	10.855	10.885	10.807	10.807	15.264	15.113
—	10.653	10.654	10.875	10.876	10.869	10.845	15.344	15.195
0.76706	0.66900	0.74988	0.77226	0.74481	0.85519	0.75639	0.79802	0.84132
0.76531	0.66837	0.74950	0.77164	0.74481	0.85499	0.75634	0.79772	0.84103
7.10	6.20	6.95	7.15	6.90	7.93	7.01	7.40	7.80
215.675	215.9179	215.1669	215.7414	215.0248	217.0682	216.7817	218.7664	218.4684
—	0.171	0.168	0.167	0.169	0.164	0.168	0.236	0.234
0.799	0.703	0.719	0.795	0.760	0.749	0.718	0.600	0.623
0.201	0.297	0.281	0.205	0.240	0.251	0.282	0.400	0.377
—	1.03948	1.03948	1.04427	1.04427	1.04448	1.04448	1.04684	1.04653
—	1.03913	1.03908	1.04392	1.04398	1.04382	1.04396	1.04628	1.04634
—	68.4	61.5	−46.7	−44.5	147.3	98.0	149.1	135.3

ions, since the rotations of the solutions do not change on standing. This also eliminates a reaction with the solvent.

Since the sugar obviously interferes with the mobility of the ions, Fig. 1 must be explained, at least partially, from this point of view. From pure water to 15 wt % dioxane, two possibilities exist: (1) the hydrogen ion is solvated by the sugar, which would cause t_c to be lower, but the sugar moving with the hydrogen ion would cause $\Delta G_{sol}{}^F$ to decrease, which is not the case (Fig. 2), and (2) the sugar and the dioxane break up the structure of water and thus decrease the Grotthus conductance of the hydrogen ion which would cause t_c to decrease.

From pure water to 15 wt % dioxane, t_c decreases to below the literature value and $\Delta G_{sol}{}^F$ increases. The sugar and the dioxane participate in the breaking up of the water structure so that the water chains formed by hydrogen bonds between water molecules are shortened or, in some cases, perhaps destroyed. The fewer hydrogen ions reaching the cathode region carry more solvent to the cathode because more of the hydrated hydrogen ions $(H_9O_4^+)^{7-9}$ with their solvent sheaths move into the cathode from the middle region, instead of numbers of the ions being released as unsolvated particles from the ends of hydrogen-bonded water chains and perhaps concomitantly becoming associated with water already in the cathode compartment.

From 15–30 wt % dioxane, t_c increases almost to the literature value and $\Delta G_{sol}{}^F$ decreases. If the hydrogen ion ties up the sugar, the sugar would be less important in breaking up the solvation structure and Grotthus conductance would again become important. This would cause t_c to increase in the presence of sugar, and the movement of the sugar would cause $\Delta G_{sol}{}^F$ to decrease because of the method of measurement used.

From 30–45 wt % dioxane, t_c decreases and $\Delta G_{sol}{}^F$ increases. The decrease in t_c with sugar present is to a value well below that recorded in the literature, but when no sugar is present, the value of t_c is near that recorded in the literature. The decrease in t_c when sugar is present is in part due, perhaps, to the continued breaking up by the

sugar and dioxane of the Grotthus conductance, but is also possibly partly due to the continuing solvation by sugar to some extent in the outer sheath of solvation of the hydrogen ion, and to the beginning of solvation by dioxane in this sheath, thus decreasing the mobility of the hydrogen ion. The amount of dioxane entering the outer solvation sheath of hydrogen ion must more than compensate for its loss in solvent-carrying capacity, due to loss of mobility and to any solvation by sugar, thus permitting $\Delta G_{sol}{}^{F}$ to increase.

From 45–60 wt % dioxane, the dioxane continues to break up the water structure. This would tend to decrease t_c and does so when sugar is absent. Also, while the effectiveness of sugar in influencing Grotthus conductance is no doubt reduced in this range of solvent composition, with the resulting decrease in dielectric constant and the consequent attraction of the sugar to a greater extent into the solvation sphere of the hydrogen ion, yet the residual effect of the sugar, in influencing the proton-jump mechanism of movement of hydrogen ion, would tend to decrease t_c. However, the inner layer of water in the chloride ion begins to be replaced by dioxane. The predominant influence on t_c in this range of solvent composition is presumably the comparative increase in bulk and mass of the chloride as contrasted with the hydrogen ion, thus causing an increase in t_c. In this range of solvent composition, the sugar in the solvation sheath of hydrogen ion perhaps excludes dioxane from extensively solvating the hydrogen ion, but does tend to cause $\Delta G_{sol}{}^{F}$ to decrease. The increased mass of solvent carried by the chloride ion compensates its lesser mobility to the extent that its net solvent-carrying capacity is increased. This effect also contributes to the decrease in $\Delta G_{sol}{}^{F}$.

Above 60 wt % dioxane, the dioxane by sheer statistical predominance gradually replaces sugar and even, to some extent, water in the solvation layers of solvated hydrogen ion, in proportions sufficient to increase the size and decrease the mobility of the ion so that t_c continually decreases. Again, however, the increased mass of solvation more than compensates for the decreased mobility as to solvent-carrying capacity of the solvated hydrogen ion, and $\Delta G_{sol}{}^{F}$ increases continually. Further, in this range of dioxane composition, the remaining Grotthus conduction no doubt rapidly vanishes, thus contributing to the decrease in t_c and to the increase in $\Delta G_{sol}{}^{F}$.

A comparison of the present data with the transference and solvation data of the ions of hydrochloric acid in water–ethanol solvents shows that α-methyl-D-glucoside does not affect the mobility of the ions in the water–ethanol system, but does affect the mobility of the ions in the water–dioxane system. Likewise, the sugar plays a role in the solvation of the hydrogen ion in the water–dioxane system, but apparently plays no part in the solvation of the hydrogen ion in the water–ethanol system, at least up to about 90 wt % ethanol. This indicates that α-methyl-D-glucoside, in certain ranges of dioxane concentration, is solvating the hydrogen ion simultaneously with the dioxane, whereas alcohol as a component of the solvent, in general prevents solvation of hydrogen ion by the sugar. This probably means a preference in solvation by the polar hydroxy alcohol as compared to the dioxane, a non-polar internal ether. This preferential solvation by the polar hydroxy alcohol completely prevented solvation by the sugar, at least up to about 90 wt % ethanol. Whether it is the non-polar or hydroxy nature of the alcohol that caused this preferential solvation could be clarified by studying the transference and solvation

phenomena of hydrochloric acid in methyl alcohol–ethyl ether or ethyl alcohol–ethyl ether solvents. The ethyl ether has a dipole moment of 1.2 debye units, which is not too different from that of the alcohols, 1.7 debye units.

ACCURACY AND PRECISION

By comparing cation transference numbers at equal solute concentrations, the average deviation from the average is $\pm 2.0\%$, which is the accuracy of the method. The average deviation from the average is $\pm 7.2\%$ for the solvation, by comparing values at equal solute concentrations.

ACKNOWLEDGEMENT

The authors thank the Atomic Energy Commission for Contract At-(40-1)-2069, which financially supported the experimental research.

SUMMARY

Transference and solvation phenomena for the ions of hydrochloric acid in water–dioxane solvents have been studied. The cation transference number and the grams of solvent transferred from anode to cathode are presented graphically as a function of solvent composition. The data are discussed in terms of the nature and extent of solvation of the ions of hydrochloric acid by the components of the solvent and the reference substance, α-methyl-D-glucoside. Comparison is made with the transference and solvation data of the ions of hydrochloric acid in the ethanol–water system.

REFERENCES

1 H. S. HARNED AND E. C. DREBY, *J. Am. Chem. Soc.*, 61 (1939) 3113.
2 J. O. WEAR, J. T. CURTIS, JR. AND E. S. AMIS, *J. Inorg. Nucl. Chem.*, 24 (1962) 93.
3a) W. T. GRUBB AND R. C. OSTHOFF, *J. Am. Chem. Soc.*, 74 (1952) 2108.
b) R. A. ROBINSON AND R. C. SELKIRK, *J. Chem. Soc.*, (1948) 1460.
4 J. O. WEAR, C. V. MCNULLY AND E. S. AMIS, *J. Inorg. Nucl. Chem.*, 18 (1961) 48.
5 D. M. MATHEWS, J. O. WEAR AND E. S. AMIS, *J. Inorg. Nucl. Chem.*, 13 (1960) 298.
6 W. V. CHILDS AND E. S. AMIS, *J. Inorg. Nucl. Chem.*, 16 (1960) 114.
7 E. WICKE, M. EIGEN AND T. ACKERMAN, *Z. Phys. Chem. N.F.*, 1 (1954) 340.
8 N. GOLDENBERG AND E. S. AMIS, *ibid.*, 30 (1961) 65.
9 N. GOLDENBERG AND E. S. AMIS, *ibid.*, 31 (1962) 145.

THE POLAROGRAPHIC MEASUREMENT OF THE FORMATION CONSTANTS OF ZINC AND CADMIUM COMPLEXES WITH BIOLOGICALLY IMPORTANT COMPOUNDS

IRWIN H. SUFFET* AND WILLIAM C. PURDY
Department of Chemistry, University of Maryland, College Park, Md. (U.S.A.)
(Received May 21st, 1965)

INTRODUCTION

As a consequence of the ability of metal ions to bind to amino acids and proteins, metallic ions influence metabolic processes upon which living organisms depend. Metals bound in co-ordination compounds of many varieties are widely distributed in the body. SCHROEDER[1] describes the essential catalytic functions in the body, of zinc, copper, cobalt and manganese. Other metallic ions that are suspected of essential activity are rubidium, boron, strontium, vanadium, chromium, nickel and aluminum. Silver and lead are known contaminants. Cadmium, tin and titanium are metals which are environmentally acquired and accumulated. Cadmium shows high accumulation in the kidneys and liver although it is absent in infants.

In vital life processes, metal ions are usually needed as part of the enzyme and transport systems. Recent investigations on the activity of drugs in the body have indicated possible metal–drug interactions. Each of these three systems shows the essential activity of metal co-ordination with amino acids and proteins.

In the present paper, the polarographic method has been applied to measure the apparent formation constants of complexes of zinc and cadmium. Among the metal-binding agents used were cysteine, penicillamine, salicylates, hydroxyquinones and alloxan. The supporting electrolyte was an orthophosphate buffer of pH 7.4. This medium was chosen as it is one of the major buffering systems of the blood. This work represents an extension of work already carried out with copper(II)[2].

EXPERIMENTAL

All polarographic studies were carried out in orthophosphate buffers of ionic strength 0.2 *M*. The directions for the preparation of these buffers have been described elsewhere[3]. Polarographic measurements were made with a Sargent Model XV polarograph. The potential settings of this instrument were calibrated with a Leeds and Northrup Model 8687 potentiometer. A Leeds and Northrup Polarotron dropping mercury electrode assembly was employed for the polarographic cell. The sample compartment of the Polarotron was thermostatted at $25 \pm 0.2°$. The sample solution was placed in the Polarotron and flushed with nitrogen gas for 15 min. During the

* Present address: Department of Environmental Science, Rutgers University, New Brunswick, New Jersey.

course of the polarogram, a nitrogen atmosphere was maintained above the sample solution. The nitrogen employed was deoxygenated by passage through two solutions of chromous sulfate and one of the supporting electrolyte before entrance into the Polarotron.

The resistance of the Polarotron was determined to be 1880 Ω as calculated by the technique of MEITES[4]. All potential measurements were corrected for iR drop.

Reversibility of the electrode reactions was tested by determining the slopes of the log $(i_d - i)/i$ *vs.* E plots. Data for these plots were obtained by manual operation of the polarograph. The calculation of the formation constants from polarographic data has been described elsewhere[5].

Thiosalicylic acid was obtained from Evans Chemetics, Inc. DL-Penicillamine and L-cysteine (free base) were purchased from Nutritional Biochemicals Corp. Lawsonne (2-hydroxy-1,4-naphthoquinone) was obtained from Dr. ERNEST PRATT of the Department of Chemistry, University of Maryland. Phthiocol (2-hydroxy-3-methyl-1,4-naphthoquinone) was synthesized by the procedure of FIESER[6]. Aspirin was synthesized by the procedure of ADAMS AND JOHNSON[7] and thioaspirin by the same procedure except that thiosalicylic acid was used as the starting material and the product was recrystallized from benzene instead of ether. Alloxan monohydrate was purchased from Eastman Organic Chemical Co. and purified by the procedure of SPEER AND DOBOVICK[8]. The polarographic maximum suppressor, Triton X-100, was provided by courtesy of Rohm and Haas Co.

RESULTS AND DISCUSSION

The polarographic data for the reduction of cadmium and zinc in a variety of orthophosphate buffers of ionic strength 0.2 M are collected in Tables 1 and 2. These data were all collected on solutions thermostatted at $25 \pm 0.2°$ and the potentials were corrected for iR drop. Cadmium was reversibly reduced over the entire pH range while zinc was irreversibly reduced over this pH range. At a pH of 7.4, zinc was found to have an α-value of 1.0. Above pH 5, colloidal suspensions develop in both the cadmium and zinc solutions and it is these colloidal suspensions that are reduced at the dropping mercury electrode (D.M.E.). Electrocapillary curves indicated that there was no adsorption of the metal orthophosphate species on the D.M.E.

TABLE 1

POLAROGRAPHIC DATA FOR THE REDUCTION OF CADMIUM AT $25 \pm 0.2°$

Supporting electrolyte is an orthophosphate buffer of ionic strength 0.2 M

pH	$m^{2/3}t^{1/6}$ $(m^{2/3}sec^{-1/2})$	$E_{1/2}$ *vs.* S.C.E. *(V)*	*Concn. (mM)*	i_d *(μA)*	I_d $(i_d/cm^{2/3}t^{1/6})$
3.00	2.18	−0.594	0.100	0.780	3.59
4.50	2.16	−0.597	0.100	0.690	3.20
5.40	2.17	−0.603	0.100	0.648	3.00
6.20	2.16	−0.604	0.100	0.648	3.00
7.40	2.16	−0.611	0.100	0.648	3.00
8.00	2.17	−0.612	0.100	0.178	0.82
9.20	2.16	−0.626	0.100	0.080	0.38
10.40	—	slight wave	0.100	—	—

Infra-red examination of the cadmium and zinc orthophosphates indicate that at pH 7.4 the colloidal suspension is a mixture of the metal mono- and di-hydrogen orthophosphate, which is reduced[9].

In Table 3 are collected the apparent formation constants for complexes formed between zinc, cadmium and nickel and several biologically important compounds. At pH 7.4, cysteine, penicillamine and 2-mercaptoethylamine compete successfully with the colloidal metal orthophosphate for the metal ion. The bonding groups in these compounds, the thiol and amino groups[10], form strong enough bonds to strip the metal from the orthophosphate compound.

TABLE 2

POLAROGRAPHIC DATA FOR THE REDUCTION OF ZINC AT 25±0.2°

Supporting electrolyte is an orthophosphate buffer of ionic strength 0.2 *M*

pH	$m^{2/3}t^{1/6}$ $(m^{2/3}sec^{-1/2})$	$E_{1/2}$ *vs. S.C.E.* *(V)*	*Concn.* *(mM)*	i_d *(μA)*	I_d $(i_d/cm^{2/3}t^{1/6})$
3.00	2.13	−1.000	0.100	0.860	4.04
4.60	2.17	−1.004	0.100	0.890	4.10
5.40	2.11	−1.022	0.100	0.780	3.68
6.50	2.17	−1.056	0.100	0.860	3.96
7.40	2.12	−1.071	0.100	0.630	2.92
8.00	2.21	−1.081	0.100	0.240	1.09
9.20	—	−1.110	0.100	0.040	—
10.40	—	No wave	0.100	—	—

TABLE 3

CALCULATED APPARENT FORMATION CONSTANTS OF METAL COMPLEXES

pH	*Ligand*	*Zn*	*p*	*Cd*	*p*	*Ni*	*p*
Group I. Cysteine, penicillamine							
7.4	L-cysteine	complex		$7.8 \cdot 10^9$	2		
7.4	DL-penicillamine	$1.3 \cdot 10^{13}$	3	$1.2 \cdot 10^{13}$	3		
7.4	2-mercaptoethylamine	$1.5 \cdot 10^6$		$1.1 \cdot 10^9$	2		
Group II. Salicylates							
7.4	salicylic acid	none		none		none	
7.4	thiosalicylic acid	complex		$4.2 \cdot 10^9$	2	$1.6 \cdot 10^{19}$	3
7.4	aspirin	none		none		none	
7.4	thioaspirin	none		$2.4 \cdot 10^4$	1	complex	
Group III. Hydroxyquinones							
7.4	lawsonne	$3.1 \cdot 10^8$	2	$3.2 \cdot 10^8$	2	complex	
7.4	phthiocol	$1.4 \cdot 10^{12}$	3	$5 \cdot 10^{11}$	3	complex	

All supporting electrolytes are orthophosphate unless otherwise noted. $\alpha = 1.0$ for zinc, $\alpha = 0.9$ for nickel.

Table 4 shows the effect of the supporting electrolyte on the apparent formation constant of the metal complexes. The potentiometric data were determined in a supporting electrolyte of 0.15 *M* potassium nitrate, a medium which does not react with the metal ions. Certain comments should be made about the data in Table 4. KUCHENSKAK AND ROSEN[12] assumed the co-ordination number, *p*, to be 2 for the zinc–penicillamine complex as this complex was comparable to the copper- and mer-

cury–penicillamine complexes. By using the approximate method of construction of MITZNER[13], p is found to be 3 for the zinc complex by the polarographic method.

RAO AND SUBRAHMANYA[14] found p to be equal to 3 for cadmium–amino acid complexes in 1 M potassium nitrate at pH-values between 11.3 and 12.3. LI AND MANNING[10] have found lead to have a co-ordination number of 3 in cysteine complexes; lead–penicillamine complexes show[12] a co-ordination number of 2.

TABLE 4

FORMATION CONSTANTS OF METAL COMPLEXES OF CYSTEINE AND RELATED LIGANDS

Cation	*Method*	*Cysteine*	*p*	*Ref.*	*Penicillamine*	*p*	*Ref.*	*2-MEA*	*p*	*Ref.*
Zn	poten.	$1.6 \cdot 10^{18}$	2	10	$7.8 \cdot 10^{18}$	2	12	$5 \cdot 10^{18}$	2	10
		$5 \cdot 10^{18}$	2	11						
Zn	polar.	complex		T.III	$1.3 \cdot 10^{16}$	3	T.III	$1.5 \cdot 10^{6}$	2	5
Cd	poten.	ppt.		11	$3.1 \cdot 10^{18}$	2	12	$5.6 \cdot 10^{19}$	2	10
Cd	polar.	$7.8 \cdot 10^{9}$	2	T.III	$1.2 \cdot 10^{13}$	3	T.III	$1.1 \cdot 10^{9}$	2	5
Cu(II)	poten.	ppt.		11	$5 \cdot 10^{21}$	2	12			
Cu(II)	polar.	$1 \cdot 10^{17}$	2	5	$1.3 \cdot 10^{15}$	2	5	$1.7 \cdot 10^{16}$	2	5

Potentiometric determination carried out in 0.15 M potassium nitrate; polarographic determination in orthophosphate buffers of ionic strength 0.2 M.
2-MEA is 2-mercaptoethylamine.
Ppt. means a precipitate was reported.
T.III means the data were taken from the previous table.

TABLE 5

FORMATION CONSTANTS OF METAL–HYDROXYQUINONE COMPLEXES

Cation	*Method*	*Solvent*	*Lawsonne*	*p*	*Ref.*	*Phthiocol*	*p*	*Ref.*
H	poten.	water	$9.1 \cdot 10^{3}$		15	$1.2 \cdot 10^{5}$		15
H	poten.	75% D–W	$1 \cdot 10^{8}$		16	$1.6 \cdot 10^{9}$		16
Cd	poten.	75% D–W	$1.7 \cdot 10^{10}$	2	16	ppt.		16
Cd	polar.	pH 7.4	$3.2 \cdot 10^{8}$	2	T.III	$5 \cdot 10^{11}$	3	T.III
Zn	poten.	75% D–W	$1.3 \cdot 10^{11}$	2	16	$1.7 \cdot 10^{12}$	2	16
Zn	polar.	pH 7.4	$3.1 \cdot 10^{8}$	2	T.III	$1.4 \cdot 10^{12}$	3	T.III

75% D–W means a 75% by volume soln. of dioxan in water.
All other terms have the same meaning as in the previous table.

Table 5 shows the effect of solvent on the apparent formation constants of hydroxyquinone complexes. Complexes of phthiocol are more stable than the corresponding lawsonne complexes. Phthiocol exhibits a co-ordination number of 3 while the value of p for lawsonne is 2. The difference in co-ordination number is apparently caused by the inductive effect of the methyl group in the 3-position on the naphthoquinone ring. The inductive effect of the methyl group is also shown by the fact that phthiocol is a weaker acid than lawsonne[15,16].

The polarographic waves of the zinc– and cadmium–lawsonne complexes show a bend before the diffusion-current plateau. This bend increases as the ratio of ligand-to-metal increases. SUBRAHMANYA[17] suggests that this is an indication of a weak equilibrium between another species of the complex and the prevalent complex species. KIDO, FERNELIUS AND HASS[16] found the instability constants of metal–phthiocol complexes to be greater than the corresponding metal–lawsonne complexes and concluded that the weaker the acid, the more stable the complex.

VINOGRADOVA AND PEDANOVA[18] found polarographically that zinc and cadmium form salicylate complexes in acid media of pH-values less than 6. The instability constant for both the cadmium and zinc complex was $2.96 \cdot 10^{-6}$. Cadmium–salicylate complexes were also studied[19] over the pH range of 5–11.

BUCHER[20] used thiosalicylic acid in a spectrophotometric procedure for the determination of nickel. He reported that this procedure was four times as sensitive as the one employing thioacetic acid. BUCHER did not attempt to formulate the nature of the complex formed.

Alloxan studies

SARTORI AND LIBERTI[21] studied alloxan by the polarographic technique in 0.1 *M* potassium nitrate. They reported two waves at pH-values less than 4. The first wave, at 0.18 V *vs.* S.C.E., was attributed to the reduction of alloxan to dialuric acid; the second wave appeared at −0.59 V *vs.* S.C.E. Above pH 5, the potential of the first wave changed with time. HLADIK[22] reported a shift of the half-wave potential of the first wave through the pH range 1.8–10.7 in Britton–Robinson buffer. HLADIK noted three reduction waves before the hydrogen wave at high pH-values. The first wave was ascribed to the reduction of anhydrous alloxan while the second wave was thought to be the reduction of parabanic acid formed from alloxan. ONO, TAKAGI AND WASU[23] studied alloxan in McIlvaine buffer of pH 3 and reported the half-wave potential of the first wave to be 0.00 V. SARTORI AND LIBERTI[21] reported that alloxanic acid was reduced at −0.59 V in 0.1 *M* potassium nitrate.

In a pH 3 orthophosphate buffer of ionic strength 0.2 *M*, two waves were observed for alloxan, before the hydrogen wave; this was in agreement with the literature[21,22]. At pH 7.4, three waves for alloxan were observed, in agreement with HLADIK[22]. The last wave, at −1.64 V *vs.* S.C.E., was observed to disappear completely with time. This last wave was diffusion-controlled and the diffusion current was proportional to the concentration of alloxan in the bulk of the solution. By following the decrease in diffusion current with time, the half-life of alloxan was determined to be 3.2 min at $25 \pm 0.2°$. This is greater than the 2.2 min that was previously reported[24] by spectrophotometric means in a phosphate medium of ionic strength 0.085 *M*.

Cobalt(II), cadmium, zinc and nickel(II) do not complex with alloxan in a phosphate buffer of pH 7.4. LANGE AND FOYE[25] prepared what they called 1:1 chelates of copper(II), cobalt(II) and nickel(II) alloxan. These appear to be salts. RESNICK AND CECIL[26] have shown that alloxan does not form a copper chelate and that the decomposition product of alloxan is alloxanic acid. They found that in the presence of a basic solution of alloxan, copper(II) does not show any complexation until decomposition to alloxanic acid has been achieved.

ACKNOWLEDGEMENT

The authors are indebted to the Office of the Surgeon General of the U. S. Army for partial support of this work under contract No. DA-49-193-MD-2593.

SUMMARY

The polarography of zinc and cadmium in orthophosphate buffers of various

pH-values has been studied. Infra-red studies of the colloidal suspension formed at pH 7.4 have shown this to be a mixture of the metal mono- and di-hydrogen orthophosphates. The nature and stability of complexes formed between zinc and cadmium and several groups of biologically important compounds has been examined. These compounds include cysteine, penicillamine, salicylates and hydroxyquinones. Finally, the polarography of alloxan has been examined briefly and complex formation between certain metals and alloxan at pH 7.4 has been attempted.

REFERENCES

1 H. A. SCHROEDER, *Metal-Binding in Medicine*, edited by M. J. SEVEN AND L. A. JOHNSON, J. B. Lippincott Co., Philadelphia, 1960, pp. 59–67.
2 P. A. PELLA AND W. C. PURDY, *J. Electroanal. Chem.*, 9 (1965) 51.
3 G. D. CHRISTIAN AND W. C. PURDY, *ibid.*, 3 (1962) 363.
4 L. MEITES, *Polarographic Techniques*, Interscience Publishers, New York, 1955.
5 E. C. KNOBLOCK AND W. C. PURDY, *J. Electroanal. Chem.*, 2 (1961) 493.
6 L. F. FIESER, *Experiments in Organic Chemistry*, D. C. Heath and Co., Boston, 3rd ed. (rev.), 1957, p. 211.
7 R. ADAMS AND J. R. JOHNSON, *Laboratory Experiments in Organic Chemistry*, The Macmillan Co., New York, 4th ed., 1949, p. 451.
8 J. SPEER AND T. DOBOVICK, *Collected Organic Syntheses*, Vol. III, edited by E. C. HORNING, J. Wiley and Sons, New York, 1955, p. 39.
9 F. MILLER AND C. H. WILKINS, *Anal. Chem.*, 24 (1953) 1253.
10 N. C. LI AND D. MANNING, *J. Am. Chem. Soc.*, 77 (1955) 5335.
11 A. ALBERT, *Biochem. J.*, 47 (1950) 531.
12 E. J. KUCHENSKAK AND Y. ROSEN, *Arch. Biochem. Biophys.*, 97 (1962) 370.
13 B. M. MITZNER, *Chemist-Analyst*, 46 (1957) 13.
14 G. N. RAO AND R. S. SUBRAHMANYA, *Current Sci., India*, 31A2 (1962) 55.
15 H. FREISER, *J. Am. Chem. Soc.*, 56 (1934) 1565.
16 H. KIDO, W. C. FERNELIUS AND C. G. HASS, JR., *Anal. Chim. Acta*, 23 (1960) 116.
17 R. S. SUBRAHMANYA, *Advances in Polarography*, Vol. II, edited by I. S. LONGMUIR, Pergamon Press, New York, 1959, p. 689.
18 E. VINOGRADOVA AND V. PEDANOVA, *Metody Analiza Redkikh i Tsvetn. Metal. Mosk. Gos. Univ.*, (1956) 25.
19 V. GOROKHOVSKII AND Y. LEVIN, *Zh. Neorgan. Khim.*, 2 (1957) 343.
20 V. M. BUCHER, *Nature*, 194 (1962) 835.
21 G. SARTORI AND A. LIBERTI, *Ric. Sci.*, 16 (1946) 313.
22 V. HLADIK, Thesis, Charles University, Prague, 1948.
23 S. ONO, M. TAKAGI AND T. WASU, *Bull. Chem. Soc., Japan*, 31 (1958) 364.
24 J. W. PATTERSON, A. LAZAROW AND S. LEVEY, *J. Biol. Chem.*, 177 (1949) 187.
25 W. E. LANGE AND W. O. FOYE, *J. Am. Pharm. Assoc., Sci. Ed.*, 45 (1956) 699.
26 P. A. RESNICK AND H. CECIL, *Arch. Biochem. Biophys.*, 61 (1956) 179.

SHORT COMMUNICATIONS

Suspensionselektrode zur Charakterisierung der Pulverkatalysatoren

Die erstmalig von E. MÜLLER UND K. SCHWABE verwendete Suspensionselektrode[1] wurde in den letzten Jahren mehrfach für elektrochemische und katalytische Untersuchungen eingesetzt[2–6]. P. BOUTRY, O. P. BLOCH UND J. C. BALACEANU[7] schlagen vor, mit Hilfe der Suspensionselektrode durch Aufnahme von Strom–Spannungskurven die katalytische Aktivität von pulverförmigen Katalysatoren zu charakterisieren. Bei sonst gleichen Bedingungen (gleiche Konzentration des Katalysators in der Suspension, gleiche Rührgeschwindigkeit und Überspannung) soll die entnommene Stromstärke ein Mass für die katalytische Aktivität darstellen.

Wir haben mit einer ähnlichen Versuchsanordnung wie diese Autoren mit platinierter und vernickelter Kohle, Raney-Nickel und Platinmohr als Katalysator Strom–Spannungskurven aufgenommen. Bei der anodischen Oxydation von Wasserstoff und Methanol in einer Suspension von platinierter Kohle erhielten wir nur sehr kleine Stromstärken (wenige mA), obwohl sich Wasserstoff und Methanol bei gleichem Katalysator an festen Elektroden sehr gut oxydieren lassen. Weiterhin zeigte sich überraschenderweise, dass diese Stromstärke von der Konzentration des Kohlepulvers in der Suspension unabhängig ist (Abb. 1). Wir konnten nachweisen,

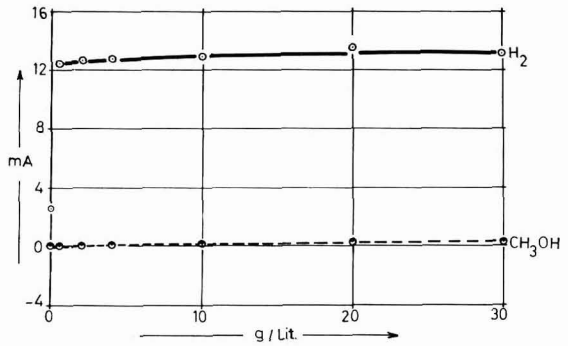

Abb. 1. Abhängigkeit der Stromstärke von der Menge der platinierten Kohle bei Überspannung von 200 mV in 1 *M* H_2SO_4.

dass sich die Suspension des Katalysators am Stromtransport nicht wesentlich beteiligt, sondern dass der Stromfluss auf die an der inerten Ableitungselektrode festhaftenden Katalysatorpartikelchen zurückzuführen ist. Ein völlig anderes Verhalten zeigten dagegen Metallpulver, an denen sich Wasserstoff sehr gut oxydieren lässt. Die Stromstärke ist der Überspannung proportional und wächst mit der Konzentration des Metallpulvers an (Abb. 2). Bei einer Konzentration des Raney-Nickels von 3 g in 50 cm^3 erhielten wir 25 mA bei einer Polarisation von 10 mV.

Wir haben in beiden Fällen katalytisch sehr aktive Pulver untersucht; trotzdem gelang es uns praktisch nicht, der Kohlesuspension einen nennenswerten Strom zu entnehmen, während sich Raney-Nickel und Platinmohr vollkommen anders verhielten. Über den Mechanismus der Ladungsübertragung in diesen Systemen hinsichtlich der Deutung des unterschiedlichen Verhaltens kann bisher nur wenig ausgesagt werden. Vorläufig nehmen wir an, dass die gemessene Stromstärke einer Katalysatorsuspension nicht nur von ihrer katalytischen Aktivität, sondern auch von der Natur der Hemmungen des Ladungsübergangs Katalysatorpartikel/

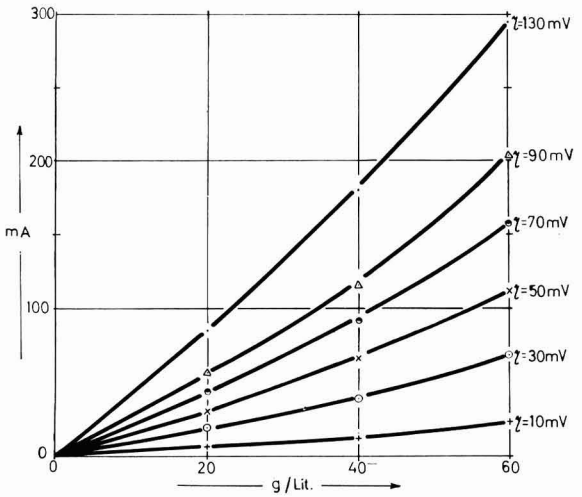

Abb. 2. Abhängigkeit der Stromstärke von der Menge des Raney-Nickels in 1 *M* NaOH mit der Wasserstoffelektrode bei verschiedenen Überspannungen.

Ableitungselektrode abhängig ist. Es wird jedenfalls kaum ein eindeutiger Zusammenhang zwischen der katalytischen Aktivität und der Grösse des Übergangswiderstands bestehen. Deshalb müssen Bedenken geäussert werden, ob die Stromstärke wirklich als ein aussagekräftiges Mass für die Aktivität von Katalysatorpulvern angesehen werden kann.

Institut für Elektrochemie und physikalische Chemie der T.U., Dresden (Deutschland)

K. SCHWABE
A. STAŠKO

1 E. MÜLLER UND K. SCHWABE, *Z. Elektrochem.*, 34 (1928) 170; *Kolloid Z.* 52 (1930) 163.
2 D. H. SOKOLSKIJ, A. B. FASMAN UND A. H. BYKOV, *Vestn. Akad. Nauk Kaz.SSR*, 18 (1962) 45.
3 H. GERISCHER, *Ber. Bunsenges.*, 67 (1963) 164, 921.
4 JU. A. PODVJAZKIN UND A. J. SCHLYGIN, *Zh. Fyz. Khim.*, 6 (1957) 1305.
5 F. BECK, *Ber. Bunsenges.*, 69 (1965) 199; R. M. LAZARENKO-MANEWITZSCH UND A. V. USCHAKOV, *Dokl. Akad. Nauk SSSR*, 161 (1965) 157.
6 K. SCHWABE, *Z. Elektrochem.*, 61 (1957) 744.
7 P. BOUTRY, O. P. BLOCH UND J. C. BALACEANU, *Compt. Rend.*, 254 (1962) 2583.

Eingegangen den 5ten September, 1965

The polarographic investigation of the composition and stability constants of the benzoate complexes of cadmium

Cadmium forms complexes with various ligands. The thiocyanate complexes of cadmium have been studied polarographically by workers[1,2] using the DeFord and Hume method for step-wise complex formation; the chloro- and bromo-complexes of cadmium have been determined by ERIKSSON[3]; the polarographic behaviour of cadmium–amino complexes has been investigated by NAGESWARA RAO AND SUBRAHMANYA[4], and SARTORI[5] has studied the oxalate and pyrophosphate complexes of cadmium polarographically. During a polarographic study of cadmium in various supporting electrolytes, it was observed that the reduction is reversible and diffusion-controlled in sodium benzoate solution. The half-wave potential shifted towards more negative values with increase in concentration of sodium benzoate, indicating the possibility of complexing between cadmium and benzoate ion[6]. The present paper reports on the composition and stability constants of the complexes formed by cadmium with benzoate ion.

Experimental

All chemicals used were of reagent-grade purity. The solution of Cd^{2+} was prepared by dissolving a weighed amount of cadmium nitrate in distilled water; it was standardised using an established method. The ionic strength (0.1) was kept constant by the addition of the requisite amount of sodium nitrate and sodium benzoate was used as a complexing agent. Triton X-100, supplied by Rohm and Hass Co., was employed as a maximum suppressor (0.001% in the final solution).

The polarograms were recorded by a Heyrovský-system L.P. 55 polarograph. The half-wave potentials were checked by a W.G. Pye Vernier potentiometer. The D.M.E. had the following characteristics: $m = 1.76$ mg/sec and $t = 3.6$ sec (at -1.0 V *vs.* S.C.E. in 0.1 *M* potassium nitrate solution). All measurements were made at $30 \pm 0.01°$. A Haake-type ultra thermostat was used for controlling the temperature. Purified nitrogen was used to remove the dissolved oxygen. The reversibility of the reduction was tested by plotting $\log i/(i_d - i)$ *vs.* $E_{d.e.}$

Solutions were 0.75 m*M* with respect to Cd^{2+} and 0.1, 0.2, 0.3, 0.4, 0.5, 0.6, 0.7, 0.8 and 1.0 *M* with respect to sodium benzoate.

The solutions, after thorough mixing, were placed in the thermostat for 48 h to ensure complete reaction. The polarograms were recorded manually after de-aeration.

Results and discussion

A well-defined single reduction wave appeared with all the solutions. The plots of $\log i/(i_d - i)$ *vs.* $E_{d.e.}$ were linear with a slope of 31 ± 2 mV, indicating a reversible reduction. The diffusion current decreased with increasing concentration of sodium benzoate. The plot of half-wave potential *vs.* $\log C_X$ (C_X = benzoate concentration) was not a straight line (Fig. 1) and showed the formation of two or more complexes in equilibrium. The classical method due to LINGANE[7] could not, therefore, be applied. The method of DEFORD AND HUME[8] (in the modified form given by IRVING[9]) for step-wise complex formation was therefore employed. The value of overall formation

constants were computed graphically as discussed below:

$$F_0([X]) = \text{antilog}\left\{\frac{0.4343\,nF}{RT}(E_{\frac{1}{2}})_s-(E_{\frac{1}{2}})_c+\log\frac{I_s}{I_c}\right\} \quad (1)$$

$$F_1([X]) = \frac{F_0([X])-\beta_0/f_s}{C_X f_X} \quad (2)$$

$$F_2([X]) = \frac{F_1([X])-\beta_1/f_{MX}}{C_X f_X} \quad (3)$$

$$F_3([X]) = \frac{F_2([X])-\beta_2/f_{MX_2}}{C_X f_X} \quad (4)$$

$$F_4([X]) = \frac{F_3([X])-\beta_3/f_{MX_3}}{C_X f_X} \quad (5)$$

where the subscripts s and c refer to the aquated cadmium ion and the complex, respectively, I_s/I_c is the ratio of the corresponding diffusion current constants, β_0, β_1, β_2 and β_3 are the overall formation constants of the zero complex and the complex containing one, two and three ligands, respectively, and f denotes the activity coefficient. The experimentally-determined values of the half-wave potentials, together with the $F_j([X])$ values calculated from eqns. (1), (2), (3), (4) and (5) are

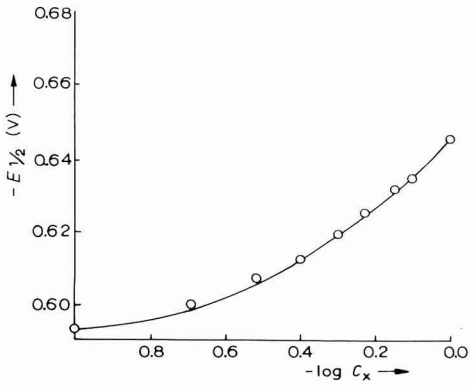

Fig. 1. Plot of $E_{\frac{1}{2}}$ *vs.* log C_X.

given in Table 1, assuming that the ionic atmosphere and, therefore, the several activity coefficients probably change very little since the ionic strength is constant. The overall formation constants given in the table were obtained by a graphical extrapolation (Fig. 2) of the $F_j([X])$ functions to the zero ligand concentration. The values of the overall formation constants for the complex ions $Cd(C_6H_5COO)^+$, $Cd(C_6H_5COO)_2$, $Cd(C_6H_5COO)_3^-$ and $Cd(C_6H_5COO)_4^{2-}$ were found to be 12, 15, 44 and 74, respectively.

Figure 3 represents the percentage distribution of cadmium present (in the cationic or anionic form) as a function of the logarithm of benzoate concentration.

TABLE 1

ANALYSIS OF $F_j([X])$ FUNCTION

C_X (moles)	$E_{\frac{1}{2}}$ (−V vs. S.C.E.)	i_d (divs.)	F_0 ([X])	F_1 ([X])	F_2 ([X])	F_3 ([X])	F_4 ([X])
0.0	0.5870	52.0					
0.1	0.5976	50.0	2.34	13.43	14.32	—	—
0.2	0.6042	47.0	4.13	15.66	18.3	—	—
0.3	0.6103	46.5	6.68	18.94	23.8	—	—
0.4	0.6152	43.0	10.48	33.7	29.2	—	—
0.5	0.6221	42.0	19.4	36.8	49.6	69.2	—
0.6	0.6288	40.0	31.99	51.65	66.1	85.1	75.0
0.7	0.6348	41.0	48.3	67.65	79.4	92.0	74.2
0.8	0.6370	38.0	61.97	76.21	82.5	99.3	73.2
1.0	0.6480	37.0	150.6	149.6	137.0	112.0	72.0

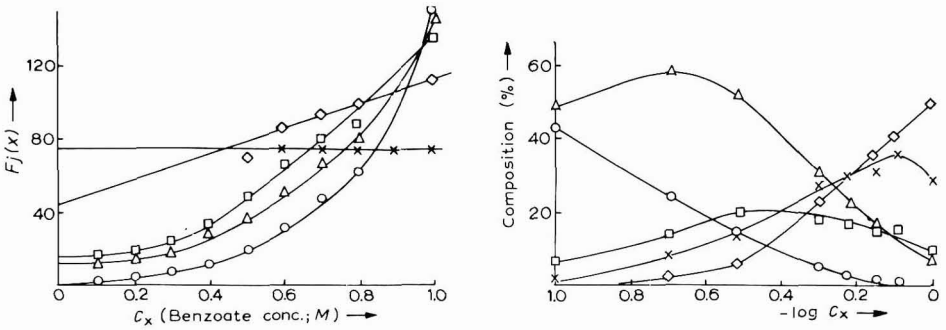

Fig. 2. $F_j([X])$ plots for cadmium–benzoate system: ○, $F_0([X])$; △, $F_1([X])$; □, $F_2([X])$; ◇, $F_3([X])$; ×, $F_4([X])$.

Fig. 3. Percentage distribution of various species present in cadmium–benzoate system: ○, Cd^{2+}; △, $Cd(C_6H_5COO)^+$; □, $Cd(C_6H_5COO)_2$; ×, $Cd(C_6H_5COO)_3^-$; ◇, $Cd(C_6H_5COO)_4^{2-}$.

Acknowledgement

The authors thank the C.S.I.R. for granting a Junior Research Fellowship to one of them (D.S.J.) and Prof. R. C. MEHROTRA for providing facilities for the investigation.

Chemical Laboratories,
University of Rajasthan,
Jaipur (India)

D. S. JAIN
J. N. GAUR

1 D. N. HUME, D. D. DEFORD AND G. B. C. CAVE, *J. Am. Chem. Soc.*, 73 (1951) 5323.
2 YA. I. TURYAN AND G. P. SEROYA, *Zh. Neorgan. Khim.*, 2 (1957) 336.
3 L. ERIKSSON, *Acta Chem. Scand.*, 7 (1951) 1176.
4 G. NAGESWARA RAO AND R. S. SUBRAHMANYA, *Current Sci. India*, 31 (1962) 55.
5 G. SARTORI, *Gazz. Chim. Ital.*, 64 (1934) 3.
6 D. S. JAIN AND J. N. GAUR, unpublished work.
7 J. J. LINGANE, *Chem. Rev.*, 29 (1941) 1.
8 D. D. DEFORD AND D. N. HUME, *J. Am. Chem. Soc.*, 73 (1951) 5321.
9 H. IRVING, *Advances in Polarography*, Vol. I, Pergamon Press, London, 1960, p. 42.

(Received June 20th, 1965)

Effect of some tetraalkylammonium hydroxides on the electrode kinetics of the chromi–chromocyanide couple

A study, similar to that of GIERST *et al.*[1] for chromate, was undertaken to determine the effect of some tetraalkylammonium hydroxides on the kinetics of the chromi–chromocyanide reaction on a mercury electrode. This couple has characteristics similar to those for chromate reduction, *viz.*, (a) reaction occurring at markedly negative potentials *versus* the point of zero charge and (b) strong repulsion of the discharged species because of its highly negative ionic valence. Results are summarized here, and a detailed report[2] is available.

Kinetic parameters were determined by the faradaic impedance method. Chromocyanide was generated *in situ* by the polarographic technique, the potential being controlled to ± 2 mV (this ion is strongly reducing and difficult to prepare). All solutions were 5 m*M* in chromicyanide and 0.1 *M* in potassium cyanide. This solution was not very stable[3] even in de-aerated solution (color change in 24 h). Electrode characteristics: 1.53 mg sec^{-1} as rate of flow; drop knocked off with magnetic hammer every 2.24 sec; bridge balanced at 1.24 sec.

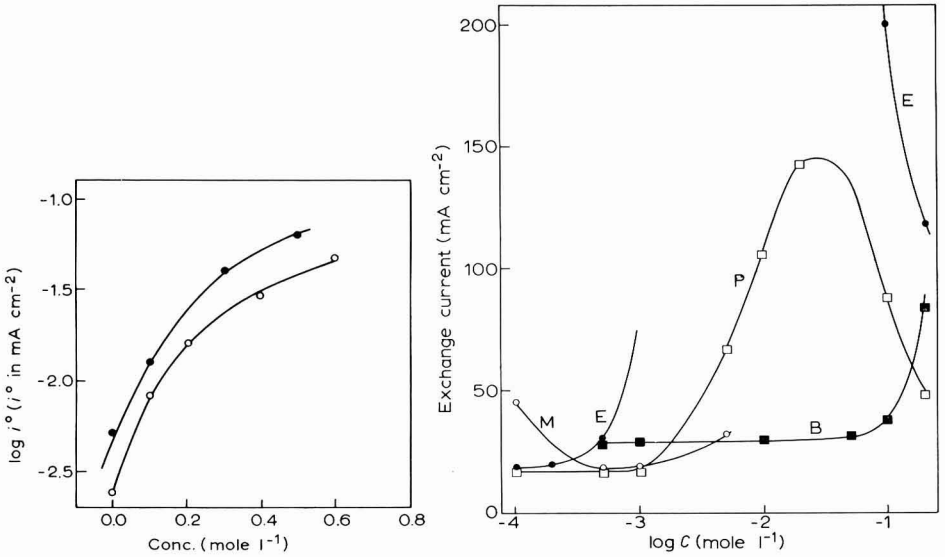

Fig. 1. Plot of log of the exchange current density, i^0, *vs.* KCl concn. for 2.5 m*M* Cr(III) + 2.5 m*M* Cr(II) in 0.1 *M* KCN. (○), this work; (●), KLEINERMAN's data.

Fig. 2. Plot of exchange current density, i^0, against the log of the concn. of tetraalkylammonium hydroxide for 2.5 m*M* Cr(III) + 2.5 m*M* Cr(II) + 0.1 *M* KCN + KCl to make an ionic concn. of 0.3 *M*. (M), methyl; (E), ethyl; (P), *n*-propyl; (B), *n*-butyl.

The solution resistance was deduced from SLUYTER's plot[4,5] and electrode impedance data were plotted according to the methods of GERISCHER[6] and RANDLES[7]. The transfer coefficient was computed from exchange currents measured at different potentials for the generation *in situ*.

Exchange current densities are plotted in Fig. 1 against potassium chloride concentration and are compared with KLEINERMAN's preliminary data[7]. These data agree with previous observations[8] and indicate a double-layer effect. The transfer coefficient, $\alpha = 0.48$, agrees quite well with an earlier result[9] of $\alpha = 0.53$ (faradaic rectification).

These results should be assessed with caution as the analysis of the faradaic impedance by the Gerischer or Randles plots deviated somewhat from the behavior expected from a simple electrode process. *Measured exchange currents should be regarded here as operational data allowing some comparison of double-layer effects.* The complexity of the chemistry of Cr(III) and Cr(II) in cyanide medium seems to preclude a simple interpretation[10].

Measurements were taken with 0.1 *M* potassium cyanide and the total ionic concentration was adjusted to 0.3 *M* with potassium chloride and tetraalkylammonium hydroxide. Desorption polarographic waves were observed for some of the hydroxides, but the potential corresponding to one-half of the total diffusion current was always taken for generation *in situ*. GERISCHER's plots in the analysis of the electrode impedance were always linear. No attempt was made to ascertain whether there was any diffusion control in the adsorption to tetraalkylammonium hydroxide but such a complication, if any, would not modify the general shape of the curves in Fig. 2 (discussed below). Each additive will be described separately.

Tetramethylammonium hydroxide (TMA). The concentration range of TMA used was rather narrow because of the formation of a precipitate. The latter dissolved in potassium cyanide but the TMA concentration could not be increased beyond 0.01 *M*. The exchange current decreased with increasing TMA concentration (Fig. 2, curve M) and reached approximately, in the limited concentration range that could be covered, the same value as in the absence of TMA.

Tetraethylammonium hydroxide (TEA). The exchange current density increased markedly at low concentrations and the reaction became diffusion-controlled in the range 10^{-3}–$5 \cdot 10^{-2}$ *M*. At higher concentrations, the exchange current again decreased (Fig. 2, curve E).

Tetra-n-propylammonium hydroxide (TPA). The behavior was similar to that of TEA but the increase in exchange current was less pronounced and occurred at higher concentrations (Fig. 2, curve P). A desorption wave was observed at rather negative potentials (≈ -1.8 *vs.* N.C.E.).

Tetra-n-butylammonium hydroxide (TBA). A desorption wave appeared at approximately -1.6 *vs.* N.C.E., and a peak showed in the differential capacity *vs.* potential curve in that range of potentials. The exchange current was constant and twice as large as in the absence of TBA up to 0.01 *M* after which it increased (Fig. 2, curve B).

These results can tentatively be interpreted in the same way as did GIERST *et al.*[1] for the chromate reduction: (a) acceleration caused by the lowering (in absolute value) of the potential in the plane of closest approach, *i.e.*, lessening of repulsion upon addition of tetraalkylammonium hydroxide; (b) decrease in rate caused by coverage of the electrode. The double-layer effect is very pronounced because of the highly negative ionic valence of Cr(III) in cyanide medium. There is a major difference between the results described here and those of GIERST *et al.*[1], in that a decreasing effect was observed from TMA to TBA whereas there was an opposite sequence for chromate reduction. This surprising difference may possibly be accounted for by

invoking ionic association (already referred to by GIERST *et al.*) and by assuming that ionic association becomes less pronounced from TMA to TBA. Differences in the solubility of tetraalkylammonium cyanides may also be invoked (*cf.* GREGOR *et al.*[11] on the behavior of tetraalkylammonium resins toward perchlorate). Finally, the complexity of the chemistry of Cr(III) and Cr(II) in cyanide media has to be taken into account.

It is concluded that the coverage and double-layer effects have a profound influence on the reduction of Cr(III) in cyanide medium and that ionic association presumably effects considerably the double-layer effect.

Acknowledgement

The author thanks Professor PAUL DELAHAY for his interest in and discussion of this problem and is indebted to the N.A.T.O. organization for a fellowship. This work was supported by the Office of Naval Research.

Coates Chemical Laboratory,
Louisiana State University,
Baton Rouge, La. 70803 (U.S.A.)

ANNA MARIA GIULIANI*

1 L. GIERST, J. TONDEUR, R. CORNELISSEN AND F. LAMY, paper presented at the Moscow CITCE meeting, 1963.
2 A. M. GIULIANI, Technical Report No. 58 to the Office of Naval research, Project NR 051-258, Louisiana State University, May 1965.
3 D. N. HUME AND I. M. KOLTHOFF, *J. Am. Chem. Soc.*, 65 (1943) 1897.
4 J. H. SLUYTERS, *Rec. Trav. Chim.*, 79 (1960) 1092.
5 M. REHBACH AND J. H. SLUYTERS, *ibid.*, 80 (1961) 469.
6 H. GERISCHER, *Z. Physik. Chem. Leipzig*, 202 (1953) 302.
7 P. DELAHAY, *Transactions of the Symposium of Electrode Processes*, edited by E. YEAGER, Wiley, New York, 1961, p. 12.
8 J. E. B. RANDLES AND K. W. SOMERTON, *Trans. Faraday Soc.*, 48 (1952) 937.
9 H. IMAI, *J. Phys. Chem.*, 66 (1962) 1744.
10 W. B. SCHAAP, unpublished work, as reported in *Chem. Eng. News*, 43 (1965), No. 39, 44.
11 H. P. GREGOR, J. BELLE AND R. A. MARCUS, *J. Am. Chem. Soc.*, 77 (1955) 2713.

Received July 21st, 1965

* On leave from Istituto di Chimica Generale ed Inorganica, Università di Roma, Rome, Italy; now in Rome.

BOOK REVIEWS

Bibliografia Polarografica (1922–1963), Parts I and II, Supplement No. 16, by L. JELLICI AND L. GRIGGIO, Consiglio Nazionale delle Ricerche, Roma, 1965, 233 pages, lire 3600 ($7.20).

The latest edition of this well-known bibliography appears with both parts, previously issued separately, in a single volume. Otherwise, the arrangement is as before, with a list of papers in alphabetical order of the first author, a separate complete author index, and a comprehensive subject index.

T. BIEGLER, University of Bristol

Chemical Thermodynamics, Basic Theory and Methods, by I. M. KLOTZ, W. A. Benjamin Inc., New York, Amsterdam, 1964, xiv + 468 pages, $10.75.
Introduction to Chemical Thermodynamics, by I. M. KLOTZ, W. A. Benjamin Inc., New York, Amsterdam, 1964, xv + 244 pages, $4.35.

The first of these books is an extremely clear and well thought out course on the techniques of classical chemical thermodynamics. The author has made no attempt to deck out the well-worn subject with new trappings, but the student who follows conscientiously through the text will have gained a thorough grounding. This would, of course, include working out the excellent, practical problems which are given at the end of each chapter. Answers are given for most of the numerical problems (none for those in the last two chapters).

The second book is a paper-back edition of the first twelve chapters of the first book which deal with the laws of thermodynamics and their application to systems in which the composition of the phases is constant. Although in some ways this is a sensible and logical division, most students would find the paper-back a false economy, because very little chemical thermodynamics can be done with these systems alone; in electrochemistry, in particular, phases of variable composition are inevitable. The second half of the main work, in fact, leads from the definition of partial molar quantities through fugacities and activities to two final chapters which deal exclusively with electrolytes. In view of the importance of thermodynamics in electrochemistry and *vice versa* it is perhaps a little surprising to find one of the main links between the two subjects, the equation $\Delta G = -zFE$, introduced almost casually on p.166. The tricky question of standard states in electrolytes is, in contrast, given close attention and explained with great clarity.

The books are well printed and laid out with very few misprints; the only one which might cause trouble is on page 99. "It should be emphasised that the second law is not an *a priori* principle, that is, it is not a statement which might be deduced from earlier principles..."

ROGER PARSONS, University of Bristol

CONTENTS